UNIVERSITA' DI NAPOLI FEDERICO II

DOTTORATO DI RICERCA
BIOCHIMICA E BIOLOGIA CELLULARE E MOLECOLARE
XXV CICLO

INTERACTION OF EUBACTERIAL LIGANDS WITH ARCHAEAL ELONGATION FACTOR 1α: MODULATION OF ITS MOLECULAR AND FUNCTIONAL PROPERTIES.

Anna Lamberti

Tutor
Prof. Paolo Arcari

Coordinator
Prof. Paolo Arcari

Co-Tutor
Prof. Mariorosario Masullo

Academic Year 2011/2012

Ringraziamenti e dediche

Scrivere i ringraziamenti per me è sempre un momento difficile! Sarà che non è facile racchiudere in un paio di pagine le emozioni e le sensazioni che si provano giunti alla fine di un percorso…
Il mio GRAZIE più grande va ai miei genitori, per aver sempre sostenuto le mie scelte, per avermi sempre tirato su il morale, per la grande fiducia che hanno in me, per il loro infinito amore e per avermi incoraggiata ad accettare il Dottorato senza borsa quando io ero indecisa, e alla mia sorellina Alessia, ormai cresciuta, per essermi stata sempre vicina (soprattutto nell'ultimo anno). Vi voglio bene!
La stesura di una tesi è sempre un momento abbastanza stressante, e c'è qualcuno che più di tutti ha subito i miei sbalzi di umore, il mio fidanzato Vincenzo. Grazie per avermi sopportata in questo periodo, ma soprattutto per essere entrato nella mia vita, che è più bella da quando ci sei tu!
Un ringraziamento sentito e doveroso va al Prof. Mariorosario Masullo, per avermi seguita fin dai primi passi che ho mosso in laboratorio, per la sua grande conoscenza, professionalità, umiltà e umanità.
Vorrei inoltre ringraziare i Proff. Paolo Arcari, Emmanuele De Vendittis, Gaetano Corso, Antonio Dello Russo e le dott.sse Rosaria Ruocco, Annalisa Lamberti e Lia Rippa per la loro grande disponibilità, perché al VI piano ci si sente davvero a casa.
Un ringraziamento particolare va ad Alba, per la sua infinita disponibilità e bontà, e per avermi aiutata a rendere la mia vita un po' meno travagliata.
Come non ringraziare tutti i ragazzi del VI piano, che hanno reso le giornate in laboratorio più leggere e spensierate. Un ringraziamento particolare va a Monica, con cui oramai condivido la mia vita tutti i giorni, in laboratorio e a casa, semplicemente ti voglio tanto bene; a Nicola, per essersi rivelato un vero amico e per il suo contributo informatico; a "Ciccio Albano" e Valentina per la loro sincera amicizia.
Infine vorrei ringraziare tutti gli amici di sempre, per essermi stati sempre vicini, in particolare Doriana, per esserci sempre, in qualsiasi

momento io ne abbia bisogno; Assunta, semplicemente perché è mia sorella, e Marialuisa, per essermi sempre vicina. Vi voglio bene!
Finalmente ho finito di scrivere i ringraziamenti che, come tutti avrete capito, non sono il mio forte! Il problema è che penso troppo al fatto che li debbano leggere gli altri e questo mi inibisce. Se ho dimenticato qualcuno non me ne voglia, chiunque leggerà questi ringraziamenti fa parte della mia vita e anche se non ha trovato citato il suo nome, si senta ringraziato lo stesso.

GRAZIE DI CUORE A TUTTI,
ANNA

Riassunto

L'attività di ricerca svolta durante il periodo di Dottorato ha riguardato lo studio dell'interazione tra il fattore di allungamento archeobatterico 1α da *Sulfolobus solfataricus* (SsEF–1α) ed alcuni ligandi eubatterici, ovvero due antibiotici, la tetraciclina e la pulvomicina, e un nucleotide guanilico modificato, il ppGpp. E' stato scelto tale fattore di allungamento perché era già stato ampiamente caratterizzato, sia dal punto di vista strutturale sia riguardo le sue proprietà funzionali, nel laboratorio dove è stato condotto il lavoro ricerca. SsEF–1α presenta caratteristiche strutturali simili all'analogo eubatterico EF–Tu e proprietà funzionali più simili all'analogo fattore eucariotico.
La tetraciclina e la pulvomicina sono antibiotici eubatterici che inibiscono la sintesi proteica. Mentre la tetraciclina impedisce il legame dell'aa–tRNA al sito A del ribosoma, la pulvomicina inibisce la formazione del complesso ternario tra il fattore di allungamento Tu (EF–Tu), il GTP e l'aa–tRNA. Lo studio dell'interazione tra la tetraciclina o la pulvomicina ed SsEF–1α è stato effettuato sia in termini degli effetti prodotti dai due antibiotici sulle proprietà biochimiche dell'enzima sia mediante spettroscopia in fluorescenza. Riguardo gli effetti sulle proprietà funzionali di SsEF–1α, entrambi gli antibiotici sono in grado di inibire la sintesi proteica in un sistema ricostituito *in vitro* contenente tutti i componenti macromolecolari purificati da *S. solfataricus*. Nelle reazioni parziali catalizzate da SsEF–1α, la pulvomicina, ma non la tetraciclina, produce una riduzione dell'affinità del fattore di allungamento per l'aa–tRNA solo in the presenza del GTP. La tetraciclina produce un aumento della velocità di scambio GDP/GTP ed una lieve inibizione dell'attività GTPasica intrinseca; viceversa, in presenza di pulvomicina, lo scambio è circa 1,5 volte più veloce per entrambi i nucleotidi guanilici, e si osserva una stimolazione dell'attività GTPasica. Inoltre, mentre la tetraciclina produce una leggera destabilizzazione della proteina alla denaturazione termica, la pulvomicina esercita un effetto protettivo su SsEF–1α nei riguardi della denaturazione chimica. Per quanto riguarda gli studi spettroscopici in fluorescenza, entrambi gli antibiotici inducono una variazione dello spettro di fluorescenza nella regione dei residui aromatici della proteina. In particolare, la tetraciclina è in grado di aumentare la resa quantica della fluorescenza di SsEF–1α e di Ss(GM)EF–1α, una sua forma troncata costituita dai domini G ed M, ma non di Ss(G)EF–1α, una sua forma troncata costituita dal solo dominio G; tale risultato indica che il dominio M è indispensabile per

l'interazione con questo antibiotico. La pulvomicina, invece, esercita un quenching della fluorescenza al massimo di assorbimento (314 nm) con la comparsa di un nuovo picco a circa 360 nm per tutte le proteine analizzate, suggerendo che la forma intatta del fattore di allungamento è necessaria per l'interazione.

Il ppGpp, chiamato anche "magic spot I", svolge la sua azione nei batteri e nelle piante durante lo "Stringent Control", ovvero in condizioni di stress cellulare e di mancanza di sostanze nutritive. Esso è in grado di inibire i fattori di allungamento della sintesi proteica in caso di carenza di amminoacidi. Ha una struttura simile a quella del GDP, ma presenta un gruppo difosfato addizionale legato all'ossigeno in posizione 3' del ribosio. E' stata studiata l'interazione tra SsEF–1α e questa molecola non solo perché tale fattore di allungamento è in grado di interagire con i nucleotidi guanilici, ma soprattutto perché il ppGpp è stato trovato legato ad SsEF–1α nella struttura cristallina di una sua forma ricombinante. Il ppGpp è in grado di inibire la sintesi proteica in un sistema ricostituito *in vitro*. Per quanto riguarda lo studio dell'effetto del nucleotide sulla formazione del complesso ternario, valutata in base alla capacità di SsEF-1α di proteggere l'aa-tRNA dalla sua deacilazione spontanea, i risultati mostrano che in presenza di ppGpp l'affinità del fattore di allungamento per l'aa–tRNA è intermedia se confrontata con quella per il GDP e per il GTP. Inoltre, la presenza del nucleotide tetrafosfato riduce l'affinità di SsEF–1α per i nucleotidi guanilici mediante un meccanismo di inibizione competitiva. In relazione all'effetto sulla GTPasi, la presenza del ppGpp provoca un aumento della K_m senza variazione della k_{cat}, indicando anche in questo caso un comportamento da inibitore competitivo. Infine, la presenza del ppGpp rende SsEF–1α più stabile al trattamento termico. Questi risultati indicano che il gruppo difosfato extra presente nel ppGpp esercita un effetto protettivo sul fattore di allungamento e tale stabilizzazione potrebbe essere spiegata da una migliore distribuzione delle cariche sulla superficie della proteina.

In conclusione, gli studi riportati nella presente tesi possono essere utili per valutare le relazioni filogenetiche tra fattori di allungamento appartenenti a diversi domini degli organismi viventi.

Summary

The interaction between the archaeal elongation factor 1α from *Sulfolobus solfataricus* (SsEF–1α) and some eubacterial ligands, such as eubacterial antibiotics, tetracycline and pulvomycin, and the modified guanosine nucleotide ppGpp was investigated. SsEF–1α had already been characterised for its structural and functional properties in the laboratory where the research work was carried out. This ubiquitous protein presents structural properties more similar to the eubacterial counterpart and functional propertis more similar to the eukaryal ones.

Tetracycline and pulvomycin are eubacterial antibiotics that inhibit protein synthesis. Tetracycline prevents the binding of aa–tRNA to the A site of the ribosome, whereas pulvomycin inhibits the formation of the ternary complex between the elongation factor Tu (EF–Tu), GTP and aa–tRNA. The interaction between SsEF–1α and these antibiotics was demonstrated either by fluorescence spectroscopy in the aromatic region of the spectrum of this protein or by the effects produced by the antibiotic on some functional properties of the elongation factor. The results indicated that both antibiotics were able to inhibit archaeal protein synthesis and that pulvomycin, but not tetracycline, was able to reduce the affinity of SsEF–1α for aa–tRNA in presence of GTP. Moreover, tetracycline produced an increase in GDP/GTP exchange rate and a slight inhibition of the intrinsic GTPase; vice versa, in the presence of pulvomycin, the exchange rate was higher for both guanosine nucleotides and a stimulation of GTPase activity was observed. Furthermore, the interaction between SsEF–1α and tetracycline caused a reduction of stability to the heat treatment, whereas pulvomycin exerted a protective effect on the elongation factor against chemical denaturation. Regarding fluorescence spectroscopy, in the presence of tetracycline an increase in the quantum yield in the fluorescence spectrum of SsEF–1α was observed. A similar behaviour was also observed for Ss(GM)EF–1α but not for Ss(G)EF–1α, two engineered forms of the elongation factor; these results indicated that the M–domain is essential for the interaction with tetracycline. Pulvomycin, instead, exerted a strong fluorescence quenching at λ_{max} which was accompanied by the appearance of a new peak at 360 nm for all proteins analysed, suggesting that the intact form of SsEF–1α is required for the interaction.

ppGpp, also called "magic spot I", is a molecule involved in the “Stringent Control” both in eubacteria and plants during amino acid starvation. It is a compound structurally similar to GDP, characterised by the presence of an additional diphosphate group, bound through a phosphoester bond to the oxygen in position 3’ of ribose. The interaction between SsEF–1α and this molecule was investigated because ppGpp was found bound to a recombinant form of the elongation factor, used for crystallographic studies. ppGpp was able to inhibit *in vitro* protein synthesis; the affinity of SsEF–1α for aa–tRNA in presence of the nucleotide tetra–phosphate resulted intermediate between that for GDP and GTP. Moreover, ppGpp reduced the affinity of SsEF–1α for guanosine nucleotides through a competitive mechanism. Regarding the effect on the intrisic GTPase, the presence of ppGpp caused an increase of K_m with any variation in k_{cat}, indicating also in this case a competitive inhibition behaviour. Finally, the presence of the nucleotide tetra–phosphate rendered SsEF–1α more stable to heat treatement.

In conclusion, the data presented demonstrated an interaction between the archaeal elongation factor 1α from *Sulfolobus solfataricus* and some eubacterial ligands. These results could be used as probe to investigate phylogenetic relationship among living domain.

Index

List of Tables

List of Figures

1. Introduction

1.1 Elongation cycle in protein biosynthesis

Protein synthesis is a process, occuring through a set of reactions, in which ribosomes advance along the mRNA introducing the appropriate aminoacyl–tRNA (aa–tRNA), giving rise to the insertion of the amino acid units for the synthesis of the encoded protein. The ribosome, therefore, can be considered a small factory in which a complex of protein and ribosomal RNA ensure, through various catalytic activities, the efficiency and effectiveness of the entire process. It requires the intervention of a considerable number of translational factors, which assist the ribosomes in the development of the three stages characterising the process: the initiation phase, the elongation cycle and termination phase. The phase certainly most studied is that of elongation, a cyclic process, which involves the binding of an amino acid residue at the carboxyl terminus of the neosinthesising polypeptide chain. In eubacteria three elongation factors, called EF–Tu, EF–Ts and EF–G, are involved. The first event is the formation of a ternary complex between the elongation factor EF–Tu, GTP and aa–tRNA (Miller et al. 1977; Forster et al. 1993), that binds the A site of the ribosome•mRNA complex only if there is a correct pairing between the mRNA codon and the anticodon of aa–tRNA (Weijland et al. 1992). Subsequently to this interaction EF–Tu elicits its intrinsic GTPase activity that produces the corresponding GDP–bound form of the factor that dissociates from the ribosome (Fasano et al. 1978). The switch from the active to the inactive form is associated with a conformational change of the enzyme (Sprinzl 1994). The regeneration of the active form of EF–Tu, complexed with GTP, is ensured by the intervention of the elongation factor Ts which catalyses the GDP/GTP exchange on the factor. In the second phase of the elongation cycle, the peptidyl–transferase activity, localised on the 50S ribosomal subunit, allows the formation of a peptide bond between the amino acid bound to the aa–tRNA placed on the A site, and the peptidyl–tRNA located on the P site of the ribosome. In the last phase of the elongation cycle, the elongation factor G bound to GTP promotes, in the order: the translocation of peptidyl–tRNA from

the A site to the P site of the ribosome, the displacement of the deacylated tRNA from the P site to the E site (Rheinberger 1991) and the simultaneous movement of an mRNA codon. The duration of the complete cycle of elongation is about 100 milliseconds (25 ms for the interaction between EF–Tu and the ribosome, 50 ms for the formation of the peptide bond and 25 ms for the event of translocation). Although the process of biosynthesis occurs with high speed, there are control mechanisms that regulate the efficiency, such as the codon–anticodon interaction and the negative cooperativity between A and E (exit site) sites of the ribosome (Rodnina et al. 2001).
The molecular mechanism of the elongation cycle was also studied from a structural point of view. In fact, the three–dimensional structure of the three elongation factors EF–Tu, EF–G, EF–Ts, as well as that of the complexes EF–Tu•EF–Ts and EF–Tu•GTP•aa–tRNA has been determined. More recently the three–dimensional structure of the ribosome has been solved (Stark 2002). Regarding the three–dimensional structure of EF–Tu from *Escherichia coli*, the presence of three structural domains, a GDP/GTP–binding domain (G–domain), a middle (M) and a C–terminal (C) domain was identified (Kjeldgaard et al. 1992; Song et al. 1999).

1.2 Antibiotics acting on EF–Tu

The details of the mechanism of action of *Escherichia coli* EF–Tu (EcEF–Tu) have also been elucidated taking advantage of specific antibiotics acting on the elongation factor. In particular, it has been reported that kirromycin freezes EF–Tu•GDP complex on the mRNA–programmed ribosome by preventing the structural rearrangement of the factor (Parmeggiani et al. 2006); tetracycline was able to inhibit the binding of aa–tRNA to the A site of mRNA–programmed ribosome (Heffron et al. 2006). In addition, pulvomycin and GE2270A interfere with ternary complex formation, preventing the interaction between EF–Tu•GTP and aa–tRNA (Parmeggiani et al. 2006; Heffron et al. 2000).

1.2.1 Tetracycline

Tetracycline (Figure 1) is a broad spectrum bacteriostatic antibiotic, that inhibits the bacterial protein synthesis (Goodman & Gilman,

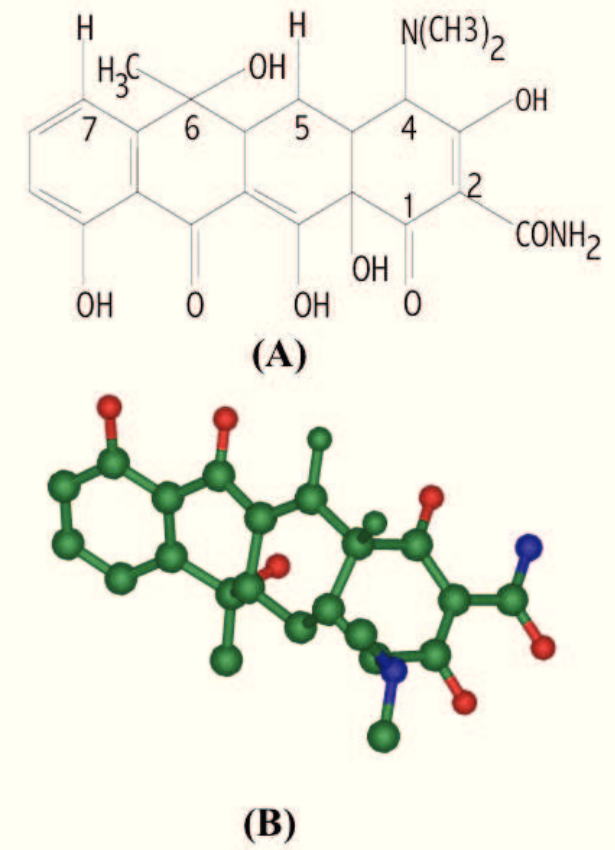

Figure 1. Chemical structure of tetracycline. *(A) molecular structure; (B) "balls and sticks structure". Carbon atoms are indicated in green, oxygen atoms in red and hydrogen atoms in blue.*

1997) through the bind to the 30S subunit of the ribosome; in this way, it prevents the access of aa–tRNA to the A site of the mRNA–ribosome complex. More recently, the resolution of the three–dimensional structure of a complex formed between tetracycline and the EF–Tu•GDP complex (Heffron et al. 2006) reopens the question of the molecular target(s) of this antibiotic that probably reflects different modes of action and / or resistant mechanisms in different

pathogens (Heffron et al. 2006). In fact, over the years several studies have been reported, in which ribosomal proteins (Connamacher et al. 1968; Maxwell et al. 1968; Williams Smith 1979) or specific sites of 16S rRNA molecules (Moazed et al. 1987; Brodersen et al. 2000; Pioletti et al. 2001; Hinrichs et al. 1994; Orth et al. 1999; Nonaka et al. 2005) are claimed to be involved in the weak interaction between tetracycline and ribosome (Epe et al. 1984). Therefore, the resolution of the structure of a complex between tetracycline and EF–Tu, in its GDP–bound form (Heffron et al. 2006), revalued early reports focusing on the involvement of this elongation factor in the mechanism of action of tetracycline (Gordon 1969; Ravel et al. 1969; Shorey et al. 1969; Skoultchi et al. 1970; Spirin et al. 1976; Semenkov et al. 1982). The details of the molecular contacts between the antibiotic and the elongation factor pointed to a binding site entirely located on the G–domain of EF–Tu; however, the crystallographic unit contains an (EF–Tu•GDP•tetracycline)$_2$ dimer, in which the two G and the two M–domains of the EF–Tu molecule formed intramolecular contacts. Therefore, the packaging of the complex might involve different portions of the proteins and it is not restricted to the nucleotide–binding domain of the elongation factor.

1.2.2 Pulvomycin

Pulvomycin (Figure 2), isolated from *Streptoverticillium netropsis*, inhibits protein synthesis in prokaryotes, blocking the formation of the ternary complex between EF–Tu, GTP and aa–tRNA. In particular, pulvomycin interacts with the three structural domains of EF–Tu through its lactone ring. The regions of EF–Tu involved in the binding of the antibiotic have been identified both by the discovery of some EF–Tu mutants, resistant to the antibiotic, and by the resolution of the three–dimensional structure of the complex EF–Tu•pulvomycin (Parmeggiani et al. 2006). The amino acid residues, interacting with the antibiotic, are located at the interface between the three structural domains of EF–Tu (Ile93, Thr94, Gln98, Glu226, Arg230, Arg233, His273, Thr334, Arg345 and Arg385) (Zeef et al. 1994; Boon et al. 1995). Pulvomycin interferes with the transition of EF–Tu from its active to its inactive form, causing a conformational change in the

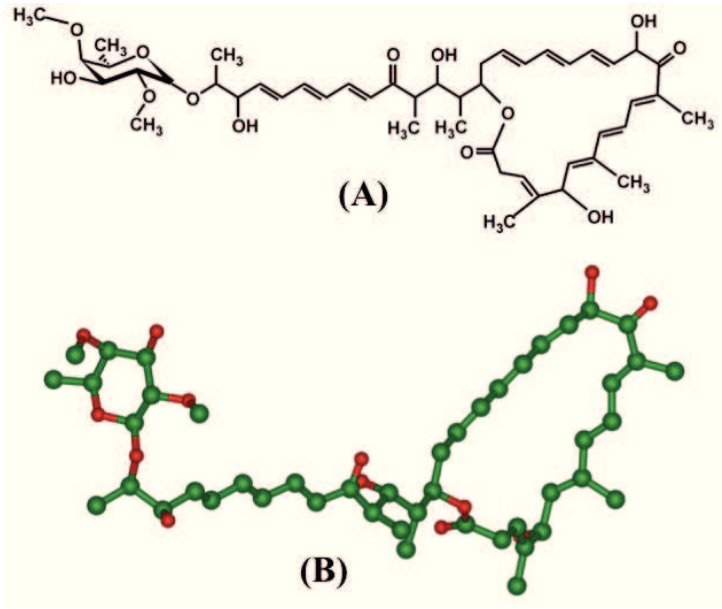

Figure 2. Chemical structure of pulvomycin*. (A) molecular structure; (B) "balls and sticks structure". Carbon atoms are indicated in green, oxygen atoms in red.*

nucleotide binding site that influences nucleotide hydrolysis (Anborgh et al. 1991; Langen et al. 1992).

1.3 (p)ppGpp interacts with EF–Tu

The accumulation of guanosine tetra– and penta–phosphates (ppGpp and pppGpp, called also magic spot I and magic spot II, respectively, or alarmones) occurs in most eubacteria during stringent control (SC) (Braeken et al. 2006 ; Magnusson et al. 2005) but not in mutant strains lacking SC (Cashel et al. 1996). Concerning eukaryotes, the presence of alarmones has been demonstrated in plants where these molecules accumulate in chloroplasts upon biotic and abiotic stresses (Takahashi et al. 2004). ppGpp, a compound structurally similar to GDP, is characterised by the presence of an additional diphosphate group, bound through a phosphoester bond to the oxygen in position 3' of

ribose (Figure 3). Its production in eubacteria can be also induced by stress conditions or nutritional starvation (Cashel et al. 1996; Battesti

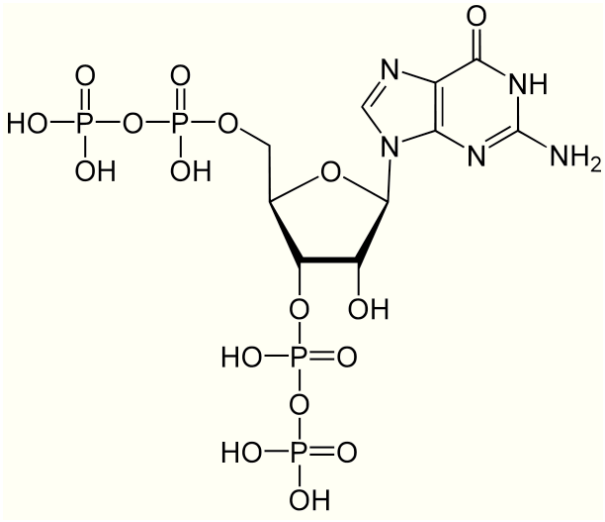

Figure 3. Chemical structure of ppGpp.

et al. 2006). The enzymes involved in magic spot synthesis are the *relA* gene product (p)ppGpp synthetase I and the *spoT* gene product (p)ppGpp synthetase II (Potrykus et al. 2008; Atkinson et al. 2011). Recently, a growing number of RelA/SpoT homologues, designated RSH, have been identified in plants (Mizusawa et al. 2008). Furthermore, the identification of such proteins in the genome of several sources including some archaea allowed the analysis of phylogenetic relationships among these proteins in the tree of life (Atkinson et al. 2011). In bacterial cells, (p)ppGpp plays a role as a negative effector of stable RNA (sRNA) levels and also in several other aspects to SC response, such as that of restricting translational errors during amino acid starvation, thus influencing translation accuracy through different proposed mechanisms (Cashel et al. 1996). One of these involves the interaction of magic spots with translation elongation factors EF–Tu and EF–G (Rojas et al. 1984) as well as with the initiation factor IF–2 (Yoshida et al. 1972; Milon et al. 2006;

Mitkevich et al. 2010). The inhibition of EF–Tu, EF–G or IF–2 functions might be involved in the control of translation fidelity during protein synthesis. In fact, ppGpp would slow down the accuracy–determining step of the reaction, acting specifically on the GTPase reactions catalysed by both elongation and initiation factors. However, a different mechanism has also been proposed in which the EF–Tu•ppGpp complex, upon its interaction with ribosome, can reduce the rate of peptide bond formation and improves proofreading by increasing the proportion of near–cognate aa–tRNAs rejected by ribosome (Rojas et al. 1984; Dix et al. 1986). In Archaea, very little is known on SC and in those so far studied there is a lack of SC with the exception of the Euryarcheota *Haloferax volcanii* showing a bacterial–like SC (Cimmino et al. 1993), and *Halococcus morrhuae*, showing a SC resembling that of eukarya (Cellini et al. 2004). In Crenarchaeota, the genus *Sulfolobus* appears to contain species that are stringent as in bacteria, but operated in the absence of magic spots; therefore, the absence of (p)ppGpp production has been proposed as an additional criteria to differentiate between Archaea and Bacteria (Cellini et al. 2004).

1.4 Scientific hypothesis and aim of the work

The aim of this experimental work has been the study of the interaction between eubacterial ligands (tetracycline, pulvomycin and ppGpp) and an archaeal elongation factor 1α, used as model to highlight the effects of these interactors on the molecular and functional properties of the enzyme. In particular, for this research we used the elongation factor 1α isolated from the thermoacidofilic archaebacterium *Sulfolobus solfataricus* (SsEF-1α) (Figure 4), endowed with a great thermophilicity and resistance to heat denaturation (Masullo et al. 1991; Granata et al 2006, 2008). In the laboratory where I developed my research activity, the molecular, functional and structural properties of SsEF–1α have been studied in detail (Masullo et al. 1991, 2004; Vitagliano et al. 2001, 2004; Granata et al. 2006, 2008), as well as those of two its engineered forms, constituted respectively by G–domain and GM–domains (Masullo et al. 1997). These studies showed a structural similarity

between SsEF–1α and eubacterial elongation factors and a functional similarity with eukaryal ones (Masullo et al. 1997). Moreover, regarding the interaction between archaeal protein synthesis elongation factors and eubacterial antibiotics, for kirromycin and

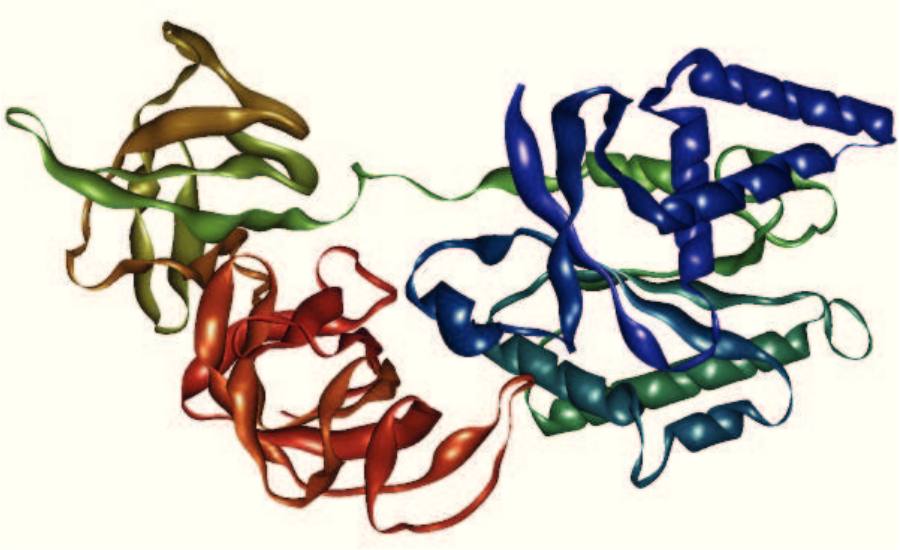

Figure 4. Three dimensional structure of SsEF–1α. *This structure has been obtained using iMol (PDB code 1JNY)*

GE2270A a functional interaction have already been reported (Masullo et al 2002, 2002; Cantiello et al. 2004). In particular, kirromycin is able to enhance the intrinsic GTPase activity of some SsEF–1α mutants, but not that of the wild–type enzyme (Masullo et al. 2002, 2002; Cantiello et al. 2004); vice versa, GE2270A was found to increase the GDP⁄GTP exchange rate and to reduce the intrinsic GTPase of the archaeal elongation factor (Masullo et al. 2004). All these considerations prompted us an investigation about the interaction between SsEF–1α and other eubacterial antibiotics, such as tetracycline and pulvomycin.

Furthermore, in a previous structural characterisation of SsEF–1α, a ppGpp molecule has been found bound to the active site of a

recombinant elongation factor (Vitagliano et al. 2004). This finding was ascribed to the ppGpp produced in *E. coli* (Cashel et al. 1996) in the heterologous expression system (Ianniciello et al. 1996). Therefore, the effects produced by ppGpp on the molecular and functional properties of SsEF–1α, have also been studied.

2. Materials and Methods

2.1 Chemicals, buffers and enzymes

Labelled compounds and chemicals were as already reported (Masullo et al. 1997). Tetracycline (Sigma–Aldrich, Milan, Italy) was prepared as 50 mM stock solution in water and stored at –80 °C. The antibiotic concentration was assessed by absorbance reading at 360 nm, using a molar extinction coefficient of 15800 M^{-1}•cm^{-1}. Pulvomycin powder was a kind gift of Prof. Andrea Parmeggiani (Ecole Polytechnique, Palaiseau, France) and it was used as 28 mM stock solution in absolute ethanol and stored at –80 °C. The spectral quality of the antibiotic was checked as reported and its concentration was determined using a molar absorbance coefficient of 74582 M^{-1}•cm^{-1} at 320 nm in methanol (Smith et al. 1985). ppGpp was purchased by TriLink BioTechnologies (USA).

The following buffers were used: buffer A: 20 mM Tris•HCl, pH 7.8, 50 mM KCl, 10 mM $MgCl_2$; buffer B: 20 mM Tris•HCl, pH 7.8, 10 mM $MgCl_2$, 1 mM DTT, 3.6 M NaCl.

SsEF–1α and its engineered forms were produced and purified as already reported (Masullo et al. 1997; Ianniciello et al. 1996; Arcari et al. 1999). SsRibosome, SstRNA, SsEF–2 and SsFRS were purified from *S. solfataricus* cell–free extract, as reported (Raimo et al. 1992; Lombardo et al. 2002).

2.2 SsEF–1α assays

The poly(U)–directed poly(Phe) synthesis was performed as already described (Masullo et al. 2002). The preparation of [^{3}H]Val–$EctRNA^{Val}$, the formation of the ternary complex between the elongation factor, aa–tRNA and GDP or GTP or ppGpp, and the protection against the spontaneous deacylation of [^{3}H]Val–$EctRNA^{Val}$ were carried out as already reported (Raimo et al. 2000).

The ability of SsEF–1α to bind [^{3}H]GDP or to exchange the radiolabelled nucleotide for GDP, GTP or ppGpp was assayed by nitrocellulose filtration as described (Masullo et al. 1997). The apparent equilibrium dissociation constant (K'_d) of the binary complex formed between SsEF–1α and [^{3}H]GDP was determined by Scatchard

plots. K'_d for GTP was derived from competitive binding experiments.
The intrinsic NaCl–dependent GTPase activity ($GTPase^{Na}$) was measured in the presence of 3.6 M NaCl as reported (Masullo et al. 1994). The k_{cat} of $GTPase^{Na}$, the K_m for [γ–^{32}P]GTP, and the inhibition constants were determined by Lineweaver–Burk plots as previously described (Masullo et al. 1994).
The effect of pulvomycin on the thermophilicity of the $GTPase^{Na}$ was evaluated by determining the initial velocity of [γ–^{32}P]GTP breakdown in the 45–75 °C interval; the data were then treated with the Arrhenius equation

$$\ln v = \ln A + E_a/R \bullet 1/T$$

in which v is the rate of GTP hydrolysis (s^{-1}) at a given temperature T (K), A is the Arrhenius constant (s^{-1}), E_a is the energy of activation ($J \bullet mol^{-1}$), and R is the gas constant (8.314 $J \bullet mol^{-1} \bullet K^{-1}$). By plotting ln v against 1/T, the E_a can be derived from the slope of the straightline obtained. The energetic parameters of activation ΔH^*, ΔS^* and ΔG^* were calculated at a given temperature by the equations

$$\Delta H^* = E_a - (RT)$$

$$\Delta S^* = R \bullet \ln(h \bullet N_A \bullet A/R \bullet T \bullet e)$$

$$\Delta G^* = \Delta H - T\Delta S$$

where h is the Plank constant ($6.624 \bullet 10^{-34}$ J•s), N_A is the Avogadro's number ($6.023 \bullet 10^{23}$ molecules/mol), and e is the base of the natural logarithm (2.718).
The effect of tetracycline on the heat inactivation of SsEF–1α was evaluated by incubating 4 µM protein in buffer A at selected temperatures in the 87–96 °C interval. After the heat treatment, 40–µL aliquots were cooled on ice for 30 min and then analysed for their residual [^{3}H]GDP–binding ability or $GTPase^{Na}$ as reported above. The data were analysed through a first–order kinetic equation, and the rate constants of the heat inactivation process obtained (k_{in}) were used to draw an Arrhenius plot, from which the energetic parameters of

activation can be derived as reported above.

The effect of pulvomycin on the chemical denaturation of SsEF–1α was evaluated by exposing the protein to guanidine hydrochloride (GuHCl, Sigma Aldrich) as already reported (Granata et al. 2006), and determining the residual $GTPase^{Na}$. To this aim, a stock solution of GuHCl (6.6 M) was prepared and mixed in different amounts with protein solutions to give a constant final value of the protein concentration (10 μM) and a variable concentration of GuHCl (0–6 M). Each sample was incubated overnight at room temperature and GuHCl–induced denaturation was evaluated by assaying the residual GTPase activity bringing each sample to a 0.6 M constant value of GuHCl concentration. Under these conditions, the $GTPase^{Na}$ of SsEF–1α was not affected at all.

2.3 Fluorescence measurements

Fluorescence spectra were recorded on a computer assisted Cary Eclipse spectrofluorimeter (Varian Inc., Mulgrave, Australia), equipped with an electronic temperature controller, at a scan rate of 60 nm⁄min using an excitation wavelength of 280 nm; excitation and emission slits were set to 10 nm. Blanks run in the absence of the protein were subtracted. Spectra recorded in the presence of tetracycline were obtained after further additions of a concentrated solution of the antibiotic, were corrected for the dilution and for the inner filter effect because of the absorbance of the antibiotic, using a molar absorption coefficient at 280 nm of 17491 $M^{-1} \cdot cm^{-1}$ determined from a linear Beer–Lambert plot of absorbance versus tetracycline concentration.

Spectra recorded in the presence of pulvomycin were obtained after further additions of a concentrated solution of the antibiotic and a correction for the dilution was applied. The analysis of the binding affinity was carried out as already reported (Johansson et al. 1998, 2000) considering that the quenched fluorescence (Q) at respective maximum is a function of the maximum possible quenching (Q_{max}) at an infinite ligand concentration. In particular, the binding affinity of the protein–pulvomycin complex (K_d) was calculated from the equation

$$Q = (Q_{max} \bullet [\text{Pulvomycin}]) / (K_d + [\text{Pulvomycin}])$$

through a double reciprocal plot.

Heat denaturation of SsEF–1α was studied by fluorescence melting curve. The excitation and emission wavelengths were 280 and 311 nm, respectively, and the excitation and emission slits were both set to 10 nm. Blanks run in the absence of the protein were carried out in parallel and subtracted. The fluorescence intensity was corrected for temperature quenching (Underfriend 1969), normalised between 0 and 100 % and plotted versus the temperature.

3. Results

3.1 Interaction between SsEF–1α and eubacterial antibiotics

3.1.1 Effect of tetracycline on the functional properties of SsEF–1α

The interaction between SsEF–1α and tetracycline was studied in terms of the effect produced by the antibiotic on the functional properties of the elongation factor. The first analysis regarded the ability of tetracycline to inhibit protein synthesis using a reconstituted system containing purified macromolecular components from *S. solfataricus*. The effect of tetracycline on the kinetics of [^{3}H]Phe polymerisation at 75°C, reported in Figure 5A, indicated that at 2 mM antibiotic, a reduction of three–fold of the rate was observed.

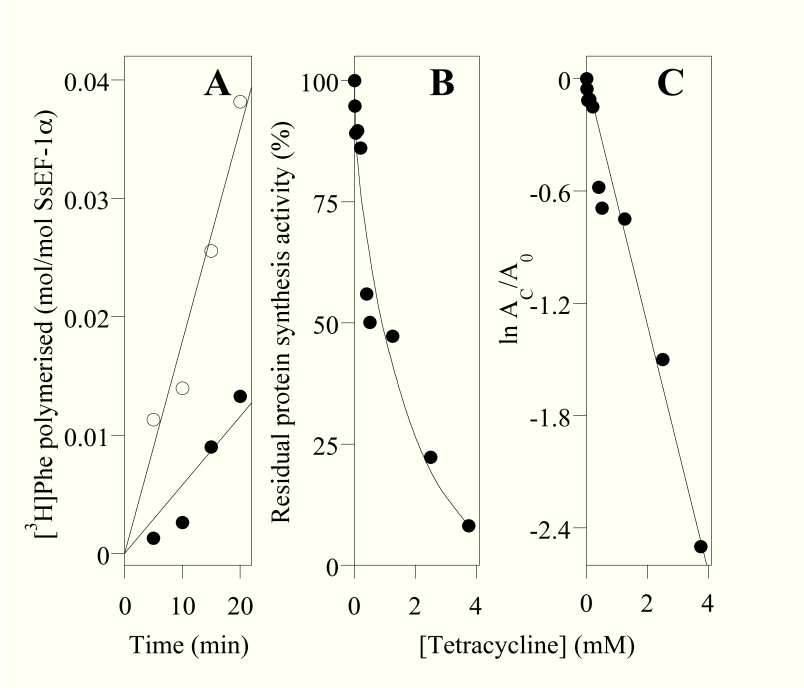

Figure 5. Effect of tetracycline on the poly(U)–directed poly(Phe) synthesis catalysed by SsEF–1α. *(A) 250 µL of the reaction mixture contained 25 mM Tris•HCl pH 7.5, 19 mM magnesium acetate, 10 mM NH_4Cl, 10 mM dithiothreitol, 2.4 mM ATP, 1.6 mM GTP, 0.16 mg/mL poly(U), 3 mM spermine, 0.25 µM Ssribosome, 80 µg/mL SstRNA, 0.1 µM SsEF–2, 2.0 µM*

[^{3}H]Phe (specific activity 1268 cpm/pmol). The reaction was started adding 0.5 μM final concentration of SsEF–1α in the absence (empty circles) or presence (filled circles) of 2 mM tetracycline and carried out at 75°C. At the times indicated, 50–μL aliquots were withdrawn, chilled on ice and then analysed for the amount of [^{3}H]Phe incorporated. (B) Effect of different concentrations of tetracycline. At each antibiotic concentration, the assay was carried out as reported in (A). (C) The data reported in (B) were treated as a first–order behaviour. A_0 represents the activity measured in the absence of the antibiotic, whereas A_C is the activity at the concentration C of tetracycline.

The effect of different concentration of tetracycline on poly(Phe) incorporation is reported in Figure 5B. The concentration of antibiotic leading to 50% inhibition was obtained from a first–order analysis of the data (Figure 5C). The value derived (1.1 mM) was identical to that previously measured using a cell–free reconstituted system (Cammarano et al. 1985), even though it was at least one order of magnitude higher than that required for the eubacterial process. To identify the partial reaction catalysed by SsEF–1α, possibly affected by this antibiotic, the ability of SsEF–1α to interact with aa–tRNA in the absence or in the presence of tetracycline was studied. As shown in Figure 6, the amount of ternary complex formed between heterologous Val–EctRNA^{Val}, SsEF–1α and nucleotides was almost identical either in the absence or in the presence of tetracycline, as revealed by the ability of the elongation factor to protect [^{3}H]Val–EctRNA^{Val} against spontaneous deacylation. In addition, the antibiotic did not affect the affinity for the nucleotide in ternary complex formation, still remaining lower for GDP (Figure 6B) than for GTP (Figure 6A).

3.1.2 Effect of pulvomycin on the functional properties of SsEF–1α

The effects of pulvomycin on the functional properties of the elongation factor was also studied. The ability of pulvomycin to inhibit protein synthesis was investigated; the antibiotic, at 200 μM concentration, reduced the poly(U)–directed poly(Phe) synthesis rate of about 4–fold (Figure 7A). The inhibition data obtained at different pulvomycin concentrations (Figure 7B), treated through a first–order

behaviour (Figure 7C), allowed the calculation of the antibiotic concentration leading to 50% inhibition (173 μM). The effect of pulvomycin was also studied on the partial reactions catalysed by SsEF–1α. Concerning ternary complex, the antibiotic was able to decrease the affinity of the elongation factor toward aa–tRNA only in the presence of GTP (Figure 8A), rendering it similar to that measured in the presence of GDP (Figure 8B).

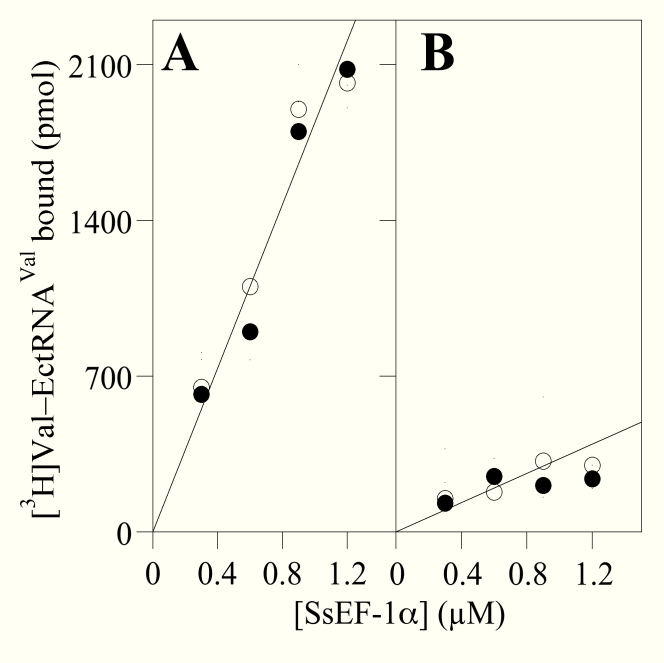

Figure 6. Effect of tetracycline on the formation of the ternary complex between SsEF–1α, [^{3}H]ValEc–tRNA^{Val} and GDP or GTP*. The mixture (30 μL) contained 25 mM Tris•HCl, pH 7.8, 10 mM NH_4Cl, 10 mM DTT, 20 mM magnesium acetate and 4.6 pmol of [^{3}H]ValEc–tRNA^{Val} (specific radioactivity 1521 cpm/pmol) and was incubated for 1h at 0°C to allow ternary complex formation in the presence of the indicated amount of SsEF-1α•GTP (A) or SsEF–1α•GDP (B), in the absence (empty circles) or in the presence (filled circles) of 50 μM tetracycline. The deacylation reaction was carried out for 1h at 50°C, and the residual [^{3}H]ValEc–tRNA^{Val} was determined as cold trichloroacetic acid insoluble material.*

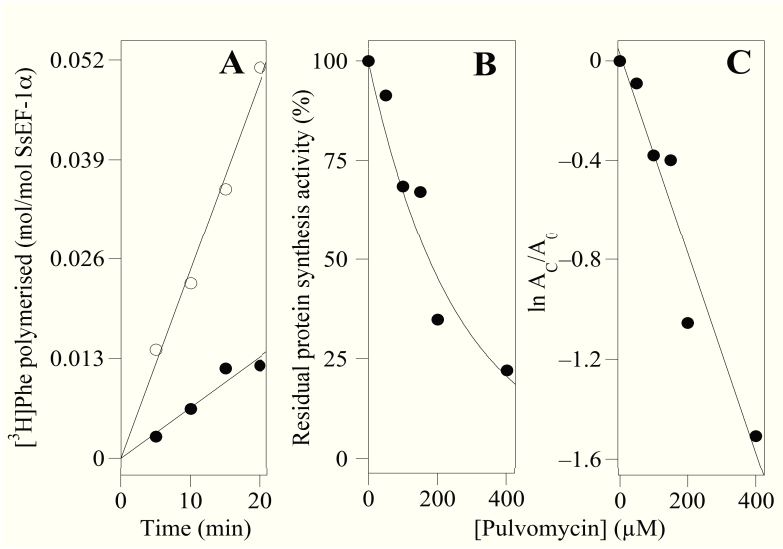

Figure 7. Effect of pulvomycin on the poly(U)–directed poly(Phe) synthesis catalysed by SsEF–1α. *(A) Kinetics of the [^{3}H]Phe incorporation in the absence (empty circles) or in the presence (filled circles) of 200 μM pulvomycin at 75°C. The reaction mixture (250 μl) contained 0.5 μM SsEF–1α, 0.25 mM Ssribosome, 80 μg/ml SstRNA, 0.1 μM SsEF–2, 2.0 μM [^{3}H]Phe (specific activity 1514 cpm/pmol), 25 mM Tris•HCl, pH 7.5, 19 mM magnesium acetate, 10 mM NH_4Cl, 10 mM dithiothreitol, 2.4 mM ATP, 1.6 mM GTP, 0.16 mg/ml poly(U) and 3 mM spermine. At the times indicated, 50 μl aliquots were withdrawn and analysed for the amount of [^{3}H]Phe incorporated. (B) Effect of different concentrations of pulvomycin. (C) The data reported in (B) were treated as a first–order behaviour. A_0 represent the activity measured in the absence of pulvomycin, whereas A_C is the activity at the concentration C of the antibiotic.*

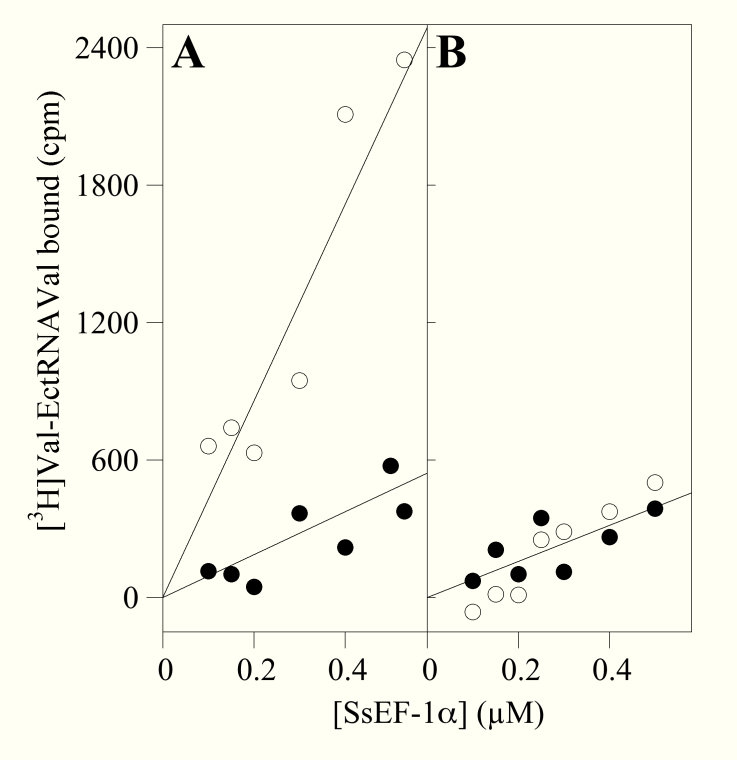

Figure 8. Effect of pulvomycin on the formation of the ternary complex between SsEF–1α, [^{3}H]ValEc–tRNA^{Val} and GTP or GDP*. The reaction mixture (30 µl) prepared in 25 mM Tris•HCl, pH 7.8 buffer, 10 mM NH_4Cl, 10 mM DTT, and 20 mM magnesium acetate, contained 4.6 pmol of [^{3}H]ValEc–tRNA^{Val} (specific radioactivity 1185 cpm/pmol). To allow ternary complex formation the mixture was incubated for 1h at 0°C in the presence of the indicated amount of SsEF-1α•GTP (A) or SsEF-1α•GDP (B), in the absence (empty circles) or in the presence (filled circles) of 20 µM pulvomycin. The deacylation reaction was then carried out for 1h at 50°C and the residual [^{3}H]ValEc–tRNA^{Val} was determined as cold trichloroacetic acid insoluble material.*

3.1.3 Effect of antibiotics on the interaction between SsEF–1α and guanosine nucleotides

The effect of the antibiotics on guanosine nucleotide exchange ability

of SsEF–1α was also investigated. As shown in Figure 9, the presence of tetracycline caused a 2.1–fold higher [^{3}H]GDP⁄GTP exchange rate on SsEF–1α (Figure 9A), whereas in the case of [^{3}H]GDP⁄GDP exchange, both rates resulted undistinguishable from each other (Figure 9B). The effect of the tetracycline on the GDP binding was also evaluated in terms of the equilibrium dissociation constant of the binary complex formed with the enzyme. The data reported in Table 1 indicated that the antibiotic slightly reduces the affinity for both guanosine nucleotides, and in the case of GDP, the reduced affinity measured in the presence of tetracycline can be ascribed to a selective reduction in the association rate constant.

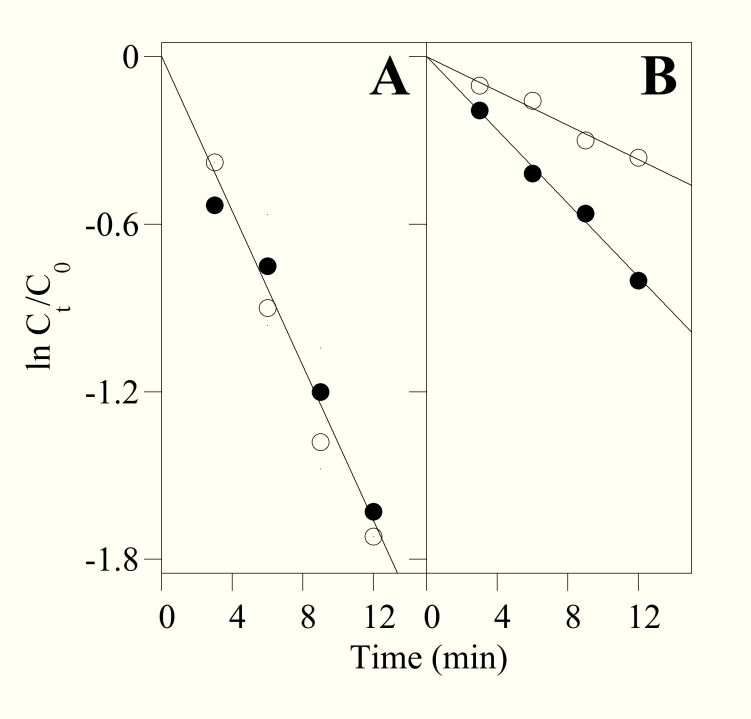

Figure 9: Effect of tetracycline on the nucleotide exchange rate catalysed by SsEF–1α. *The reaction mixture (300 µL) prepared in buffer A contained 0.5 µM SsEF–1α•[3H]GDP in the absence (empty circles) or in the presence (filled circles) of 50 µM tetracycline. The nucleotide exchange reaction was*

started at 60°C by adding 1 mM GDP (A) or GTP (B) final concentration. At the times indicated, the amount of the residual radiolabelled binary complex was determined on 30–µL aliquots by nitrocellulose filtration. The data were treated according to a first–order kinetic.

In presence of pulvomycin, instead, the guanosine nucleotides exchange rate on the archaeal elongation factor was 1.5–fold faster for both GDP (Figure 10A) and GTP (Figure 10B). In addition, in the presence of the antibiotic, the guanosine nucleotides apparent equilibrium dissociation constants for GDP and GTP were slightly lower (Table 1) and the effect produced was more evident in the case of GTP. Regarding the slight increased affinity for GDP, the effect of pulvomycin can be ascribed to a higher increase of the association constant with the respect to the dissociation one.

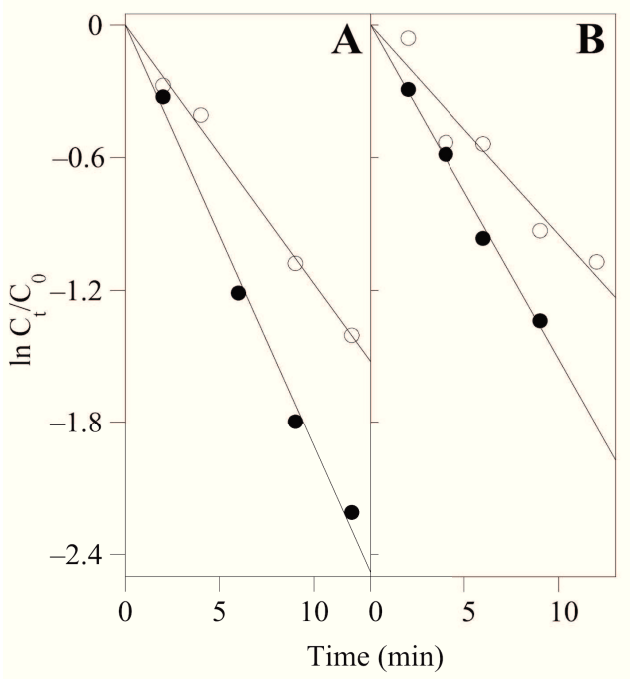

Figure 10: Effect of pulvomycin on the nucleotide exchange rate catalysed by SsEF–1α. *The reaction mixture (250 µl) prepared in buffer A contained*

0.5 μM SsEF–1α•[^{3}H]GDP in the absence (empty circles) or in the presence (filled circles) of 20 μM pulvomycin. The nucleotide exchange reaction was started at 60°C by adding 1 mM GDP (A) or GTP (B) final concentration. At the times indicated, the amount of the residual radiolabelled binary complex was determined on 50–μl aliquots by nitrocellulose filtration. The data were treated according to a first–order kinetic.

Table 1. Effect of tetracycline and pulvomycin on the affinity of SsEF-1α for guanosine nucleotides at 60°C. *The K_d' and k_{-1} values represent the average of 3–4 different determinations. k_{+1} was calculated as k_{-1}/K_d'.*

SsEF-1α	K'd		k-1	k+1
	GDP (μM)	GTP (μM^{-1})	GDP (min^{-1})	GDP (μM^{-1}•min^{-1})
w/o antibiotic	0.33 ± 0.09	5.35 ± 1.40	0.13 ± 0.03	0.40
+ tetracycline	0.50 ± 0.10	9.00 ± 2.00	0.12 ± 0.04	0.24
+ pulvomycin	0.30 ± 0.11	2.60 ± 2.00	0.19 ± 0.01	0.63

To better evaluate the effect of the antibiotics on the interaction between SsEF–1α and guanosine nucleotides, we have verified whether tetracycline affected the intrinsic GTPase of the elongation factor and its truncated forms triggered by high concentration of NaCl (Masullo et al. 1994, 1997). The results shown in Figure 11 indicate that tetracycline inhibited the GTPase^{Na} of SsEF–1α but not that elicited by two its engineered forms, lacking the C–terminal (Ss(GM)EF–1α) or both the C– and the M–domains (Ss(G)EF–1α) (Masullo et al. 1997). The inhibition level observed for SsEF–1α depended on the antibiotic concentration (Figure 11A), even though a complete inhibition was not reached even in the presence of 120 μM antibiotic, a concentration corresponding to about 200–fold molar excess over that of SsEF–1α. However, the concentration of tetracycline for half inhibition of SsEF–1α GTPase can be calculated as about 322 μM (Figure 11B). The effect of the antibiotic on the kinetic parameters of the reaction (Table 2) indicated that tetracycline exerted a mixed inhibition; in fact, besides a reduced maximum

hydrolytic rate, also a slight reduced affinity for the nucleotide was observed.

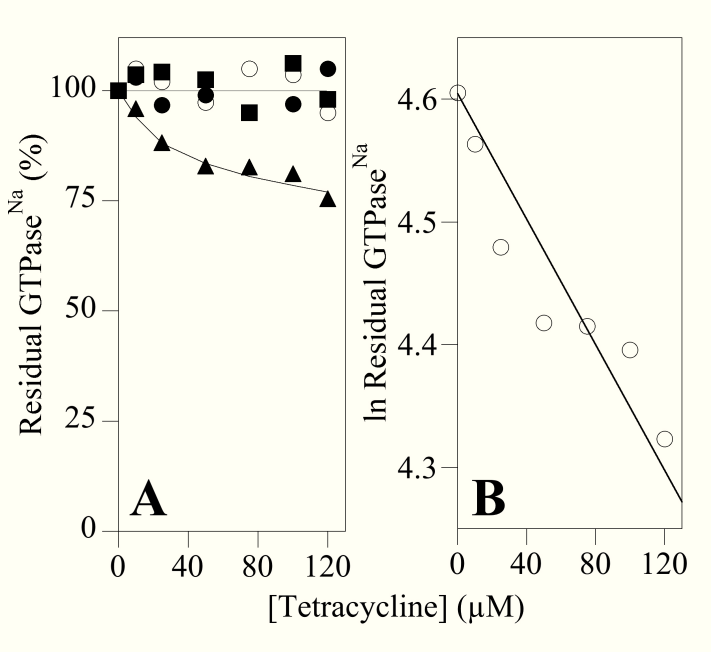

Figure 11. Effect of tetracycline on the intrinsic GTPase of SsEF–1α and its engineered forms. *(A) The GTPase^{Na} activity of SsEF–1α (filled triangles), Ss(GM)EF–1α (empty circles), Ss(G)EF–1α (filled circles) was determined in the presence of the indicated tetracycline concentration. The kinetic parameters were determined in buffer B using 0.5 μM SsEF–1α and 1.5–30 μM [γ–^{32}P]GTP (specific radioactivity 8582–551 cpm/pmol). The reaction was followed kinetically at 60°C and the amount of $^{32}P_i$ released determined on 50–μL aliquots. The data were referred to the value measured in the absence of the antibiotic. (B) The data referring to SsEF–1α were linearised using a first–order behaviour equation.*

Regarding the effect of pulvomycin on GTPase activity, we observed an opposite behaviour. In fact, as reported in Figure 12A, increasing antibiotic concentration increased the rate of the intrinsic GTPase

Table 2. Effect of tetracycline and pulvomycin on kinetic parameters of the intrinsic GTPase catalysed by SsEF–1α.

	K_m	k_{cat}	k_{cat}/K_m
SsEF–1α	(μM)	(min^{-1})	(min^{-1}•μM^{-1})
w/o antibiotic	3.4 ± 1.2	0.44 ± 0.12	0.13
+ tetracycline	4.5 ± 1.3	0.36 ± 0.14	0.08
+ pulvomycin	2.6 ± 1.0	1.04 ± 0.20	0.40

catalysed by SsEF–1α, reaching its maximum stimulation effect at 30 μM. This stimulation was not observed for the truncated forms. The data reported for SsEF–1α up to a concentration of pulvomycin of 30 μM followed a saturation behaviour and, through a double reciprocal plot (Figure 12B), the concentration of pulvomycin required for 50% stimulation (5.4 μM) can be derived from the X–axis intercept. The effect of the antibiotic on the kinetic parameters of the $GTPase^{Na}$ was also studied. The data reported in Table 2 indicated that the increased catalytic efficiency, measured in the presence of 20 μM pulvomycin can be ascribed to an increased affinity for the substrate together with an higher hydrolytic rate. Furthermore, the $GTPase^{Na}$ was competitively inhibited by GDP and GTP also in the presence of pulvomycin (Table 2). In particular, the inhibition power, evaluated through the comparison of the inhibition constants by GDP or GppNHp (a slowly hydrolysable GTP analog), was reduced by 4–fold for both nucleotides, thus confirming the observed increased affinity for the guanosine nucleotides in the presence of the antibiotic (not shown). The effect of pulvomycin on the thermophilicity of $GTPase^{Na}$ was also analysed in the 45–75 °C temperature interval and the antibiotic exerted its stimulatory effect at all the tested temperatures (Figure 13A). The analysis of data through the Arrhenius equation, gave a straight–line also in the presence of the antibiotic, but with a different slope with respect to that obtained in its absence (Figure 13B). From these data the energetic parameters of activation of $GTPase^{Na}$ in absence or in presence of pulvomycin were calculated and reported in Table 3. The antibiotic reduced the energy of activation of the hydrolytic reaction without changing the free energy

of activation. However, a differential effect on the other thermodynamic parameters of activation was observed; in particular, pulvomycin produced a favourable variation of enthalpy of activation that is accompanied by an unfavourable variation of the entropy.

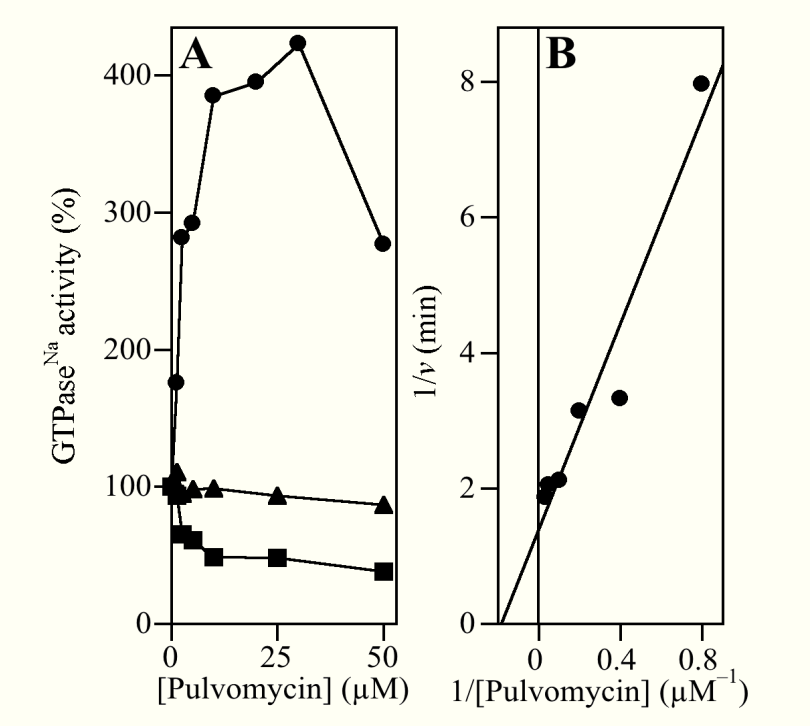

Figure 12. Effect of pulvomycin on the intrinsic GTPase of SsEF–1α and its engineered forms. *(A) The GTPase^{Na} of SsEF–1α (filled circles), Ss(GM)EF–1α (filled squares) and Ss(G)EF–1α (filled triangles), was determined in the presence of the indicated pulvomycin concentration. The reaction mixture contained 0.5 μM SsEF–1α and 25 μM [γ–^{32}P]GTP (specific activity 400–900 cpm/pmol) in 200 μL of buffer B. The reaction was followed kinetically at 50°C, and the amount of $^{32}P_i$ released was determined on 40–μl aliquots. The data were reported as a percentage of the activity measured in the absence of the antibiotic. (B) The data referring to SsEF–1α up to 30 μM pulvomycin were treated by the Lineweaver–Burk equation after the subtraction of the GTPase^{Na} activity of SsEF–1α measured in the absence of pulvomycin (0.166 min^{-1}).*

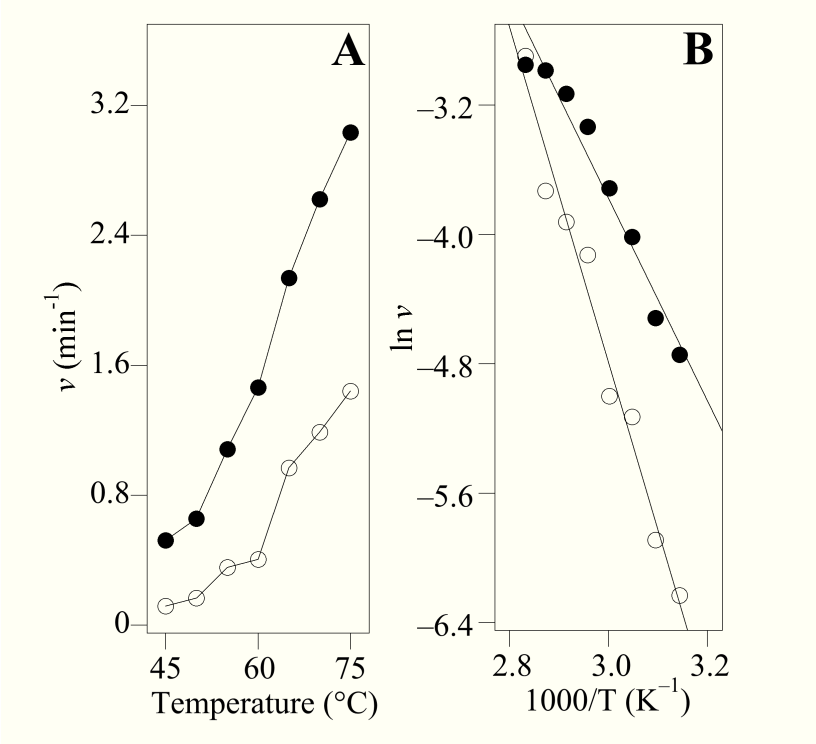

Figure 13. Effect of pulvomycin on the thermophilicity of the GTPase^{Na} catalysed by SsEF–1α. *(A) The rate of GTP breakdown was determined as reported in the Materials and Methods section at the indicated temperature, in the absence (empty circles) or in the presence (filled circles) of 20 μM pulvomycin. At each temperature, the times used for the determination were selected in order to give a linear relationship between the time and the amount of [γ–^{32}P]GTP hydrolysed. (B) Arrhenius analysis of the data reported in (A).*

Table 3. Effect of pulvomycin on the energetic parameters of activation of the GTPase^{Na} catalysed by SsEF–1α. *ΔH, ΔS* and ΔG* were calculated at 60°C.*

	E_a	Δ*H**	Δ*S**	Δ*G**
SsEF–1α	(kJ·mol^{-1})	(kJ·mol^{-1})	(J·mol·K^{-1})	(kJ·mol)
– pulvomycin	86	83	– 36	95
+ pulvomycin	53	50	– 127	92

3.1.4 Effect of tetracycline on the heat stability of SsEF–1α

The interaction between tetracycline and SsEF–1α was also investigated through the effect exerted by the antibiotic on the heat inactivation kinetics of the $GTPase^{Na}$ catalysed by SsEF–1α in the 87–96 °C interval. As shown in Figure 14A, the antibiotic did not affect the first–order behaviour of the heat inactivation kinetic at all tested temperature. The analysis according to the Arrhenius equation of the kinetic constants of the heat inactivation process (Figure 14B) allowed the calculation of the energetic parameters of the activation. The data reported in Table 4 indicated that tetracycline increased the rate of the heat inactivation through a reduction of the energy of activation without affecting the free energy associated with the process.

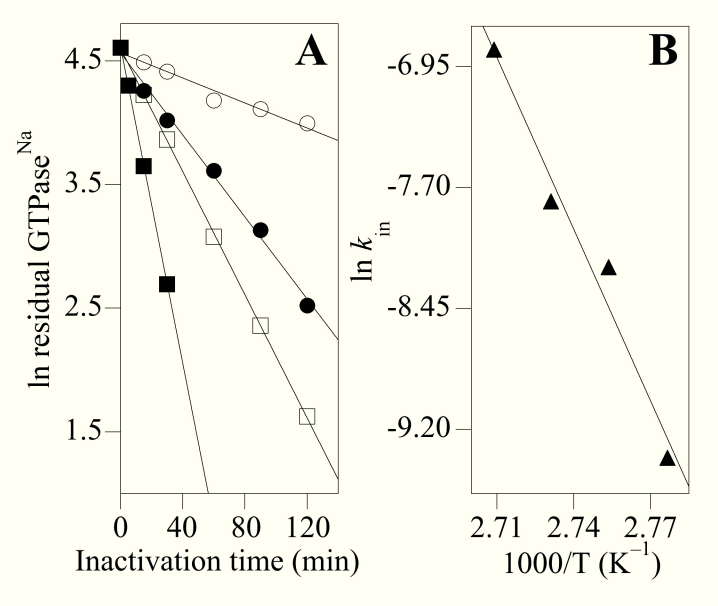

Figure 14. Effect of tetracycline on the heat inactivation kinetics of SsEF–1α. *(A) 4 μM SsEF–1α was incubated at 87 (empty circles), 90 (filled circles), 93 (empty squares) or 96°C (filled squares) in the presence of 16 μM tetracycline, and at the indicated time intervals, aliquots were withdrawn and placed at 0°C. The residual GTPase activity was determined as reported in Materials and Methods and referred to an untreated sample kept at 0°C*

for all the experiment of the heat treatment. The data were treated as a first–order kinetic and reported as the natural logarithm of the residual activity. (B) Arrhenius analysis of the heat inactivation kinetic rate constants (k_{in}) derived from the slope of the equations reported in (A).

Table 4. Effect of tetracycline on the energetic parameters of activation of the inactivation process of the GTPase^{Na} catalysed by SsEF–1α. *ΔH, ΔS* and ΔG* were calculated at 87°C.*

	E_a	ΔH*	ΔS*	ΔG*
SsEF–1α	(kJ·mol^{-1})	(kJ·mol^{-1})	(J·mol·K^{-1})	(kJ·mol)
– tetracycline	361	358	665	119
+ tetracycline	177	174	164	115

3.1.5 Effect of pulvomycin on chemical denaturation of SsEF–1α

The effect of antibiotic on the resistance of SsEF–1α against guanidine hydrochloride denaturation was verified by measuring its residual GTPase activity in the presence of guanidine hydrochloride at increasing concentrations, in the presence or in the absence of 20 μM pulvomycin (Figure 15). The concentration of denaturant agent to get 50% inactivation of the GTPase^{Na} was 3.0 M in the absence and 3.6 M in the presence of the antibiotic. These results indicated that pulvomycin exerted a protective action against chemical denaturation of SsEF–1α.

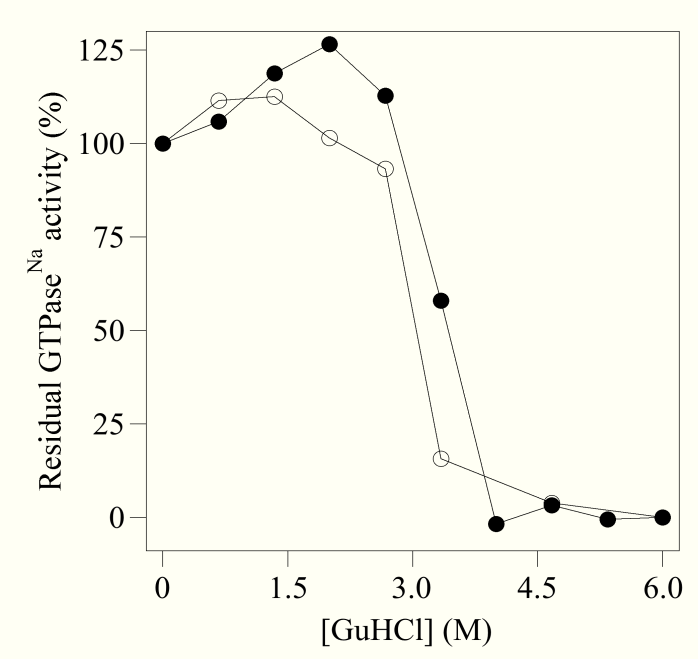

Figure 15. Effect of pulvomycin on the chemical denaturation of SsEF–1α. *The residual GTPase^{Na} was determined, after incubation of the samples at indicated guanidine hydrocloride concentration, as reported in Materials and methods, in the absence (empty circles) or in the presence (filled circles) of pulvomycin.*

3.1.6 Effect of tetracycline on the molecular properties of SsEF–1α

The primary structure of SsEF–1α contains 10 tyrosine residues (7 in the G domain, 1 in the M domain and 2 in the C domain), 18 of phenylalanine (11 in the G domain, 3 in the M domain and 4 in the C domain) and two tryptophans. In particular, the tryptophan 209 is contained in the catalytic domain of SsEF–1α (domain G) whereas the other (W334) is located in the C–terminal domain. The fluorescence spectrum of SsEF–1α is characterised by an emission maximum at 314 nm (Granata et al. 2006, 2008). The addition of different concentrations of tetracycline caused a gradual increase in the quantum yield (Figure 16A) and a slight shift of the emission maximum to higher wavelengths (about 318 nm). These results

indicate that tetracycline is able to bind SsEF–1α and, probably, in the regions containing aromatic residues. In order to better evaluate the binding of the antibiotic to SsEF–1α, the effect of different concentration of tetracycline was also assessed on the fluorescence spectrum of the truncated forms of the elongation factor.

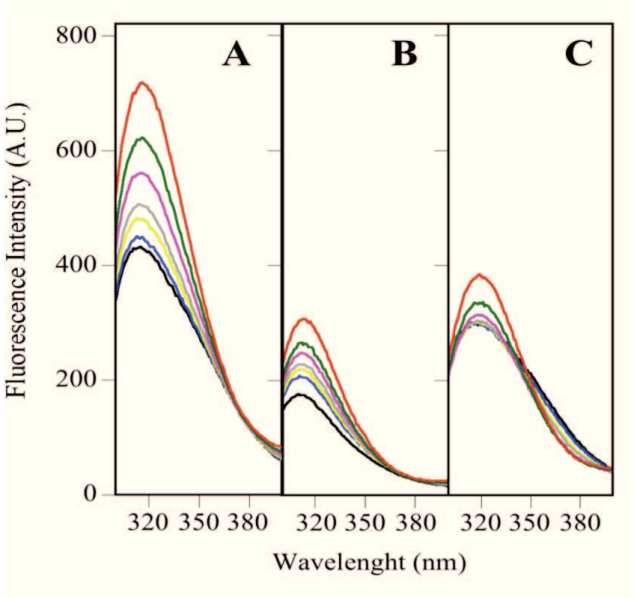

Figure 16. Effect of tetracycline on fluorescence spectra of SsEF–1α and its engineered forms. *Spectra were recorded in buffer A in the presence of 4 μM SsEF–1α (A), Ss(GM)EF–1α (B) or Ss(G)EF–1α (C) in the absence (black line) or in the presence of increasing concentration of tetracycline ranging between 4 (blue) and 38 μM (red) shown by different colors.*

As reported in Figure 16B, the removal of both M and C domains caused no variation of fluorescence maximum (314 nm); whereas a decrease in the quantum yield (about 50%) was observed, probably due to the presence of a lower number of aromatic residues. Regarding Ss(GM)EF–1α, the fluorescence spectrum was very similar to that of SsEF–1α, with an emission maximum at about 310 nm. Moreover, the

addition of the antibiotic, caused a gradual increase in the quantum yield and a slight shift of the maximum towards higher wavelengths (about 316 nm) (Figure 16C). These results indicated that the M domain was essential for the interaction between tetracycline and the elongation factor and that this interaction rendered the aromatic residues less exposed to the solvent.

For SsEF–1α and Ss(GM)EF–1α an increase in the quantum yield at increasing tetracycline concentration with a saturation behaviour was observed (Figure 17A). In fact, using a double reciprocal plot, in which the reciprocal of antibiotic concentration was reported on the abscissa axis and the reciprocal of fluorescence variation on the ordinate ones, straight lines were obtained (Figure 17B). From the intercept on the abscissa axis, a value of antibiotic concentration to reach half the maximum fluorescence can be calculated; in particular, the value derived for SsEF–1α (229 μM, F_{max} 490) was significantly higher than that found for Ss(GM)EF–1α (50 μM, F_{max} 222) but also for EcEF–Tu (57 μM, F_{max} 87) (not shown). These findings, besides indicating that eubacterial EcEF–Tu has an affinity for tetracycline higher than archaeal SsEF–1α, confirm that the M–domain of the elongation factor plays a role in the antibiotic binding.

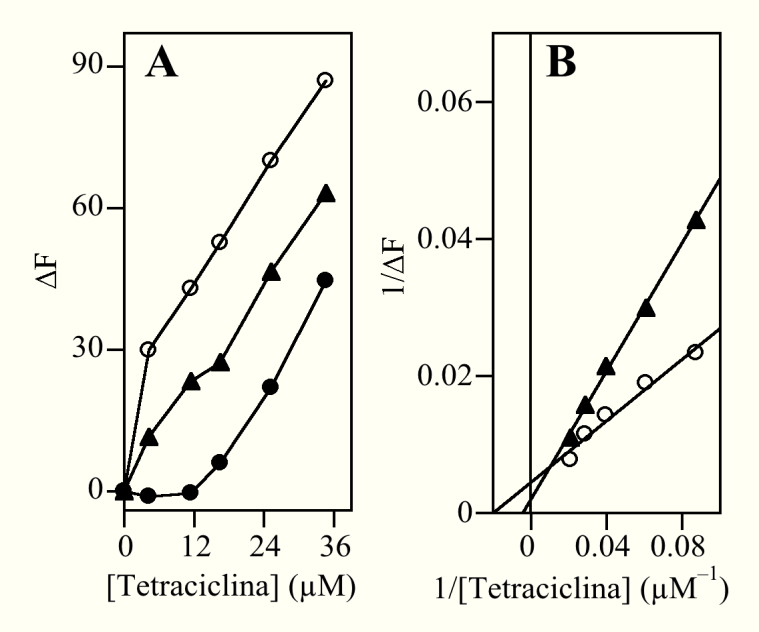

Figure 17. Effect of tetracycline on the fluorescence increase. *(A) The increase in the fluorescence intensity upon excitation at 280 nm caused by tetracycline was measured at 314 nm for SsEF–1α (filled triangles), 310 nm for Ss(GM)EF–1α (empty circles), 314 nm for Ss(G)EF–1α (filled circles). The concentration of each protein was 4.5 μM. (B) The data reported in (A) were treated as a double reciprocal plot, except that referred to Ss(G)EF–1α.*

3.1.7 Effect of pulvomycin on the molecular properties of SsEF–1α

The effect of pulvomycin on the molecular properties was also studied by fluorescence spectroscopy in the aromatic region of the fluorescence spectrum (λ_{exc} 280 nm) of SsEF–1α and its truncated forms. As shown in Figure 18, pulvomycin exerted for all proteins investigated, a strong fluorescence quenching at λ_{max} which was accompanied by the appearance of a new peak at 360 nm; this behaviour can be explained by a combination of both a static and a dynamic quenching (Lakowicz 2006), as well as by an inner filter effect (Parker et al. 1962) due to the absorption of pulvomycin at the emission region of spectrum (λ_{max} 320 nm); therefore, all these

findings impaired the correction for the inner filter effect (Lakowicz 2006). Moreover, the presence of a new peak at a higher wavelength could indicate a conformational modification induced by antibiotic involving specific aromatic residues, mainly tryptophans (Lakowicz 2006). However, a differential effect on quenching and new peak appearance was exerted by pulvomycin on the different proteins investigated. In particular, a prevalence on the quenching effect was observed in the case of SsEF–1α (Figure 18A), whereas a higher effect on the new peak appearance was observed in the case of the truncated forms of the elongation factor lacking the C–terminal (Figure 18B) or both the C– and M– domains (Figure 18C).

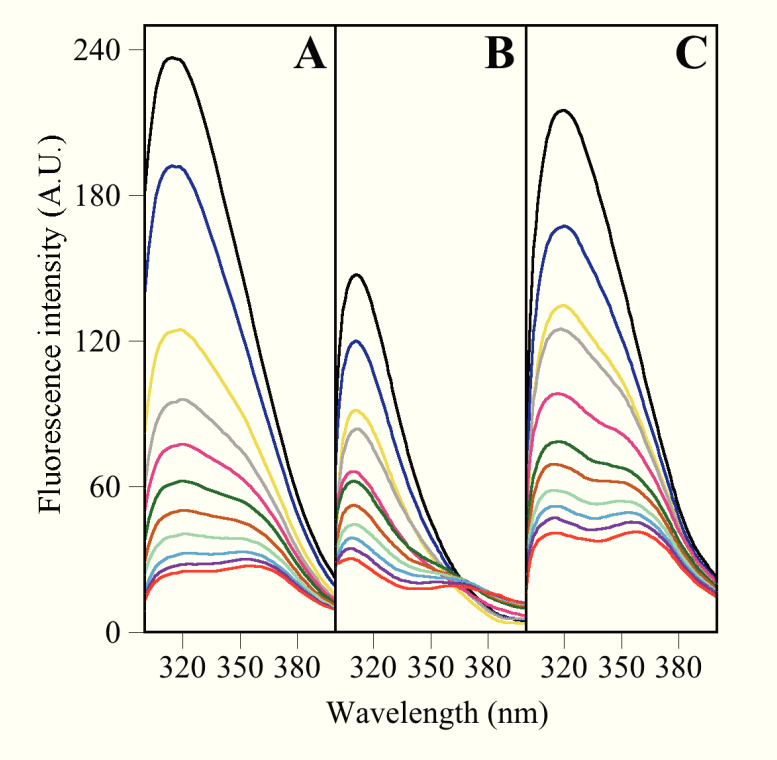

Figure 18. Effect of pulvomycin on the fluorescence spectra of SsEF–1α and its engineered forms. *Spectra were recorded in buffer A in the presence of 4 μM SsEF–1α (A), Ss(GM)EF–1α (B) or Ss(G)EF–1α (C) in the absence*

(black line) or in the presence of increasing concentration of pulvomycin ranging between 4 (blue) and 38 μM (red) shown by different colors.

The analysis of the quenching effect allowed an evaluation of the binding process (Johansson et al. 1998; Lakowicz 2006) through the variation of the quenched fluorescence (Q) against pulvomycin concentration (Figure 19A).

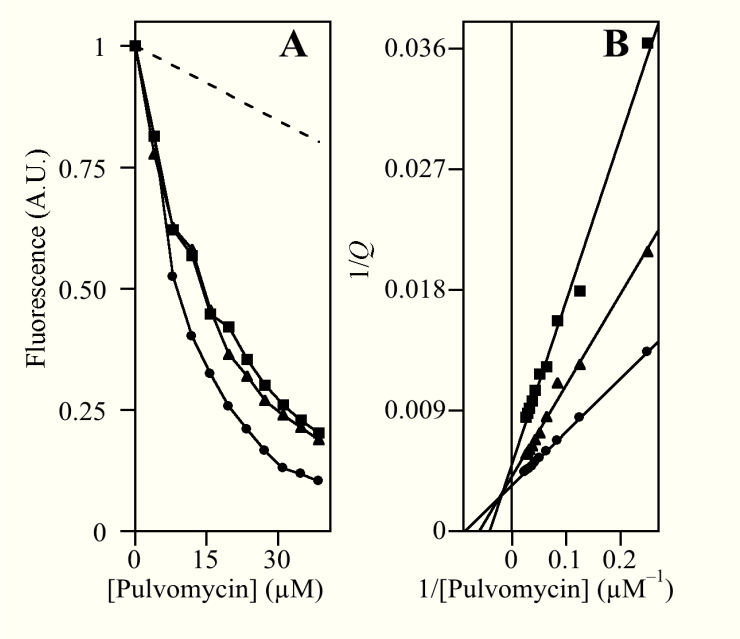

Figure 19. Effect of pulvomycin on the fluorescence quenching. *(A) The fluorescence at the respective maximum was plotted against increasing concentration of pulvomycin for SsEF–1α (filled circles, 314 nm), Ss(GM)EF–1α (filled squares, 311 nm) and Ss(G)EF–1α (filled triangles, 319 nm). The dashed line reports the effect on the fluorescence of bovine serum albumin (346 nm), used as a negative control for the interaction. (B) Double reciprocal plot of the data reported in (A).*

In fact, the linearity of the double reciprocal plot (Figure 19B), allowed the extrapolation of the binding constant from the abscissa axis intercept. The values obtained indicated that intact SsEF–1α showed an affinity similar to that reported for EcEF–Tu, being the K_d 11.6 μM and 13.9 μM, respectively. In the case of SsEF–1α, the lacking of C–terminal domain lowered the affinity of the elongation factor towards pulvomycin (K_d = 23.9 μM), whereas the truncation of both the C– and M–domains induced a less evident effect (K_d = 16.6 μM).

3.2 Interaction between SsEF–1α and ppGpp

3.2.1 Effect of ppGpp on the functional properties of SsEF–1α

The ability of ppGpp to affect archaeal poly(U)–directed poly(Phe) synthesis was assessed using a purified cell–free system reconstituted *in vitro* with the required components isolated from *Sulfolobus solfataricus* (De Vendittis et al. 2002). As reported in Figure 20A, ppGpp exerted only a weak inhibitory effect on the rate of poly[^{3}H]Phe synthesis catalysed by SsEE–1α; in fact, in the presence of 550 μM ppGpp, a 20% reduction of the phenylalanine incorporation rate was observed. From the analysis of the effect exerted by different concentrations of ppGpp on poly(Phe) incorporation (Figure 20B), the concentration leading to 50 % inhibition (IC_{50} = 2.1 mM) was calculated from a semi–logarithmic plot, as reported in Figure 20C. Moreover, we have also investigated the ability of SsEF–1α to form an heterologous ternary complex with aa–tRNA also in the presence of ppGpp, through the protection against spontaneous deacylation exerted by SsEF–1α on aa–tRNA; the results reported in Figure 21 showed that ppGpp induced an intermediate affinity of the elongation factor for aa–tRNA when compared with that induced by GDP or GTP.

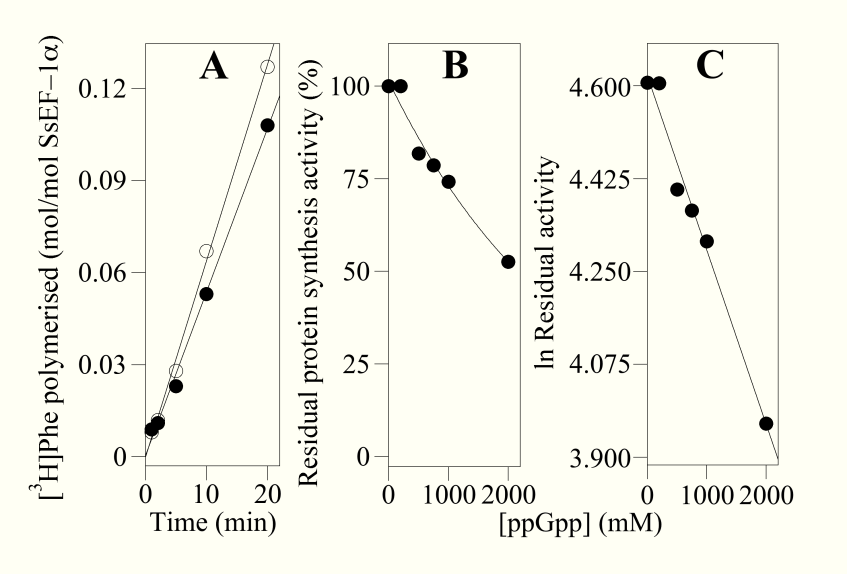

Figure 20. Effect of ppGpp on the poly(U)–directed poly(Phe) synthesis catalysed by SsEF–1α. *(A) 250 µl of the reaction mixture contained 25 mM Tris•HCl pH 7.5, 19 mM magnesium acetate, 10 mM NH_4Cl, 10 mM dithiothreitol, 2.4 mM ATP, 1.6 mM GTP, 0.16 mg/ml poly(U), 3 mM spermine, 0.25 µM Ssribosome, 80 µg/ml SstRNA, 0.1 µM SsEF–2, 2.0 µM [^{3}H]Phe (specific radioactivity 3094 cpm/pmol). The reaction was started by addition of 0.5 µM final concentration of SsEF–1α in the absence (empty circles) or in presence (filled circles) of 550 µM ppGpp and carried out at 75°C. At the times indicated, 50–µl aliquots were withdrawn, chilled on ice and then analysed for the amount of [^{3}H]Phe incorporated as hot trichloroacetic acid insoluble material. (B) The assay was carried out as reported in (A) at the indicated guanosine tetra–phosphate concentration. (C) The data reported in (B) were treated as a semi–logarithmic plot.*

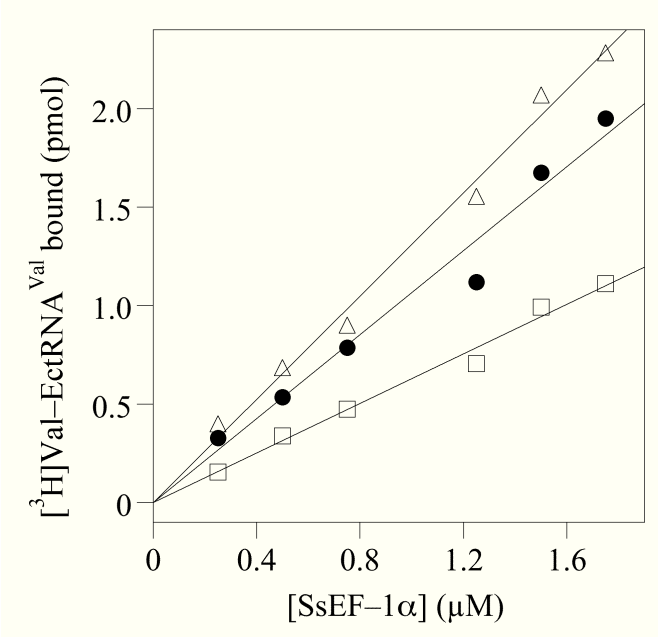

Figure 21. Formation of the ternary complex between SsEF–1α, [^{3}H]ValEc–tRNA^{Val} and ppGpp or GDP or GTP. *The mixture (30 μl) contained 25 mM Tris•HCl, pH 7.8, 10 mM NH_4Cl, 10 mM DTT, 20 mM magnesium acetate and 4.6 pmol of [^{3}H]ValEc–tRNA^{Val} (specific radioactivity 847 cpm/pmol) and was incubated for 1h at 0°C to allow ternary complex formation in the presence of the indicated amount of SsEF–1α•GDP (empty squares) or SsEF–1α•ppGpp (filled circles) or SsEF–1α•GTP (empty triangles). The deacylation reaction was carried out for 1h at 50°C and the residual [^{3}H]ValEc–tRNA^{Val} was determined as cold trichloroacetic acid insoluble material.*

3.2.2 Effect of ppGpp on the interaction between SsEF–1α and guanosine nucleotides

The affinity of ppGpp for the archaeal elongation factor was assessed by competitive binding experiments between ppGpp and [^{3}H]GDP. As reported in Figure 22A, the addition of increasing concentration of the nucleotide tetra–phosphate reduced the amount of the SsEF–1α•[^{3}H]GDP complex formation, thus indicating an inhibitory

competitive effect. From a semi–logarithmic plot of the data (Figure 22B), the concentration leading to 50 % inhibition (252 μM) was calculated.

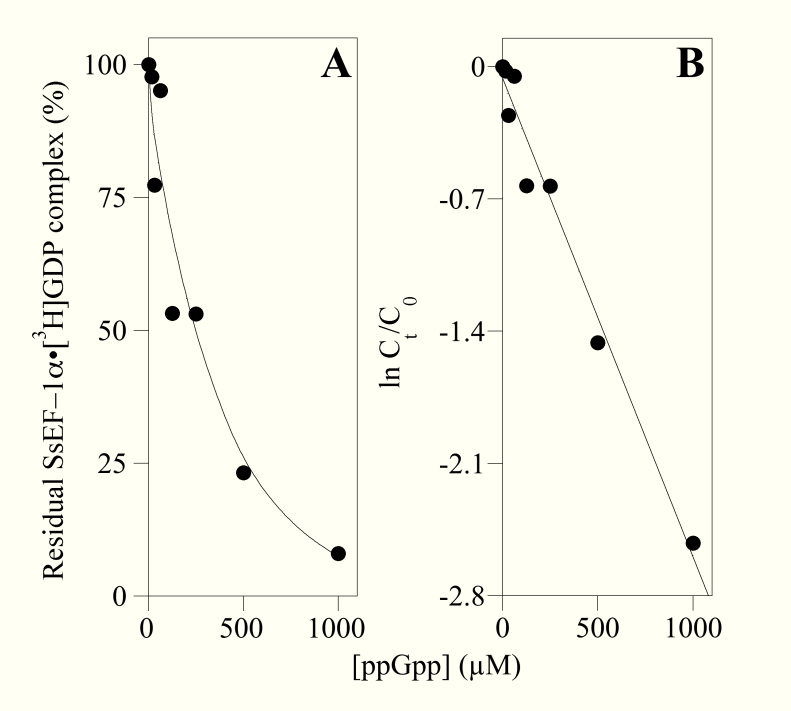

Figure 22. ppGpp competitively inhibited the [^{3}H]GDP binding to SsEF–1α. *(A) The reaction mixture (50 μl), containing 20 mM Tris•HCl, pH 7.8, 50 mM KCl, 10 mM $MgCl_2$, 25 μM [^{3}H]GDP (specific radioactivity 512 cpm/pmol), 1 μM SsEF-1α and increasing concentration of ppGpp (3–1000 μM), was incubated for 30 min at 60°C to reach the equilibrium. The amount of the residual SsEF–1α•[^{3}H]GDP complex was determined on 40–μl aliquots by nitrocellulose filtration. (B) Semi–logarithmic plot of data reported in (A).*

This value allowed the derivation of the equilibrium dissociation constant for ppGpp which was about one order of magnitude higher than that previously reported for GDP and slightly lower than that for GTP (Table 5) (Ianniciello et al. 1996). Moreover, SsEF–1α was able

to exchange bound [^{3}H]GDP for free guanosine nucleotides (Figure 23) and the exchange rate for GDP was faster than that for GTP.

Table 5. Effect of ppGpp on the affinity of SsEF–1α for guanosine nucleotides at 60°C. *The K_d' and k_{-1} values represent the average of 3–4 different determinations. k_{+1} was calculated as k_{-1}/K_d'.*

SsEF–1α	K'_d (μM)	k_{-1} (min^{-1})	k_{+1} ($\mu M^{-1} \cdot min^{-1}$)
GDP	1.6	0.10 ± 0.03	0.063
GTP	35	0.06 ± 0.03	0.002
ppGpp	15.7 ± 2.8	0.08 ± 0.02	0.005

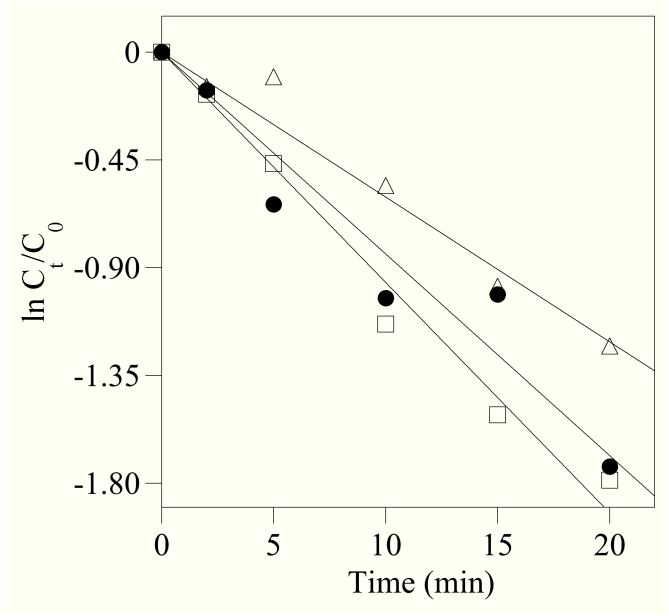

Figure 23. Effect of ppGpp on the nucleotide exchange rate on SsEF–1α. *The reaction mixture (150 μl) prepared in buffer A contained 1 μM SsEF–1α•[^{3}H]GDP. The nucleotide exchange reaction was started at 60°C by adding 333 μM GDP (empty squares) or ppGpp (filled circles) or GTP*

(empty triangles) final concentration. At the times indicated, 30–µl aliquots were filtered on nitrocellulose and the radioactivity retained on the filters was counted. The data were treated according to a first–order kinetic. C_t represents the concentration of SsEF–1α•[^{3}H]GDP at the time t, whereas C_0 is its concentration at the time 0.

The intermediate ability of ppGpp to exchange bound [^{3}H]GDP to SsEF–1α confirmed the results observed for the equilibrium dissociation constant (Table 5). The interaction between SsEF–1α and ppGpp was also studied analysing the effect of the nucleotide on the intrinsic GTPase^{Na}. The catalytic activity of SsEF–1α was sensitive to the presence of tetra–phosphate; the data reported in Figure 24 indicated that in the presence of different amounts of ppGpp, the rate of GTP breakdown catalysed by SsEF–1α was lower (Figure 24A and 24B).

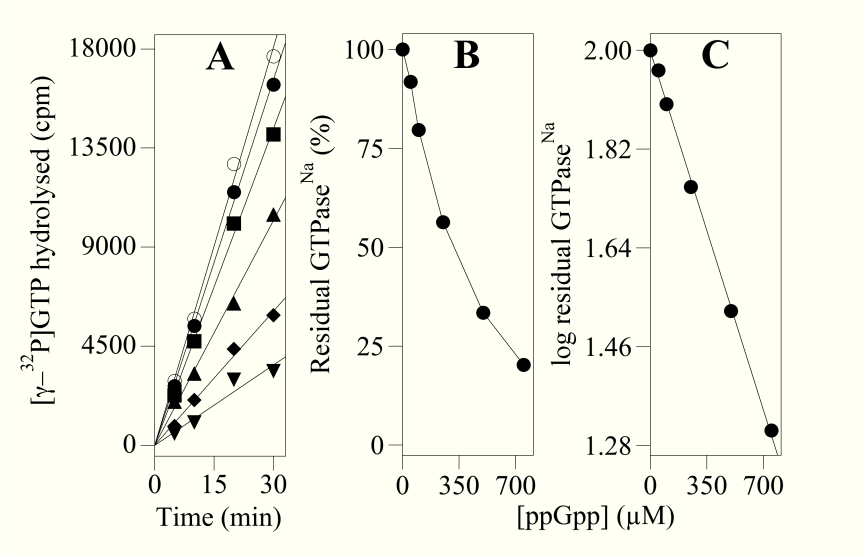

Figure 24. Effect of ppGpp on the GTPase^{Na} of SsEF–1α. *(A) The GTPase activity was assayed at the times indicated, in the absence (empty circles) or in the presence of 50 (filled circles), 100 (filled squares), 250 (filled upright triangles), 500 (filled diamonds) or 750 (filled inverted triangles) µM of ppGpp. The reaction mixture contained 0.1–0.3 µM SsEF–1α and 50 µM [γ–*

^{32}P]GTP (specific activity 150–300 cpm/pmol). The reaction was followed kinetically up to 30 min at 60°C; the amount of $^{32}P_i$ released was determined on 50–µl aliquots. (B) The rate of GTP hydrolysis carried out as in (A) were plotted against ppGpp concentration as a percentage of that measured in the absence of the nucleotide tetra–phosphate. (C) The data reported in (B) were linearized using a semi–logarithmic plot.

The data, linearised using a first–order behaviour equation (Figure 24C), allowed the evaluation of ppGpp concentration required to get 50 % inhibition of the intrinsic GTPase^{Na} of SsEF-1α (320.5 µM). In order to get an insight on the inhibition mechanism, the kinetic parameters of the GTPase^{Na} were determined in the presence of different ppGpp concentration (Figure 25).

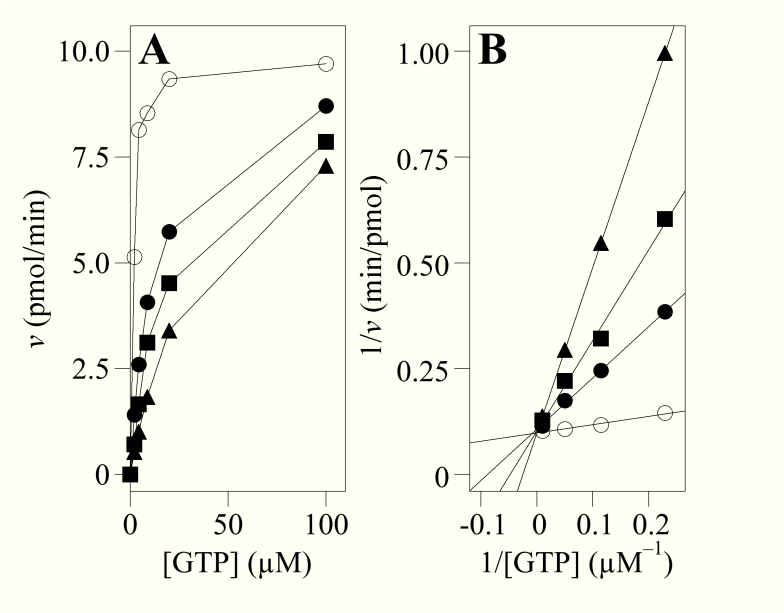

Figure 25. ppGpp competitively inhibited the GTPase^{Na} catalysed by SsEF–1α. *(A) The initial hydrolysis rate (v) was determined at the indicated [γ–^{32}P]GTP concentration in the absence (empty circles) or in the presence of 75 (filled circles), 150 (filled squares) or 300 (filled triangles). The reaction mixture contained 0.1–0.3 µM SsEF–1α and 50 µM [γ-^{32}P]GTP (specific activity 150–300 cpm/pmol). The reaction was followed kinetically at 60°C;*

the amount of $^{32}P_i$ released was determined on 50–µl aliquots. (B) The data reported in (A) were treated with the Lineweaver–Burk equation.

The data treated according to the Lineweaver–Burk equation showed that ppGpp induced an increase of K_m without any variation in the k_{cat} values (Table 6), thus indicating that the nucleotide tetra–phosphate acted as a competitive inhibitor. It is relevant that the calculated K_i value (15.5 ± 0.3 µM) was almost identical to the value of the equilibrium dissociation constant, determined with the competitive binding experiments reported in Figure 22.

Table 6. Effect of ppGpp on kinetic parameters of the intrinsic GTPase catalyzed by SsEF–1α.

SsEF–1α	K_m (µM)	k_{cat} (min^{-1})	k_{cat}/K_m (min^{-1}•μM^{-1})
w/o ppGpp	2.0 ± 0.3	0.80 ± 0.22	0.20
+ 75 µM ppGpp	11.3 ± 1.9	0.73 ± 0.26	0.07
+ 150 µM ppGpp	21.0 ± 2.4	0.77 ± 0.29	0.04
+ 300 µM ppGpp	40.0 ± 6.1	0.80 ± 0.35	0.02

3.2.3 Effect of ppGpp on the thermostability of SsEF–1α

The effect of temperature on the stability of SsEF–1α in the presence of ppGpp was analised by fluorescence monitored thermal denaturation. As shown in Figure 26, the denaturation profile of the elongation factor in the presence of ppGpp was shifted towards higher temperatures with a denaturation midpoint (96.4 °C) about 2 °C higher with respect to that observed for the elongation factor bound to GDP. These findings indicated that the extra diphosphate group present in the magic spot I exerted a protective effect against SsEF–1α thermal denaturation.

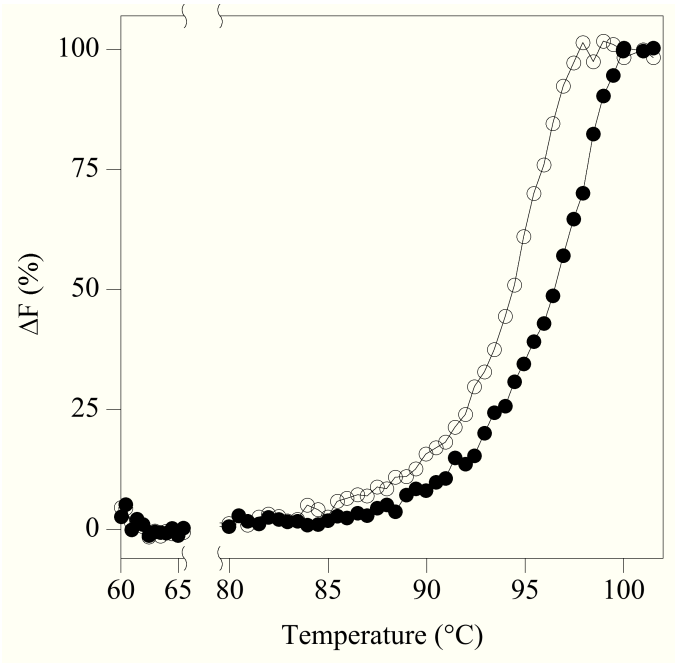

Figure 26. Effect of ppGpp on the fluorescence melting profile of SsEF–1α. *The increase in fluorescence intensity was measured in buffer A at the indicated temperatures using 2 μM SsEF–1α•GDP, in the absence (empty circles) or in the presence of 20 μM ppGpp (filled circles). The temperature increasing rate was set to 0.2°C/min. In the 65–80°C interval (omitted in the figure) no fluorescence variation was observed.*

4. Discussion/Conclusions

In this research thesis, several aspects of the action of eubacterial ligands on SsEF–1α functions were investigated. The interaction between SsEF–1α and two eubacterial antibiotics was demonstrated either by fluorescence spectroscopy in the aromatic region of the spectrum or by the effects produced by the antibiotic on some functional properties of the elongation factor; in particular, spectroscopic data showed in the presence of tetracycline an increase in the quantum yield in the fluorescence spectrum of SsEF–1α. A similar behaviour was also observed for Ss(GM)EF–1α but not for Ss(G)EF–1α. Therefore, these results indicated that the M–domain is essential for the interaction with tetracycline.

Regarding pulvomycin, the data obtained from fluorescence spectroscopy, suggested a conformational change induced by the antibiotic upon its interaction with SsEF–1α and confirmed those already reported for EcEF–Tu (Parmeggiani et al. 2006, 2006). However, the integrity of the archaeal elongation factor is required to bind the antibiotic with higher affinity. Furthermore, the appearance of a fluorescence band at 360 nm in the presence of pulvomycin for all proteins investigated, is indicative of the exposition to the aqueous solvent of tryptophan residues, even though a resonance energy transfer between close tyrosines and tryptophan(s) residues (Lakowicz 2006) cannot be excluded. In the primary structure of SsEF–1α two tryptophans and ten tyrosines are present, most of them in the nucleotide binding domain (W209, Y84, Y122, Y161, Y166, Y180, Y210, Y218). Therefore, the finding that the appearance of the 360 nm band was also evident on the truncated forms of the elongation factor, indicated that the main target of the solvent exposition upon antibiotic binding, was the region comprising Trp209 (Figure 27) to which the resonance energy transfer could occur from tyrosines 161, 166 and 210, surrounding this residue.

The effects on the functional properties of the enzyme and the results obtained pointed to the finding that both antibiotics were able to inhibit protein synthesis.

Regarding the effects on the partial reactions, any detectable effect was observed on ternary complex formation in presence of

tetracycline. Pulvomycin, instead, reduced the ability of SsEF–1α to form a ternary complex only in the presence of GTP, and the affinity for the aa–tRNA became very similar to that measured using GDP.

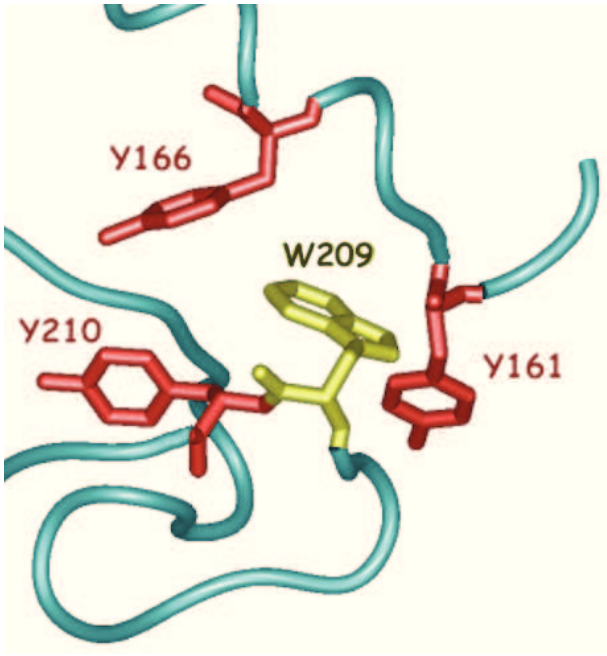

Figure27. Close–up of the SsEF–1α 3D structure surrounding the W209. *Tyrosines 161, 166 and 210 are indicated in red; tryptophan 209 in yellow. The picture was generated using the software iMol (http://www.pirx.com/iMol) and the PDB code 1JNY.*

These findings indicated that, as found for EcEF–Tu, even for an archaeal elongation factor the impairment of the ternary complex formation was the target of this antibiotic action (Wolf et al. 1978).
Furthermore, tetracycline slightly reduced the affinity of SsEF–1α for guanosine nucleotides. In the case of GDP, the increased equilibrium dissociation constant of the binary complex SsEF–1α•GDP can be ascribed to a greater decrease in the association rate constant than the dissociation one. In the case of the GDP⁄GTP exchange reaction on

SsEF–1α, the antibiotic has a more pronounced effect, making it faster and more similar to GDP⁄GDP. Pulvomycin, instead, increased the rate of nucleotide exchange for both GDP and GTP.

The effects of the tetracycline on the intrinsic GTPase catalysed by the elongation factor in the presence of NaCl appeared limited and undetectable on the engineered forms of the factor. This result, in contrast with the data reported on the spectroscopic properties, can be attributed to the high concentration of NaCl (3.6 M) needed to induce the GTPase activity of both intact (Masullo et al. 1994) and truncated forms of SsEF–1α (Masullo et al. 1997; Arcari et al. 1999). However, the concentration of antibiotic needed to get a 50% inhibition of the intrinsic GTPase of SsEF–1α (322 μM) is very similar to that obtained from fluorescence titration and of the same order of magnitude than that required to inhibit to 50% the *in vitro* protein synthesis in some micropathogens (400–850 μM) but also in a cell–free reconstituted system of *S. solfataricus* and *S. acidocaldarius* (Cammarano et al. 1985; Katiyar et al. 1991).

Pulvomycin had an opposite effect on $GTPase^{Na}$ catalysed by SsEF–1α. In particular, the antibiotic was able to stimulate the intrinsic GTPase catalysed by the elongation factor in presence of NaCl, a finding that was already reported for the intrinsic GTPase of EcEF–Tu (Parmeggiani et al. 2006), even though in that case the stimulatory effect was more pronounced. However, the stimulatory effect cannot be detected for the catalytic activity exerted by the truncated forms of SsEF–1α lacking the C– or both the C– and M–domains. These results indicated that the integrity of the elongation factor was required to observe the effect, and that the C–terminal domain was essential for the interaction. The analysis of the energetic parameters of activation could give an explanation of the increased hydrolytic rate of the reaction, measured in the presence of pulvomycin. In fact, the reduced energy of activation, induced by the antibiotic, was essentially due to a reduced enthalpy of activation, even though an unfavourable entropy factor leads to an unvaried free energy of activation.

Moreover, the interaction between SsEF–1α and tetracycline caused a reduction of the heat inactivation of the archaeal elongation factor, as demonstrated by a lower value of the energy of activation of the

process. The analysis of the thermodynamic parameters of the heat inactivation process at 87°C (Table 4) indicated that the antibiotic reduced both the enthalpy and the entropy of activation without affecting the free energy associated with the process. This finding can be explained by a less favourable entropic factor induced by the antibiotic in the attainment of the activation state of the inactivation process. The interaction between SsEF–1α and tetracycline was also analysed in terms of amino acid residues of the elongation factor involved, through the alignment between the primary structures of EcEF–Tu and SsEF–1α (Figure 28).

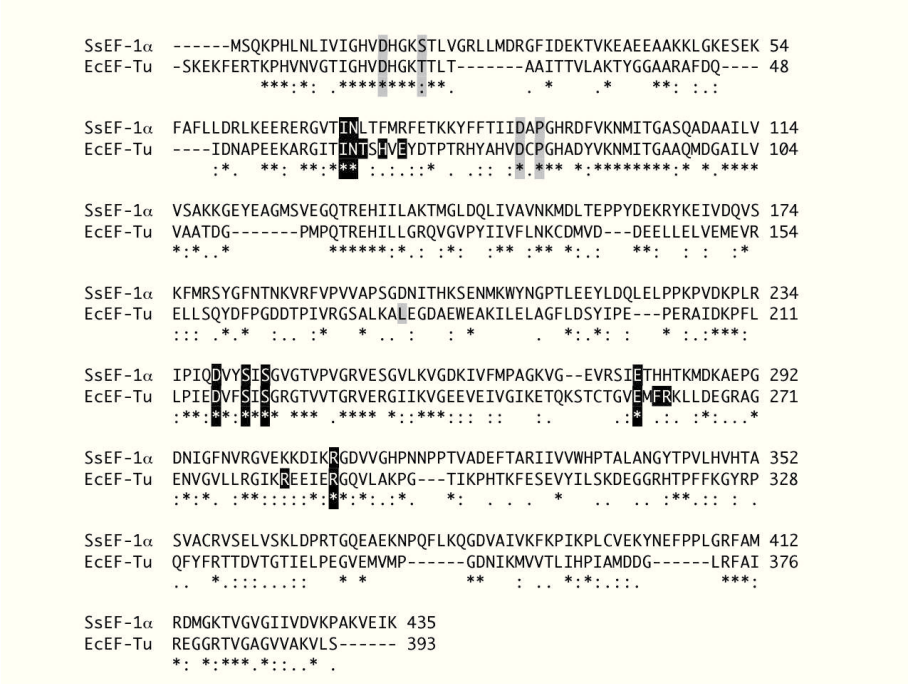

Figure 28. Primary structure alignment between EcEF–Tu and SsEF–1α. *The alignment was carried out using the proteomics tools available at http://www.expasy.ch. Residues involved in tetracycline binding in EcEF–Tu belonging to the G–domain are highlighted in grey. Those participating in the dimerisation induced by tetracycline are in white and shaded in black. Conserved residues are indicated by an asterisk, conservative substitutions by a colon and semi–conservative substitutions by a dot.*

Among the residues identified in the catalytic domain of EcEF–Tu involved in the binding of the antibiotic (Heffron et al. 2006), those of the consensus sequences of guanosine nucleotide–binding proteins (Asp21, Thr25, Asp80, and Pro82, EcEF–Tu numbering) as expected are conserved in SsEF–1α. Regarding the other residues involved in the interaction with the antibiotic and belonging to this domain (Thr64, Ser65, Val67 and Leu178, EcEF–Tu numbering), although a Ser65→Thr and a Val67→Met were found as conservative substitutions, the other two residues were not conserved in SsEF–1α (Thr65→Leu and Leu178→Asp, EcEF–Tu numbering, respectively). Concerning the amino acid residues involved in the dimer formation through protein–protein interaction, those participating in the stabilisation of the conserved flexible region Ile220→Arg223 were also present in SsEF–1α; vice versa, differences were found in the residues belonging to the Arg262→Leu264 loop, even though some of the residues involved in its stabilisation were conserved (Asp216 and Glu259).

The interaction between the archaeal elongation factor and pulvomycin was also demonstrated by the finding that the antibiotic rendered SsEF–1α slightly more resistant to guanidine hydrochloride denaturation. This finding is indicative of a more compact molecular organisation of the elongation factor observed in the presence of pulvomycin. However, a direct stabilising effect of the antibiotic on the protein in the complex cannot be excluded.

The interaction between SsEF–1α and ppGpp, a molecule involved in the stringent control both in eubacteria and plants during amino acid starvation, was also demonstrated. In line with previous crystallographic data showing that ppGpp was found bound to SsEF–1α in the crystalline state (Vitagliano et al. 2004), the ability of magic spot I to interact with the elongation factor was confirmed using different experimental approaches based on the competitive inhibition exerted by ppGpp on the GDP or GTP binding to the SsEF–1α. The affinity of SsEF–1α for ppGpp was intermediate between that obtained for GDP or GTP. The interaction of the guanosine tetra–phosphate with the enzyme affected also both the thermostability and the catalytic activity of SsEF–1α. The binding of ppGpp to SsEF–1α

produced an increase of the temperature for half denaturation by 2°C when compared to GDP. This finding was somehow surprising as the extra diphosphate group present in the ppGpp is solvent exposed and does not make any short–range interaction with the protein (Figure 29).

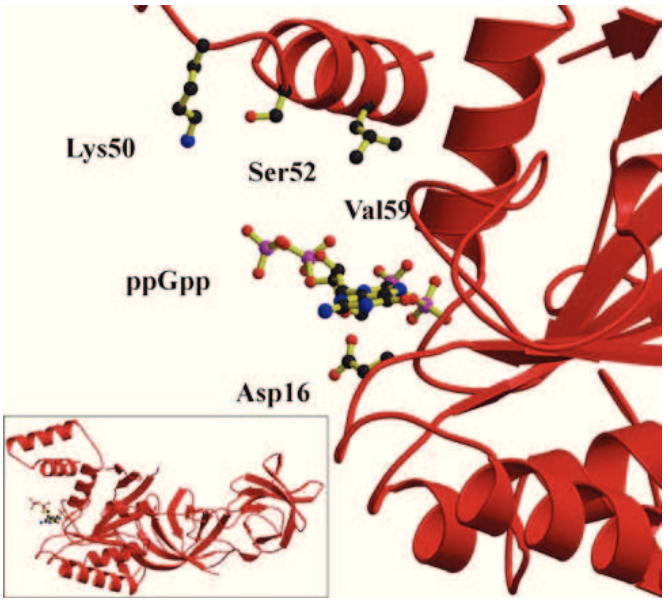

Figure 29. 3D structure of the SsEF–1α•ppGpp complex. *The model was generated using the coordinates of SsEF–1α reported in the Worldwide Protein Data Bank (PDB ID: 1SKQ). The position of the terminal phosphate group is indicative as it is not involved in interactions with the protein atoms closer than 8.0 Ä and is free to rotate.*

Therefore, the over–stabilisation of protein by ppGpp binding may be explained by considering that SsEF–1α shows a remarkable overall positive charge being its isoelectric point 9.1 (Masullo et al. 1991). The presence of additional negative charges in ppGpp compared to GDP could lead to an improved charge distribution of the surface of the elongation factor upon magic spot binding. Significant effects were also observed on the partial reactions catalysed by SsEF–1α.

Indeed, ppGpp was able to inhibit the intrinsic $GTPase^{Na}$ of SsEF–1α with a dose response behaviour as also recently reported for plant chloroplasts (Nomura et al. 2012). Furthermore, kinetic experiments indicated that the nucleotide tetra–phosphate acted as a competitive inhibitor. It is relevant that the inhibition constant obtained (15.5 μM) was almost identical to that determined for the equilibrium dissociation constant of SsEF–1α•ppGpp binary complex (15.7 μM) determined in the absence of NaCl. ppGpp was also able to inhibit protein synthesis *in vitro*, although the concentration required to get half–inhibition (IC50 = 2.1 mM) was significantly higher than that required for the eubacterial (Legault et al. 1972) and eukaryal systems (Nomura et al. 2012; Manzocchi et al. 1973). The explanation of the difference in the concentration of nucleotide to measure an effect is probably due to the finding that the protein synthesis assay was carried out in the presence of several other components, mainly ribosomes, EF–2 and synthetic mRNA, rendering the effect of guanosine tetra–phosphate less powerful.

Apparently, the results described are in disagreement with the findings that in the genome of *S. solfataricus* the genes coding for RelA and SpoT have not been found, no accumulation of magic spots was found in cell extracts of this archaeon (Cellini et al. 2004) and a BLAST search of amino acid sequences of RSH family (Atkinson et al. 2011) towards the genome of *S. solfataricus* gives no significative matches (not shown). Although a physiological role of ppGpp in *S. Solfataricus* is yet to be demonstrated, the effects on SsEF–1α can be ascribed to common structural/functional features of elongation factors isolated from different organisms, independently on the role that magic spots play in different species.

In conclusion, the data presented demonstrated an interaction between the archaeal elongation factor 1α from *Sulfolobus solfataricus* and two eubacterial antibiotics (tetracyline or pulvomycin), as well as with a nucleotide tetra–phosphate. These results could be used as probe to investigate phylogenetic relationship among living domain. Therefore, the binding of ppGpp, characterised requiring structural determinants similar to those for GDP, could indicate that the regulation of some cellular processes can be achieved without interfering with the

GDP/GTP balance which is important for many other metabolic ways, a finding already reported in *Saccharomyces cerevisiae* (Iglesias-Gato et al. 2011).

5. References

Anborgh, P.H. and Parmeggiani, A. (1991). New antibiotic that acts specifically on the GTP–bound form of elongation factor Tu. EMBO J. 10, 779–784.

Arcari, P., Masullo, M.,Arcucci, A.,Ianniciello, G., de Paola, B., Bocchini, V. (1999). A chimeric elongation factor containing the putative guanine nucleotide binding domain of archaeal EF-1 alpha and the M and C domains of eubacterial EF–Tu. Biochem. 38, 12288–12295.

Atkinson, G.C., Tenson, T., Hauryliuk, V. (2011). The RelA/SpoT homolog (RSH) superfamily: distribution and functional evolution of ppGpp synthetases and hydrolases across the tree of life. PLoS One 6, e23479.

Battesti, A., Bouveret, E. (2006). Acyl carrier protein/SpoT interaction, the switch linking SpoT–dependent stress response to fatty acid metabolism. Mol. Microbiol. 62, 1048–1063.

Boon, K., Krab, I.M., Parmeggiani, A., Bosch, L., and Kraal, B. (1995). Substitution of Arg230 and Arg233 in *Escherichia coli* elongation factor Tu strongly enhances its pulvomycin resistance. Eur. J. Biochem. 22, 816–822.

Braeken, K., Moris, M., Daniels, R., Vanderleyden, J., Michiels, J. (2006). New horizons for (p)ppGpp in bacterial and plant physiology. J. Trends Microbiol. 14, 45–54.

Brodersen, D.E., Clemons, W.M. Jr, Carter, A.P., Morgan–Warren, R.J., Wimberly, B.T., Ramakrishnan, V. (2000). The structural basis for the action of the antibiotics tetracycline, pactamycin, and hygromycin B on the 30S ribosomal subunit. Cell 103, 1143–1154.

Cammarano, P., Teichner, A., Londei, P., Acca, M., Nicolaus, B., Sanz, J.L., Amils, R. (1985). Insensitivity of archaebacterial ribosomes to protein synthesis inhibitors. Evolutionary implications. EMBO J. 4, 811–816.

Cantiello, P., Castellano, I., De Vendittis, E., Lamberti, A., Longo, O., Masullo, M., Raimo, G., Ruocco, M.R., Arcari, P. (2004). Interaction of archaeal translation elongation factors with eubacterial protein synthesis inhibitors. Curr. Top. Biochem. Res. 6, 145–154.

Cashel, M., Gentry, D.R., Hernandez, V.J., Vinella, D. (1996). The stringent response. In: Neidhardt, F.C., Curtiss, R. III, Ingraham, J.L., Lin, E.C.C., Low, K.B., Magasanik, B., Reznicoff, W., Riley, M., Schaechter, M., Umbarger, A.E. (eds)

Escherichia coli and *Salmonella*: cellular and molecular biology, 2nd edn. ASM Press, Washington DC, 1458–1496.

Cellini, A., Scoarughi, G.L., Poggiali, P., Santino, I., Sessa, R., Donini, P., Cimmino, C. (2004). Stringent control in the archaeal genus Sulfolobus. Res. Microbiol. 155, 98–104.

Cimmino, C., Scoarughi, G.L., Donini, P. (1993). Stringency and relaxation among the halobacteria. J Bacteriol. 175, 6659–6662.

Connamacher, R.H., Mandel, H.G., (1968). Studies on the intracellular localization of tetracycline in bacteria. Biochim. Biophys. Acta 166, 475–486.

De Vendittis, E., De Paola, B., Gogliettino, M.A., Adinolfi, B.S., Fiengo, A., Duvold, T., Bocchini, V. (2002). Fusidic and helvolic acid inhibition of elongation factor 2 from the archaeon *Sulfolobus solfataricus*. Biochemistry 41, 14879–14884.

Dix, D.B., Thompson, R.C. (1986). Elongation factor Tu•guanosine 3'–diphosphate 5'–diphosphate complex increases the fidelity of proofreading in protein biosynthesis: mechanism for reducing translational errors introduced by amino acid starvation. Proc. Natl. Acad. Sci. USA 83, 2027–2031.

Epe, B., Woolley, P. (1984). The binding of 6-demethylchlortetracycline to 70S, 50S and 30S ribosomal particles: a quantitative study by fluorescence anisotropy. EMBO J. 3, 121–126.

Fasano, O., Bruns, W., Crechet, J.B., Sander, G., Parmeggiani, A. (1978). Modification of elongation-factor-Tu•guanine–nucleotide interaction by Kirromycin. A comparison with the effect of aminoacyl-tRNA and elongation factor Ts. Eur. J. Biochem. 89, 557–565.

Forster, C., Limmer, S., Ribeiro, S., Hilgenfeld, R., Sprinzl, M. (1993). Ternary complex between elongation factor Tu•GTP and Phe–tRNA^{Phe}. Biochimie 75, 1159–1166.

Goodman & Gilman (1997). "Le basi farmacologiche della terapia", McGraw-Hill, ninth edition, p.1095.

Gordon J. (1969). Hydrolysis of guanosine 5'–triphosphate associated with binding of aminoacyl transfer ribonucleic acid to ribosomes. J. Biol. Chem. 244, 5680–5686.

Granata, V., Graziano, G., Ruggiero, A., Raimo, G., Masullo, M., Arcari, P., Vitagliano, L., Zagari, A. (2006). Chemical denaturation of the elongation

factor 1α isolated from the hyperthermophilic archaeon *Sulfolobus solfataricus*. Biochemistry 45, 719–726.

Granata, V., Graziano, G., Ruggiero, A., Raimo, G., Masullo, M., Arcari, P., Vitagliano, L., Zagari, A. (2008). Stability against temperature of *Sulfolobus solfataricus* elongation factor 1 alpha, a multi-domain protein. Biochim. Biophys. Acta 1784, 573–581.

Heffron, S.E., Jurnak, F. (2000). Structure of an EF–Tu complex with a thiazolyl peptide antibiotic determined at 2.35 A resolution: atomic basis for GE2270A inhibition of EF–Tu. Biochemistry 39, 37–45.

Heffron, S.E., Mui, S., Aorora, A., Abel, K., Bergmann, E., Jurnak, F. (2006). Molecular complementarity between tetracycline and the GTPase active site of elongation factor Tu. Acta Cryst. Sect. D D62, 1392–1400.

Hinrichs, W., Kisker, C., Düvel, M., Müller, A., Tovar, K., Hillen, W., Saenger, W. (1994). Structure of the Tet repressor–tetracycline complex and regulation of antibiotic resistance. Science 264, 418–420.

Ianniciello, G., Masullo, M., Gallo, M., Arcari, P., Bocchini, V. (1996). Expression in *Escherichia coli* of thermostable elongation factor 1 alpha from the archaeon *Sulfolobus solfataricus*. Biotechnol. Appl. Biochem. 23, 41–45.

Iglesias-Gato, D., Martín-Marcos, P., Santos, M.A., Hinnebusch, A.G., Tamame, M. (2011). Guanine nucleotide pool imbalance impairs multiple steps of protein synthesis and disrupts GCN4 translational control in *Saccharomyces cerevisiae*. Genetics 187, 105–122.

Johansson, J.S., Gibney, B.R., Rabanal, F., Reddy, K.S., Dutton, P.L. (1998). A designed cavity in the hydrophobic core of a four–α–helix bundle improves volatile anesthetic binding affinity. Biochemistry 37, 1421–1429.

Johansson, J.S., Scharf, D., Davies, L.A., Reddy, K.S., Eckenhoff, R.G. (2000). A designed four-α-helix bundle that binds the volatile general anesthetic halothane with high affinity. Biophis. J. 78, 982–993.

Katiyar, S.K., Edlind, T.D. (1991). Enhanced antiparasitic activity of lipophilic tetracyclines: role of uptake. Antimicrob. Agents Chemother. 35, 2198–2202.

Kjeldgaard, M., Nyborg, J. (1992). Refined structure of elongation factor Tu from *E.Coli*. J. Mol. Biol. 223, 721–42.

Lakowicz, J.R. (2006). Principles of Fluorescence Spectroscopy, third ed., Springer, New York.

Langen, R., Schweins, T., and Warshel, A. (1992). On the mechanism of guanosine triphosphate hydrolysis in ras p21 proteins. Biochemistry 31, 8691–8696.

Legault, L., Jeantet, C., Gros, F. (1972). Inhibition of in vitro protein synthesis by ppGpp. FEBS Lett. 27, 71–75.

Lombardo, B., Raimo, G., Bocchini, V. (2002). Molecular and functional properties of an archaeal phenylalanyl-tRNA synthetase from the hyperthermophile *Sulfolobus solfataricus*. Biochim. Biophys. Acta 1596, 246–252.

Magnusson, L.U., Farewell, A., Nyström, T. (2005). ppGpp: a global regulator in *Escherichia coli*. Trends Microbiol. 13, 236–242.

Manzocchi, L.A., Tarragó, A., Allende, J.E. (1973). The effect of ppGpp on in vitro protein synthesis by a wheat embryo system. FEBS Lett. 29, 309–312.

Masullo, M., Raimo, G., Parente, A., Gambacorta, A., De Rosa, M., Bocchini, V. (1991). Properties of the elongation factor 1α in the thermoacidophilic archaebacterium *Sulfolobus solfataricus*. Eur. J. Biochem. 199, 529–537.

Masullo, M., De Vendittis, E., Bocchini, V. (1994). Archaebacterial elongation factor 1 alpha carries the catalytic site for GTP hydrolysis. J. Biol. Chem. 269, 20376–20379.

Masullo, M., Ianniciello, G., Arcari, P., Bocchini, V. (1997). Properties of truncated forms of the elongation factor 1alpha from the archaeon *Sulfolobus solfataricus*. Eur. J. Biochem. 243, 468–473.

Masullo, M., Cantiello, P., de Paola, B., Catanzano, F., Arcari, P., Bocchini, V. (2002). G13A substitution affects the biochemical and physical properties of the elongation factor 1 alpha. A reduced intrinsic GTPase activity is partially restored by kirromycin. Biochemistry 41, 628–633.

Masullo, M., Cantiello, P., de Paola, B., Fiengo, A., Vitagliano, L., Zagari A., Arcari, P. (2002). Valine 114 replacements in archaeal elongation factor 1 alpha enhanced its ability to interact with aminoacyl–tRNA and kirromycin. Biochemistry 41, 14482–14488.

Masullo, M., Cantiello, P., Arcari, P. (2004). Archaeal elongation factor 1α from *Sulfolobus solfataricus* interacts with the eubacterial antibiotic GE2270A. Extremophiles 8, 499–505.

Maxwell, I.H. (1968). Studies of the binding of tetracycline to ribosomes in vitro. Mol. Pharmacol. 4, 25–37.

Miller, D.L., Weissbach, H. (1977). In "Molecular mechanism of protein synthesis", Edited by Pestka, M. and Weissbach, H., Academic Press, New York, 323–373.

Milon, P., Tischenko, E., Tomsic, J., Caserta, E., Folkers, G., La Teana, A., Rodnina, M.V., Pon, C.L., Boelens, R., Gualerzi, C.O. (2006). The nucleotide–binding site of bacterial translation initiation factor 2 (IF2) as a metabolic sensor. Proc. Natl. Acad. Sci. USA 103, 13962–13967.

Mitkevich, V.A., Ermakov, A., Kulikova, A.A., Tankov, S., Shyp, V., Soosaar, A., Tenson, T., Makarov, A.A., Ehrenberg, M., Hauryliuk, V. (2010). Thermodynamic characterization of ppGpp binding to EF–G or IF2 and of initiator tRNA binding to free IF2 in the presence of GDP, GTP, or ppGpp. J. Mol. Biol. 402, 838–846.

Mizusawa, K., Masuda, S., Ohta, H. (2008). Expression profiling of four RelA/SpoT–like proteins, homologues of bacterial stringent factors, in *Arabidopsis thaliana*. Planta 228, 553–562.

Moazed, D., Noller, H.F. (1987). Interaction of antibiotics with functional sites in 16S ribosomal RNA. Nature 327, 389–394.

Nomura, Y., Takabayashi, T., Kuroda, H., Yukawa, Y., Sattasuk, K., Akita, M., Nozawa, A., Tozawa, Y. (2012). ppGpp inhibits peptide elongation cycle of chloroplast translation system in vitro. Plant Mol. Biol. 78, 185–196.

Nonaka, L., Connell, S.R., Taylor, D.E. (2005). 16S rRNA mutations that confer tetracycline resistance in *Helicobacter pylori* decrease drug binding in *Escherichia coli* ribosomes. J. Bacteriol. 187, 3708–3712.

Orth, P., Saenger, W., Hinrichs, W. (1999). Tetracycline–chelated Mg^{2+} ion initiates helix unwinding in Tet repressor induction. Biochemistry 38, 191–198.

Parker, C.A., Rees W.T. (1962). Fluorescence spectrometry. A review. Analyst 87, 83–111.

Parmeggiani, A., Nissen, P. (2006). Elongation factor Tu–targeted antibiotics: four different structures, two mechanisms of action. FEBS Lett. 580, 4576–4581.

Parmeggiani, A., Krab, I.M., Okamura, S., Nielsen, R.C., Nyborg, J., Nissen, P. (2006). Structural basis of the action of pulvomycin and GE2270A on elongation factor Tu. Biochemistry 45, 6846–6857.

Pioletti, M., Schlünzen, F., Harms, J., Zarivach, R., Glühmann, M., Avila, H., Bashan, A., Bartels, H., Auerbach, T., Jacobi, C., Hartsch, T., Yonath, A., Franceschi, F. (2001). Crystal structures of complexes of the small ribosomal subunit with tetracycline, edeine and IF3. EMBO J. 20, 1829–1839.

Potrykus, K., Cashel, M. (2008). (p)ppGpp still magical? Annu. Rev. Microbiol. 62, 35–51.

Raimo, G., Masullo, M., Parente, A., Dello Russo, A., Bocchini, V. (1992). Molecular, functional and structural properties of an archaebacterial elongation factor 2. Biochim. Biophys. Acta 1132, 127–132.

Raimo, G., Masullo, M., Lombardo, B., Bocchini, V. (2000). The archaeal elongation factor 1alpha bound to GTP forms a ternary complex with eubacterial and eukaryal aminoacyl–tRNA. Eur. J. Biochem. 267, 6012–6018.

Ravel, J.M., Shorey, R.L., Garner, C.W., Dawkins, R.C., Shive, W. (1969). The role of an aminoacyl–tRNA–GTP–protein complex in polypeptide synthesis. Cold Spring Harb. Symp. Quant. Biol. 34, 321–330.

Rheinberger, H.J. (1991). The function of the translating ribosome: allosteric three–site model of elongation. Biochimie 73, 1067–1088.

Rodnina, M.V., Wintermeyer, W. (2001). Fidelity of aminoacyl–tRNA selection on the ribosome: kinetics and structural mechanisms. Annu. Rev. Biochem. 70, 415–435.

Rojas, A.M., Ehrenberg, M., Andersson, S.G., Kurland, C.G. (1984). ppGpp inhibition of elongation factors Tu, G and Ts during polypeptide synthesis. Mol. Gen. Genet. 197, 36–45.

Semenkov, Yu.P., Makarov, E.M., Makhno, V.I., Kirillov, S.V. (1982). Kinetic aspects of tetracycline action on the acceptor (A) site of *Escherichia coli* ribosomes. FEBS Lett. 144, 125–129.

Shorey, R.L., Ravel, J.M., Garner, C.W., Shive, W. (1969). Formation and properties of the aminoacyl transfer ribonucleic acid–guanosine triphosphate–protein complex. J. Biol. Chem. 244, 4555–4564.

Skoultchi, A., Ono, Y., Waterson, J., Lengyel, P. (1970). Peptide chain elongation; indications for the binding of an amino acid polymerization factor, guanosine 5'–triphosphate–aminoacyl transfer ribonucleic acid complex to the messenger–ribosome complex. Biochemistry 9, 508–514.

Smith, R.J., Williams, D.H., Barna, J.C.J., McDermott, I.R., Haegele, K.D., Piriou, F., Wagner, J., Higgins, W. (1985). Structure revision of the antibiotic pulvomycin, J. Am. Chem. Soc. 107, 2849–2857.

Song, H., Parsons, M.R., Roswell, S., Leonard, G., Phillips, S.E. (1999). Crystal structure of intact elongation factor EF-Tu from *Escherichia coli* in GDP conformation at 2.05 Å resolution. J. Mol. Biol. 285, 1245–1256.

Spirin, A.S., Kostiashkina, O.E., Jonák, J. (1976). Contribution of the elongation factors to resistance of ribosomes against inhibitors: comparison of the inhibitor effects on the factor–free translation systems. J. Mol. Biol. 101, 553–562.

Sprinzl, M. (1994). Elongation factor Tu: a regulatory GTPase with an integrated effector. Trends Biochem. Sci. 19, 245–250.

Stark, H. (2002). Three–dimensional electron cryomicroscopy of ribosomes. Curr. Protein Pept. Sci. 3, 79–91.

Takahashi, K., Kasai, K., Ochi, K. (2004). Identification of the bacterial alarmone guanosine 5'-diphosphate 3'-diphosphate (ppGpp) in plants. Proc. Natl. Acad. Sci. USA 101, 4320–4324.

Underfriend, S. (1969). Fluorescence assay in biology and medicine, vol 2nd. Academic Press, London.

Vitagliano, L., Masullo, M., Sica, F., Zagari, A., Bocchini, V. (2001). The crystal structure of *Sulfolobus solfataricus* elongation factor 1alpha in complex with GDP reveals novel features in nucleotide binding and exchange. EMBO J. 20, 5305–5311.

Vitagliano, L., Ruggiero, A., Masullo, M., Cantiello, P., Arcari, P., Zagari, A. (2004). The crystal structure of *Sulfolobus solfataricus* elongation factor 1 alpha in complex with magnesium and GDP. Biochemistry 43, 6630–6636.

Weijland, A., Hamark, K., Cool, R.H., Anborgh, P.H., Parmeggiani, A. (1992). Elongation factor Tu: a molecular switch in protein biosynthesis. Mol. Biol. 132, 253–256.

Williams Smith, H. (1979). Antibiotic–resistant *Escherichia coli* in market pigs in 1956–1979: the emergence of organisms with plasmid–borne trimethoprim resistance. J. Hyg. 84, 467–477.

Wolf, H., Assmann, D., Fisher, E. (1978). Pulvomycin, an inhibitor of protein biosynthesis preventing ternary complex formation between elongation factor Tu, GTP, and aminoacyl–tRNA. Proc. Natl. Acad. Sci. USA 75, 5324–5328.

Yoshida, M., Travers, A., Clark, B.F. (1972). Inhibition of translation initiation complex formation by MS1. FEBS Lett. 23, 163–166.

Zeef ,L.H.A., Bosch, L., Anborgth ,P.H., Centin, R., Parmeggiani, A. and Hilgenfeld, R. (1994). Pulvomycin–resistant mutants of *E. coli* elongation factor Tu, Embo J. 13, 5113–5120.

LIST OF PUBLICATIONS OF DR. ANNA LAMBERTI

Full Papers

1. Nicola M. Martucci, **Anna Lamberti**, Luigi Vitagliano, Piergiuseppe Cantiello, Immacolata Ruggiero, Paolo Arcari, Mariorosario Masullo. The magic spot ppGpp influences *in vitro* the molecular and functional properties of the elongation factor 1a from the archaeon *Sulfolobus solfataricus*. Extremophiles (2012) 16:743-749.

2. Luciana Esposito, Alessia Ruggiero, Mariorosario Masullo, Maria Rosaria Ruocco, **Anna Lamberti**, Paolo Arcari, Adriana Zagari, Luigi Vitagliano. Crystallographic and spectroscopic characterizations of *Sulfolobus solfataricus* TrxA1 provide insights into the determinants of thioredoxin fold stability. Journal of Structural Biology (2012) 177:506-512.

3. Nicola M. Martucci, **Anna Lamberti**, Paolo Arcari, Mariorosario Masullo. The eubacterial protein synthesis inhibitor pulvomycin interacts with archaeal elongation factor 1alpha from *Sulfolobus solfataricus*. Biochimie (2012) 94:503-509.

4. **Anna Lamberti**, Nicola M. Martucci, Immacolata Ruggiero, Paolo Arcari, Mariorosario Masullo. Interaction between the antibiotic tetracycline and the elongation factor 1a from the archaeon *Sulfolobus solfataricus*. Chemical Biology and Drug Design (2011) 78:260-268.

5. Immacolata Ruggiero, Piergiuseppe Cantiello, **Anna Lamberti**, Angela Sorrentino, Nicola M. Martucci, Alessia Ruggiero, Rosaria Arcone, Luigi Vitagliano, Paolo Arcari. Biochemical characterisation of the D60A mutant of the elongation factor 1a from the archaeon *Sulfolobus solfataricus.* Biochimie (2009) 91:835-842.

Abstracts to National and International Meetings

1. **Anna Lamberti**, Nicola M. Martucci, Piergiuseppe Cantiello, Immacolata Ruggiero, Paolo Arcari, Mariorosario Masullo. The magic spot ppGpp regulates the molecular and functional properties of the elongation factor 1α from the archaeon *Sulfolobus solfataricus*. The FEBS Journal 279, suppl 1 (2012) 476, 37th FEBS Congress "From single molecules to systems biology" – Seville (Spain) 2012

2. **Anna Lamberti**, Nicola M. Martucci, Immacolata Ruggiero, Paolo Arcari, Mariorosario Masullo. Interaction between some eubacterial antibiotics and the elongation factor 1α from the archaeon *Sulfolobus solfataricus*.The FEBS Journal 278, suppl 1 (2011) 115, 36th FEBS Congress "Biochemistry for Tomorrow's Medicine" - Torino (Italy) 2011

3. Francesco Albano, Giuseppina Granato, Nicola M. Martucci, **Anna Lamberti**, Maria Rosaria Ruocco. Analysis in vitro of photocytotoxic effects on cell cultures system during 5-aminolevulinic acid PDT. The FEBS Journal 278, suppl 1 (2011) 332, 36th FEBS Congress "Biochemistry for Tomorrow's Medicine" - Torino (Italy) 2011

4. **Lamberti A.,** Martucci N.M., Ruggiero I., Arcari P., Masullo M. Interazione tra il fattore di allungamento 1a dall'archeobatterio *Sulfolobus solfataricus* e l'antibiotico eubatterico tetraciclina. XV Giornate Scientifiche - Polo delle Scienze e delle Tecnologie per la Vita Università degli Studi di Napoli Federico II

5. Albino A., **Lamberti A**., Rullo R., De Vendittis E., Masullo M. Il sistema preposto alla sintesi del glutatione nell'eubatterio psicrofilo *Pseudoalteromonas haloplanktis*. XV Giornate Scientifiche - Polo delle Scienze e delle Tecnologie per la Vita Università degli Studi di Napoli Federico II

6. Masullo M, Ruggiero I, Cantiello P, **Lamberti A**, Sorrentino A, Martucci NM, Ruggiero A, Arcone R, Vitagliano L, Arcari P. Characterisation of the D60A mutant of the elongation factor 1a from the archaeon *Sulfolobus solfataricus*. The FEBS Journal 276, suppl 1 (2009) 153, 34th FEBS Congress "LIFE'S MOLECULAR INTERACTIONS" - Prague (Czech Republic) 2009

7. Sorrentino A., **Lamberti A.**, Ruggiero I., Arcari P., Masullo M. Caratterizzazione biochimica della forma mutata D60A del fattore di allungamento 1α dall'archeobatterio *Sulfolobus solfataricus*. Giornate scientifiche 2008 - Polo delle Scienze e delle Tecnologie per la Vita Università degli Studi di Napoli Federico II

FULL PAPERS CO-AUTHORED BY

DR. ANNA LAMBERTI

DURING DOCTORAL TRAINING

Extremophiles (2012) 16:743–749
DOI 10.1007/s00792-012-0470-z

ORIGINAL PAPER

The magic spot ppGpp influences in vitro the molecular and functional properties of the elongation factor 1α from the archaeon *Sulfolobus solfataricus*

Nicola M. Martucci · Anna Lamberti · Luigi Vitagliano · Piergiuseppe Cantiello · Immacolata Ruggiero · Paolo Arcari · Mariorosario Masullo

Received: 11 April 2012 / Accepted: 21 June 2012 / Published online: 7 July 2012

Abstract Guanosine tetra-phosphate (ppGpp), also known as "magic spot I", is a key molecule in the stringent control of most eubacteria and some eukarya. Here, we show that ppGpp affects the functional and molecular properties of the archaeal elongation factor 1α from *Sulfolobus solfataricus* (SsEF-1α). Indeed, ppGpp inhibited archaeal protein synthesis in vitro, even though the concentration required to get inhibition was higher than that required for the eubacterial and eukaryal systems. Regarding the partial reactions catalysed by SsEF-1α the effect produced by ppGpp on the affinity for aa-tRNA was lower than that measured in the presence of GTP but higher than that for GDP. Magic spot I was also able to bind SsEF-1α with an intermediate affinity in comparison to that displayed by GDP and GTP. Furthermore, ppGpp inhibited the intrinsic GTPase of SsEF-1α with a competitive behaviour. Finally, the binding of ppGpp to SsEF-1α rendered the elongation factor more resistant to heat treatment and the analysis of the molecular model of the complex between SsEF-1α and ppGpp suggests that this stabilisation arises from the charge optimisation on the surface of the protein.

Keywords Elongation factor 1α · *Sulfolobus solfataricus* · Stringent control · ppGpp · Magic spot · Intrinsic GTPase

Communicated by S. Albers.

N. M. Martucci and A. Lamberti equally contributed to this work.

N. M. Martucci · A. Lamberti · M. Masullo (✉)
Dipartimento di Studi delle Istituzioni e dei Sistemi Territoriali, Università degli Studi di Napoli "Parthenope", Via Medina 40, 80133 Naples, Italy
e-mail: mario.masullo@uniparthenope.it

N. M. Martucci · M. Masullo
Dipartimento di Scienze Farmacobiologiche, Università degli Studi "Magna Graecia" di Catanzaro, Complesso "Ninì Barbieri", 88021 Roccelletta di Borgia (CZ), Italy

A. Lamberti · P. Cantiello · I. Ruggiero · P. Arcari (✉) · M. Masullo
Dipartimento di Biochimica e Biotecnologie Mediche, Università degli Studi di Napoli Federico II, Via S. Pansini 5, 80131 Naples, Italy
e-mail: arcari@unina.it

L. Vitagliano
Istituto di Biostrutture e Bioimmagini, CNR, Via Mezzocannone 16, 80134 Naples, Italy

P. Arcari
CEINGE Biotecnologie Avanzate s.c.a r.l, Via G. Salvatore 486, 80145 Naples, Italy

Abbreviations

SC	Stringent control
Ss	*Sulfolobus solfataricus*
Ec	*Escherichia coli*
EF	Elongation factor
$GTPase^{Na}$	GTPase activity of SsEF-1α measured in the presence of 3.6 M NaCl
ppGpp	Guanosine tetra-phosphate

Introduction

The accumulation of guanosine tetra- and penta-phosphates (ppGpp and pppGpp, called also magic spot I and magic spot II, respectively, or alarmones) occurs in most eubacteria during stringent control (SC) (Braeken et al. 2006; Magnusson et al. 2005) but not in mutant strains lacking SC, which have been defined relaxed strains (Cashel et al.

1996). Concerning eukaryotes, the presence of alarmones has been demonstrated in plants where these molecules accumulate in chloroplasts upon biotic and abiotic stresses (Takahashi et al. 2004). ppGpp, a compound structurally similar to that of GDP, is characterised by the presence of an additional diphosphate group, bound through a phosphoester bond to the oxygen in position 3′ of ribose. Its production in eubacteria can be also induced by stress conditions or nutritional starvation (Cashel et al. 1996; Battesti and Bouveret 2006). The enzymes involved in magic spot synthesis are the *relA* gene product (p)ppGpp synthetase I and the *spoT* gene product (p)ppGpp synthetase II (Potrykus and Cashel 2008; Atkinson et al. 2011). The latter enzyme possess both synthetic and degrading activity and is responsible for the production of (p)ppGpp regardless SC and amino acid starvation, thus presumably explaining the basal level of (p)ppGpp always present in some bacteria (Potrykus and Cashel 2008; Atkinson et al. 2011). Recently, a growing number of RelA/SpoT homologues, designated RSH, have been identified in plants (Mizusawa et al. 2008) and their role in plant physiology/growth was previously reported (Kasai et al. 2002; van der Biezen et al. 2000). Furthermore, the identification of such proteins in the genome of several sources including some archaea allowed the analysis of phylogenetic relationships among these proteins in the tree of life (Atkinson et al. 2011). Finally, SpoT orthologs have also been recently identified in metazoa, and their involvement in body growth and starvation response in *Drosophila melanogaster* have been demonstrated (Sun et al. 2010).

In bacterial cells, (p)ppGpp plays a role as a negative effector of stable RNA (sRNA) levels and also in several other aspects to SC response such as that of restricting translational errors during amino acid starvation, thus influencing translation accuracy through different proposed mechanisms (Cashel et al. 1996). One of these involves the interaction of magic spots with translation elongation factors EF-Tu and EF-G (Rojas et al. 1984) as well as with the initiation factor IF-2 (Yoshida et al. 1972; Milon et al. 2006; Mitkevich et al. 2010). The inhibition of EF-Tu, EF-G or IF-2 functions might be involved in the control of translation fidelity during protein synthesis. In fact, ppGpp would slow down the accuracy-determining step of the reaction, acting specifically on the GTPase reactions catalysed by both elongation and initiation factors. However, a different mechanism has also been proposed in which the EF-Tu·ppGpp complex, upon its interaction with ribosome, can reduce the rate of peptide bond formation and improves proofreading by increasing the proportion of near-cognate aminoacyl-tRNAs rejected by ribosome (Rojas et al. 1984; Dix and Thompson 1986).

In Archaea very little is known on SC and in those so far studied there is a lack of SC with the exception of the Euryarcheota *Haloferax volcanii* showing a bacterial-like SC (Cimmino et al. 1993), and *Halococcus morrhuae*, showing a SC resembling that of eukarya (Cellini et al. 2004). In Crenarchaeota, the genus *Sulfolobus* appears to contain species that are stringent as in bacteria, but operated in the absence of magic spots; therefore, the absence of (p)ppGpp production has been proposed as an additional criteria to differentiate between Archaea and Bacteria (Cellini et al. 2004). In a previous structural characterisation of the elongation factor 1α, an enzyme isolated from the thermoacidophilic archaebacterium *Sulfolobus solfataricus* (SsEF-1α) endowed with a great thermophilicity and resistance to heat denaturation (Masullo et al. 1991; Granata et al. 2006, 2008), we found a ppGpp molecule bound to the active site of the recombinant protein (Vitagliano et al. 2004). This finding was ascribed to the ppGpp produced in *E. coli* (Cashel et al. 1996) in the heterologous expression of SsEF-1α (Ianniciello et al. 1996). In order to evaluate and to quantify the impact of binding of ppGpp to the properties of translational elongation factors, we here report a functional and molecular characterisation of SsEF-1α in the presence of the magic spot I.

Materials and methods

Chemicals, buffers and enzymes

Labelled compounds and chemicals were as already reported (Masullo et al. 1997). ppGpp was purchased by TriLink BioTechnologies (USA).

The following buffers were used: buffer A: 20 mM Tris·HCl, pH 7.8, 50 mM KCl, 10 mM $MgCl_2$; buffer B: 20 mM Tris·HCl, pH 7.8, 10 mM $MgCl_2$, 1 mM DTT, 3.6 M NaCl.

SsEF-1α was produced and purified as already reported (Ianniciello et al. 1996). SsRibosome, SstRNA, SsEF-2 and SsFRS were purified as reported (Raimo et al. 1992; Lombardo et al. 2002).

SsEF-1α assays

The poly(U)-directed poly(Phe) synthesis was performed at 75 °C as already described (Masullo et al. 2002). The preparation of [^{3}H]Val-EctRNA^{Val}, the formation of the ternary complex between the elongation factor, aa-tRNA and GDP or GTP or ppGpp, and the protection against the spontaneous deacylation of [^{3}H]Val-EctRNA^{Val} were carried out as already reported (Raimo et al. 2000).

The ability of SsEF-1α to exchange [^{3}H]GDP for unlabelled GDP, GTP or ppGpp, the determination of the apparent dissociation rate constant of the SsEF-1α·[^{3}H]GDP complex and the determination of the

equilibrium dissociation constant of the SsEF-1α·ppGpp complex were assessed by the nitrocellulose filtration method as reported (Masullo et al. 1991). Values are indicated as the mean of at least three different experiments with the indication of the standard error.

The GTPase activity was measured in the presence of 3.6 M NaCl ($GTPase^{Na}$) (Masullo et al. 1994). Unless otherwise indicated the reaction mixture contained 0.1–0.3 μM SsEF-1α and 50 μM [γ-^{32}P]GTP (specific activity 150–300 cpm/pmol). The reaction was followed kinetically up to 30 min at 60 °C; the amount of $^{32}P_i$ released was determined on 50 μl aliquots as already reported (Masullo et al. 1994); the catalytic constant of $GTPase^{Na}$, the affinity for [γ-^{32}P]GTP and the inhibition constants for ppGpp of $GTPase^{Na}$ were determined as reported previously (Masullo et al. 1997).

Fluorescence measurements

Heat denaturation of SsEF-1α was studied by fluorescence melting curve realised on a computer assisted Cary Eclipse spectrofluorimeter (Varian) equipped with an electronic temperature controller. The excitation and emission wavelengths were 280 and 311 nm, respectively, and the excitation and emission slits were both set to 10 nm. Blanks run in the absence of the protein were carried out in parallel and subtracted. The fluorescence intensity was corrected for temperature quenching (Underfriend 1969), not observed for the blank, normalised between 0 and 100 % and plotted versus the temperature.

Results

ppGpp inhibited the archaeal protein synthesis in vitro

The ability of ppGpp to affect archaeal poly(U)-directed poly(Phe) synthesis was assessed using a purified cell-free system reconstituted in vitro with the required components isolated from *Sulfolobus solfataricus* (De Vendittis et al. 2002). As reported in Fig. 1a, ppGpp exerted only a weak inhibitory effect on the rate of poly[^{3}H]Phe synthesis catalysed by SsEE-1α; in fact, in the presence of 550 μM ppGpp, a 20 % reduction of the phenylalanine incorporation rate was observed. From the analysis of the effect exerted by different concentrations of ppGpp on poly(Phe) incorporation (Fig. 1b), the concentration leading to 50 % inhibition (IC_{50} = 2.1 mM) was derived from a semi-logarithmic plot, as reported in Fig. 1c.

Moreover, we have also investigated the ability of SsEF-1α to form an heterologous ternary complex with aa-tRNA also in the presence of ppGpp, through the protection exerted by the elongation factor on aa-tRNA against spontaneous deacylation; the results reported in Fig. 2 showed that ppGpp induced an intermediate affinity of SsEF-1α for aa-tRNA when compared with that induced by GDP or GTP.

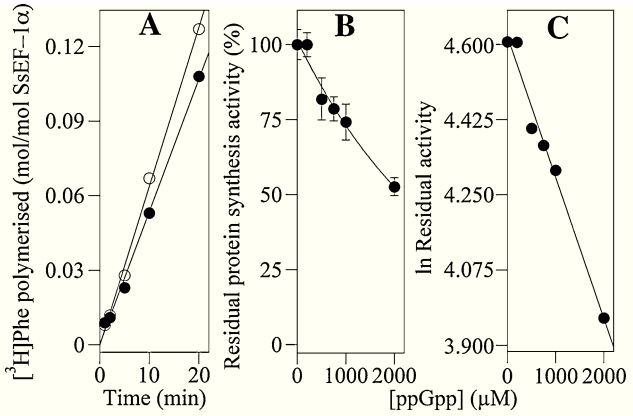

Fig. 1 Effect of ppGpp on the poly(U)-directed poly(Phe) synthesis catalysed by SsEF-1α. **a** 250 μl of the reaction mixture contained 25 mM Tris·HCl pH 7.5, 19 mM magnesium acetate, 10 mM NH_4Cl, 10 mM dithiothreitol, 2.4 mM ATP, 1.6 mM GTP, 0.16 mg/ml poly(U), 3 mM spermine, 0.25 μM Ssribosome, 80 μg/ml SstRNA, 0.1 μM SsEF-2, 2.0 μM [^{3}H]Phe (specific radioactivity 3094 cpm/pmol). The reaction was started by addition of 0.5 μM final concentration of SsEF-1α in the absence (*open circle*) or in presence (*filled circle*) of 550 μM ppGpp and carried out at 75 °C. At the times indicated, 50-μl aliquots were withdrawn, chilled on ice and then analysed for the amount of [^{3}H]Phe incorporated as hot trichloroacetic acid insoluble material. **b** The assay was carried out in triplicate as reported in **a** at the indicated guanosine tetra-phosphate concentration. The standard *error bars* are reported. **c** The data reported in **b** were treated as a semi-logarithmic plot

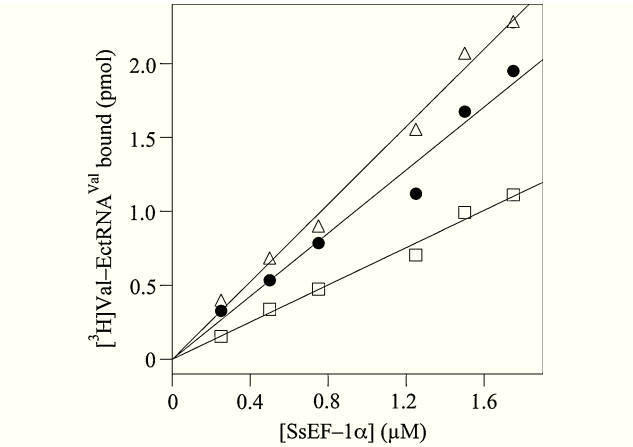

Fig. 2 Formation of the ternary complex between SsEF-1α, [^{3}H]Val-lEc-tRNA^{Val} and ppGpp or GDP or GTP. The mixture (30 μl) contained 25 mM Tris·HCl, pH 7.8, 10 mM NH_4Cl, 10 mM DTT, 20 mM magnesium acetate and 4.6 pmol of [^{3}H]ValEc-tRNA^{Val} (specific radioactivity 847 cpm/pmol) and was incubated for 1 h at 0 °C to allow ternary complex formation in the presence of the indicated amount of SsEF-1α·GDP (*open square*) or SsEF–1α·ppGpp (*filled circle*) or SsEF-1α·GTP (*unfilled triangle*). The deacylation reaction was carried out for 1 h at 50 °C and the residual [^{3}H]ValEc-tRNA^{Val} was determined as cold trichloroacetic acid insoluble material

ppGpp interacted with SsEF-1α

The affinity of ppGpp for the archaeal elongation factor was measured by competitive binding experiments. SsEF-1α binds [^{3}H]GDP with an affinity in the micromolar range (Ianniciello et al. 1996); as reported in Fig. 3a, the addition of increasing concentration of the tetra-phosphate nucleotide reduced the amount of the SsEF-1α·[^{3}H]GDP complex formation, thus indicating an inhibitory competitive effect. From a semi-logarithmic plot of the data (Fig. 2b), the concentration leading to 50 % inhibition (252 μM) was derived. This value allowed the calculation of the equilibrium dissociation constant for ppGpp (15.7 ± 2.8 μM) which was about one order of magnitude higher than that previously reported for GDP (1.6 μM) and slightly lower than that for GTP (35 μM) (Ianniciello et al. 1996).

Furthermore, SsEF-1α was able to exchange bound [^{3}H]GDP for free guanosine nucleotides (Fig. 4) and the exchange rate for GDP (first order rate constant, $k_{-1} = 0.10 \pm 0.03$ min^{-1}) was faster than that for GTP ($k_{-1} = 0.06 \pm 0.03$ min^{-1}). The intermediate ability of ppGpp to exchange bound [^{3}H]GDP on SsEF-1α ($k_{-1} = 0.08 \pm 0.02$ min^{-1}) confirmed the results observed for the equilibrium dissociation constant.

The interaction between SsEF-1α and ppGpp was also studied analysing the effect of the nucleotide on the intrinsic GTPase^{Na}. The catalytic activity of SsEF-1α was sensitive to the presence of tetra-phosphate; the data reported in Fig. 5 indicated that in the presence of different concentrations of

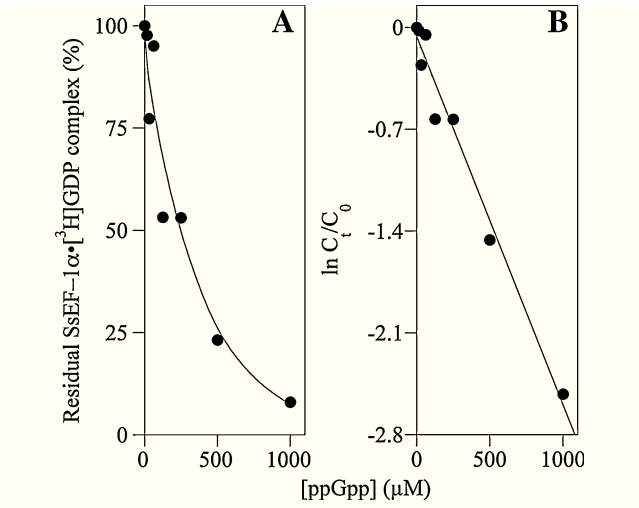

Fig. 3 Competitive binding of [^{3}H]GDP and ppGpp to SsEF-1α. **a** The reaction mixture (50 μl), containing 20 mM Tris·HCl, pH 7.8, 50 mM KCl, 10 mM $MgCl_2$, 25 μM [^{3}H]GDP (specific radioactivity 512 cpm/pmol), 1 μM SsEF-1α and increasing concentration of ppGpp (3–1000 μM), was incubated for 30 min at 60 °C to reach the equilibrium. The amount of the residual SsEF-1α·[^{3}H]GDP complex was determined on 40-μl aliquots by nitrocellulose filtration. **b** Semi–logarithmic plot of data reported in **a**

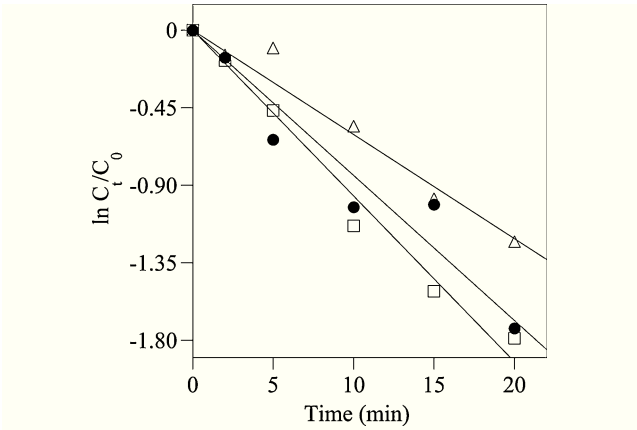

Fig. 4 Guanosine nucleotides exchange rate catalysed by SsEF-1α. The reaction mixture (150 μl) prepared in buffer A contained 1 μM SsEF-1α·[^{3}H]GDP. The nucleotide exchange reaction was started at 60 °C by adding 333 μM GDP (*open square*) or ppGpp (*filled circle*) or GTP (*unfilled triangle*) final concentration. At the times indicated, 30-μl aliquots were filtered on nitrocellulose and the radioactivity retained on the filters was counted. The data were treated according to a first-order kinetic. C_t represents the concentration of SsEF-1α·[^{3}H]GDP at the time t, whereas C_0 is its concentration at the time 0

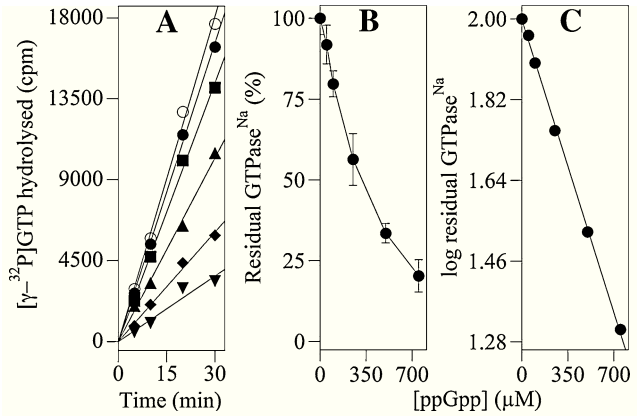

Fig. 5 Effect of ppGpp on the GTPase^{Na} of SsEF-1α. **a** The GTPase activity was assayed at the times indicated, as described in "Materials and methods", in the absence (*open circle*) or in the presence of 50 (*filled circle*), 100 (*filled square*), 250 (*filled upright triangle*), 500 (*filled diamond*) or 750 (*filled inverted triangle*) μM of ppGpp. **b** The rate of GTP hydrolysis derived from three experiments carried out as in **a** were plotted against ppGpp concentration as a percentage of that measured in the absence of the nucleotide tetra-phosphate. Standard *error bars* are indicated. **c** The data reported in **b** were linearised using a semi-logarithmic plot

ppGpp, the rate of GTP breakdown catalysed by SsEF-1α was lower (Fig. 5a, b). The data, linearised using a first-order behaviour equation (Fig. 5c), allowed the evaluation of ppGpp concentration required to get 50 % inhibition of the intrinsic GTPase^{Na} of SsEF-1α (320.5 μM).

In order to get an insight on the inhibition mechanism, the kinetic parameters of the GTPase^{Na} were determined in

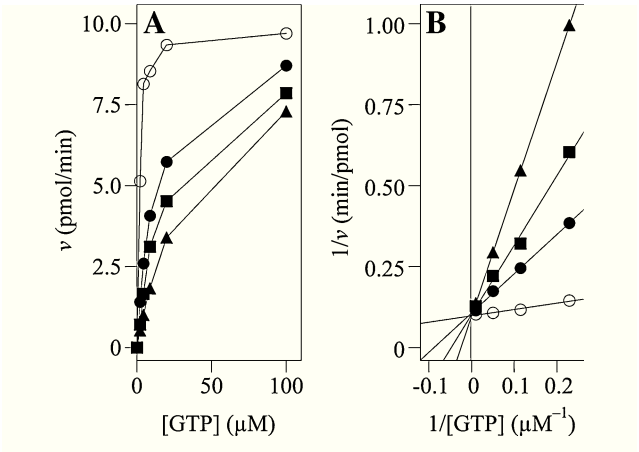

Fig. 6 Affinity of SsEF-1α for ppGpp in GTPase^{Na}. **a** The initial hydrolysis rate (v) was determined at the indicated [γ-^{32}P]GTP concentration in the absence (*open circle*) or in the presence of 75 (*filled circle*), 150 (*filled square*) or 300 (*filled triangle*) μM ppGpp as reported in "Materials and methods". **b** The data reported in **a** were treated with the Lineweaver–Burk equation

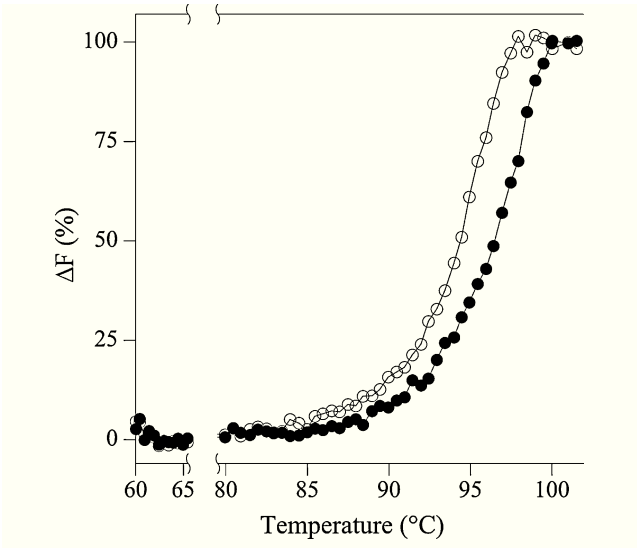

Fig. 7 Effect of ppGpp on the heat denaturation profile of SsEF-1α·GDP. The increase in fluorescence intensity was measured in buffer A at the indicated temperatures using 2 μM SsEF-1α·GDP, in the absence (*open circle*) or in the presence of 20 μM ppGpp (*filled circle*). The temperature increasing rate was set to 0.2 °C/min. In the 65–80 °C interval (omitted in the figure) no fluorescence variation was observed

the presence of different ppGpp concentration (Fig. 6a). The data analysed according to the Lineweaver–Burk equation showed that ppGpp induced an increase of K_m (from 2.0 ± 0.3 μM in the absence to 11.3 ± 1.9, 21.0 ± 2.4 and 40.0 ± 6.1 μM in the presence of 75, 150, and 300 μM ppGpp, respectively) without any variation in the k_{cat} values (from 0.80 ± 0.22 min^{-1} in the absence to a mean value of 0.75 ± 0.26 min^{-1} in the presence of the three ppGpp concentration), thus indicating that the nucleotide tetra-phosphate acted as a competitive inhibitor. It is relevant that the calculated K_i value (15.5 ± 0.3 μM) was almost identical to the value of the equilibrium dissociation constant determined with the competitive binding experiments reported in Fig. 3.

Effect of ppGpp on the thermostability of SsEF-1α

The effect of temperature on the stability of SsEF-1α in the presence of ppGpp was here evaluated by fluorescence-monitored thermal denaturation. As shown in Fig. 7, the denaturation profile of the elongation factor in the presence of ppGpp was shifted towards higher temperatures with a denaturation midpoint (96.4 °C) about 2 °C higher with respect to that observed for the elongation factor bound to GDP. These findings indicated that the extra diphosphate group present in the magic spot I exerted a protective effect against SsEF-1α thermal denaturation.

Discussion

In this work, we have demonstrated that ppGpp, a molecule involved in the stringent control both in eubacteria and plants during amino acid starvation, was able to interact with the archaeal elongation factor 1α from *S. solfataricus* and to influence its molecular and functional properties. A number of experiments here reported unveiled the effects produced by ppGpp on the molecular and functional properties of SsEF-1α. In line with previous crystallographic data showing that ppGpp was found bound to SsEF-1α in the crystalline state (Vitagliano et al. 2004), the ability of magic spot I to interact with the protein was confirmed using different experimental approaches based on the competitive inhibition exerted by ppGpp on the GDP or GTP binding to the elongation factor. The affinity of SsEF-1α towards ppGpp was thoroughly intermediate between that elicited for GDP or GTP.

The interaction of the guanosine tetra-phosphate with the protein affected also both the thermostability and the catalytic activity of SsEF-1α. We have previously shown that the binding of GDP to SsEF-1α increased its thermal stability by approximately 4 °C (Granata et al. 2008). This was not unexpected as this nucleotide makes extensive interaction with protein residues (Vitagliano et al. 2001, 2004). The binding of ppGpp to SsEF-1α produced a further increase of the temperature by 2 °C when compared to GDP. This finding was somehow surprising as the extra diphosphate group present in the ppGpp is solvent exposed and does not make any short range interaction with the protein (Fig. 8). Therefore, the over-stabilisation of protein by ppGpp binding may be explained by considering that SsEF-1α shows, under the experimental conditions used in

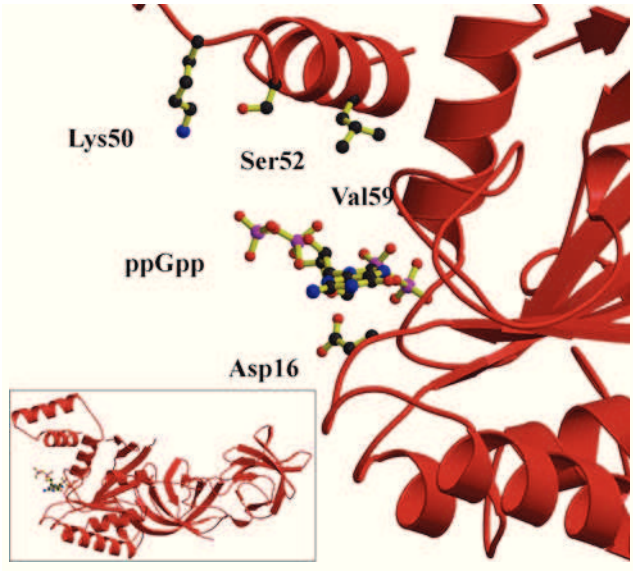

Fig. 8 SsEF-1α nucleotide binding site. The model was generated using the coordinates of SsEF-1α reported in the Worldwide Protein Data Bank (PDB ID: 1SKQ). The position of the terminal phosphate group is indicative as it is not involved in interactions with the protein atoms closer than 8.0 Å and is free to rotate. *Inset* Overall structure of the SsEF-1α·ppGpp complex. The diphosphate group bond to the oxygen in position 3′ of ribose is fully exposed to the solvent

this work but also in the crystallisation experiments, a remarkable overall positive charge being its isoelectric point 9.1 (Masullo et al. 1991). The presence of additional negative charges in ppGpp compared to GDP could lead to an improved charge distribution of the surface of the protein upon magic spot binding.

Significant effects were also observed on the partial reactions catalysed by the elongation factor. Indeed, ppGpp was able to inhibit the intrinsic GTPase^{Na} of SsEF-1α with a dose response behaviour as also recently reported for plant chloroplasts (Nomura et al. 2012). Furthermore, kinetic experiments indicated that the nucleotide tetra-phosphate acted as a competitive inhibitor. It is relevant that the inhibition constant obtained (15.5 μM) was almost identical to that determined for the equilibrium dissociation constant of SsEF-1α·ppGpp binary complex (15.7 μM) determined in the absence of NaCl. Therefore, the interaction between the archaeal elongation factor and ppGpp takes place regardless of the presence of the high salt concentration.

The guanosine nucleotide tetra-phosphate was also able to inhibit protein synthesis in vitro, although the concentration required to get half–inhibition (IC_{50} = 2.1 mM) was significantly higher than that required for the eubacterial (Legault et al. 1972) and eukaryal systems (Nomura et al. 2012; Manzocchi et al. 1973). Compared to the effects caused by ppGpp on the GTPase^{Na} of SsEF-1α, protein synthesis inhibition required concentration of the magic spot one order of magnitude higher. The explanation of the difference in the concentration of nucleotide to measure an effect is probably due to the finding that the protein synthesis assay was carried out in the presence of several other components, mainly ribosomes, EF-2 and synthetic mRNA, rendering the effect of guanosine tetra-phosphate less powerful.

Not only do the overall results reported in this paper confirm previous crystallographic indication about the possibility of ppGpp to interact with SsEF-1α, but also demonstrate that magic spot I interferes with the functional properties of the enzyme.

Apparently, the results here described are in disagreement with the findings that (a) in the genome of this archaeon the genes coding for RelA and SpoT have not been identified, (b) no accumulation of magic spots was found in cell extracts of *S. solfataricus* (Cellini et al. 2004) and (c) a BLAST search using amino acid sequences of RSH family (Atkinson et al. 2011) towards the genome of *S. solfataricus* gives no significative matches (not shown). Although a physiological role of ppGpp in *S. Solfataricus* is yet to be demonstrated, the effects here reported can be ascribed to common structural/functional features of elongation factors isolated from different organisms, independently on the role that magic spots play in different species. Along this line, the finding that ppGpp interacts with an archaeal elongation factor could be exploited to shed light on the molecular mechanisms on which the effect of magic spots on the elongation cycle takes place.

In conclusion, the inhibitory effect exerted by ppGpp on the protein synthesis, here quantified on an archaeal elongation factor is comparable to that recently reported for guanosine nucleotides in other sources (Nomura et al. 2012). Therefore, the binding of ppGpp, characterised by structural requirements similar to those required by GDP, could indicate that the regulation of some cellular processes can be achieved without interfering with the GDP/GTP balance which is important for many other metabolic ways as reported for *Saccharomyces cerevisiae* (Iglesias-Gato et al. 2011).

Acknowledgments This work was supported by MiUR (Rome), PRIN 2009 to MM, and PRIN 2008 to PA.

References

Atkinson GC, Tenson T, Hauryliuk V (2011) The RelA/SpoT homolog (RSH) superfamily: distribution and functional evolution of ppGpp synthetases and hydrolases across the tree of life. PLoS One 6:e23479

Battesti A, Bouveret E (2006) Acyl carrier protein/SpoT interaction, the switch linking SpoT-dependent stress response to fatty acid metabolism. Mol Microbiol 62:1048–1063

Braeken K, Moris M, Daniels R, Vanderleyden J, Michiels J (2006) New horizons for (p)ppGpp in bacterial and plant physiology. J Trends Microbiol 14:45–54

Cashel M, Gentry DR, Hernandez VJ, Vinella D (1996) The stringent response. In: Neidhardt FC, Curtiss R III, Ingraham JL, Lin ECC, Low KB, Magasanik B, Reznicoff W, Riley M, Schaechter M, Umbarger AE (eds) *Escherichia coli* and *Salmonella*: cellular and molecular biology, 2nd edn. ASM Press, Washington DC, pp 1458–1496

Cellini A, Scoarughi GL, Poggiali P, Santino I, Sessa R, Donini P, Cimmino C (2004) Stringent control in the archaeal genus Sulfolobus. Res Microbiol 155:98–104

Cimmino C, Scoarughi GL, Donini P (1993) Stringency and relaxation among the halobacteria. J Bacteriol 175:6659–6662

De Vendittis E, De Paola B, Gogliettino MA, Adinolfi BS, Fiengo A, Duvold T, Bocchini V (2002) Fusidic and helvolic acid inhibition of elongation factor 2 from the archaeon *Sulfolobus solfataricus*. Biochemistry 41:14879–14884

Dix DB, Thompson RC (1986) Elongation factor Tu·guanosine 3′-diphosphate 5′-diphosphate complex increases the fidelity of proofreading in protein biosynthesis: mechanism for reducing translational errors introduced by amino acid starvation. Proc Natl Acad Sci USA 83:2027–2031

Granata V, Graziano G, Ruggiero A, Raimo G, Masullo M, Arcari P, Vitagliano L, Zagari A (2006) Chemical denaturation of the elongation factor 1alpha isolated from the hyperthermophilic archaeon *Sulfolobus solfataricus*. Biochemistry 45:719–726

Granata V, Graziano G, Ruggiero A, Raimo G, Masullo M, Arcari P, Vitagliano L, Zagari A (2008) Stability against temperature of *Sulfolobus solfataricus* elongation factor 1 alpha, a multi-domain protein. Biochim Biophys Acta 1784:573–581

Ianniciello G, Masullo M, Gallo M, Arcari P, Bocchini V (1996) Expression in *Escherichia coli* of thermostable elongation factor 1 alpha from the archaeon *Sulfolobus solfataricus*. Biotechnol Appl Biochem 23:41–45

Iglesias-Gato D, Martín-Marcos P, Santos MA, Hinnebusch AG, Tamame M (2011) Guanine nucleotide pool imbalance impairs multiple steps of protein synthesis and disrupts GCN4 translational control in *Saccharomyces cerevisiae*. Genetics 187:105–122

Kasai K, Usami S, Yamada T, Endo Y, Ochi K, Tozawa Y (2002) A RelA-SpoT homolog (Cr-RSH) identified in *Chlamydomonas reinhardtii* generates stringent factor in vivo and localizes to chloroplasts in vitro. Nucleic Acids Res 30:4985–4992

Legault L, Jeantet C, Gros F (1972) Inhibition of in vitro protein synthesis by ppGpp. FEBS Lett 27:71–75

Lombardo B, Raimo G, Bocchini V (2002) Molecular and functional properties of an archaeal phenylalanyl-tRNA synthetase from the hyperthermophile *Sulfolobus solfataricus*. Biochim Biophys Acta 1596:246–252

Magnusson LU, Farewell A, Nyström T (2005) ppGpp: a global regulator in *Escherichia coli*. Trends Microbiol 13:236–242

Manzocchi LA, Tarragó A, Allende JE (1973) The effect of ppGpp on in vitro protein synthesis by a wheat embryo system. FEBS Lett 29:309–312

Masullo M, Raimo G, Parente A, Gambacorta A, De Rosa M, Bocchini V (1991) Properties of the elongation factor 1 alpha in the thermoacidophilic archaebacterium *Sulfolobus solfataricus*. Eur J Biochem 18:529–537

Masullo M, De Vendittis E, Bocchini V (1994) Archaebacterial elongation factor 1 alpha carries the catalytic site for GTP hydrolysis. J Biol Chem 269:20376–20379

Masullo M, Ianniciello G, Arcari P, Bocchini V (1997) Properties of truncated forms of the elongation factor 1alpha from the archaeon *Sulfolobus solfataricus*. Eur J Biochem 243:468–473

Masullo M, Cantiello P, de Paola B, Fiengo A, Vitagliano L, Zagari A, Arcari P (2002) Valine 114 replacements in archaeal elongation factor 1 alpha enhanced its ability to interact with aminoacyl-tRNA and kirromycin. Biochemistry 41:14482–14488

Milon P, Tischenko E, Tomsic J, Caserta E, Folkers G, La Teana A, Rodnina MV, Pon CL, Boelens R, Gualerzi CO (2006) The nucleotide-binding site of bacterial translation initiation factor 2 (IF2) as a metabolic sensor. Proc Natl Acad Sci USA 103:13962–13967

Mitkevich VA, Ermakov A, Kulikova AA, Tankov S, Shyp V, Soosaar A, Tenson T, Makarov AA, Ehrenberg M, Hauryliuk V (2010) Thermodynamic characterization of ppGpp binding to EF-G or IF2 and of initiator tRNA binding to free IF2 in the presence of GDP, GTP, or ppGpp. J Mol Biol 402:838–846

Mizusawa K, Masuda S, Ohta H (2008) Expression profiling of four RelA/SpoT-like proteins, homologues of bacterial stringent factors, in *Arabidopsis thaliana*. Planta 228:553–562

Nomura Y, Takabayashi T, Kuroda H, Yukawa Y, Sattasuk K, Akita M, Nozawa A, Tozawa Y (2012) ppGpp inhibits peptide elongation cycle of chloroplast translation system in vitro. Plant Mol Biol 78:185–196

Potrykus K, Cashel M (2008) (p)ppGpp still magical? Annu Rev Microbiol 62:35–51

Raimo G, Masullo M, Parente A, Dello Russo A, Bocchini V (1992) Molecular, functional and structural properties of an archaebacterial elongation factor 2. Biochim Biophys Acta 1132:127–132

Raimo G, Masullo M, Lombardo B, Bocchini V (2000) The archaeal elongation factor 1alpha bound to GTP forms a ternary complex with eubacterial and eukaryal aminoacyl-tRNA. Eur J Biochem 267:6012–6018

Rojas AM, Ehrenberg M, Andersson SG, Kurland CG (1984) ppGpp inhibition of elongation factors Tu, G and Ts during polypeptide synthesis. Mol Gen Genet 197:36–45

Sun D, Lee G, Lee JH, Kim HY, Rhee HW, Park SY, Kim KJ, Kim Y, Kim BY, Hong JI, Park C, Choy HE, Kim JH, Jeon YH, Chung J (2010) A metazoan ortholog of SpoT hydrolyzes ppGpp and functions in starvation responses. Nat Struct Mol Biol 17:1188–1194

Takahashi K, Kasai K, Ochi K (2004) Identification of the bacterial alarmone guanosine 5′-diphosphate 3′-diphosphate (ppGpp) in plants. Proc Natl Acad Sci USA 101:4320–4324

Underfriend S (1969) Fluorescence assay in biology and medicine, vol 2nd. Academic Press, London

van der Biezen EA, Sun J, Coleman MJ, Bibb MJ, Jones JD (2000) Arabidopsis RelA/SpoT homologs implicate (p)ppGpp in plant signaling. Proc Natl Acad Sci USA 28:3747–3752

Vitagliano L, Masullo M, Sica F, Zagari A, Bocchini V (2001) The crystal structure of *Sulfolobus solfataricus* elongation factor 1alpha in complex with GDP reveals novel features in nucleotide binding and exchange. EMBO J 20:5305–5311

Vitagliano L, Ruggiero A, Masullo M, Cantiello P, Arcari P, Zagari A (2004) The crystal structure of *Sulfolobus solfataricus* elongation factor 1 alpha in complex with magnesium and GDP. Biochemistry 43:6630–6636

Yoshida M, Travers A, Clark BF (1972) Inhibition of translation initiation complex formation by MS1. FEBS Lett 23:163–166

Biochimie 94 (2012) 503–509

Contents lists available at SciVerse ScienceDirect

Biochimie

journal homepage: www.elsevier.com/locate/biochi

Research paper

The eubacterial protein synthesis inhibitor pulvomycin interacts with archaeal elongation factor 1α from *Sulfolobus solfataricus*

Nicola M. Martucci[a,b,1], Anna Lamberti[b,1], Paolo Arcari[b,c,**], Mariorosario Masullo[b,c,d,*]

[a] Dipartimento di Scienze Farmacobiologiche, Università degli Studi "Magna Graecia" di Catanzaro, Complesso "Ninì Barbieri", I-88021 Roccelletta di Borgia (CZ), Italy
[b] Dipartimento di Biochimica e Biotecnologie Mediche, Università degli Studi di Napoli Federico II, Via S. Pansini 5, I-80131 Napoli, Italy
[c] CEINGE Biotecnologie Avanzate s.c.a r.l., Via Gaetano Salvatore 486, I-80145 Napoli, Italy
[d] Dipartimento di Studi delle Istituzioni e dei Sistemi Territoriali, Università degli Studi di Napoli "Parthenope", Via Medina 40, I-80133 Napoli, Italy

ARTICLE INFO

Article history:
Received 25 May 2011
Accepted 27 August 2011
Available online 10 September 2011

Keywords:
Elongation factor 1α
Sulfolobus solfataricus
Pulvomycin
Protein–antibiotic interaction
Intrinsic GTPase

ABSTRACT

The effect of pulvomycin on the biochemical and fluorescence spectroscopic properties of the archaeal elongation factor 1α from *Sulfolobus solfataricus* (SsEF-1α), the functional analog of eubacterial EF-Tu, was investigated. The antibiotic was able to reduce in vitro the rate of protein synthesis however, the concentration of pulvomycin leading to 50% inhibition (173 μM) was two order of magnitude higher but one order lower than that required in eubacteria and eukarya, respectively. The effect of the antibiotic on the partial reactions catalysed by SsEF-1α indicated that pulvomycin was able to decrease the affinity of the elongation factor toward aa-tRNA only in the presence of GTP, to an extent similar to that measured in the presence of GDP. Moreover, the antibiotic produced an increase of the intrinsic GTPase catalysed by SsEF-1α, but not that of its engineered forms. Finally, pulvomycin induced a variation in fluorescence spectrum of the aromatic region of the elongation factor and its truncated forms. These spectroscopic results suggested that a conformational change of the elongation factor takes place upon interaction with the antibiotic. This finding was confirmed by the protection against chemical denaturation of SsEF-1α, observed in the presence of pulvomycin. However, a stabilising effect of the antibiotic directly on the protein in the complex could takes place.

1. Introduction

Archaeal elongation factor 1α from *Sulfolobus solfataricus* (SsEF-1α) plays a fundamental role in the elongation cycle of protein biosynthesis [1]. SsEF-1α is the functional homologue of the eubacterial elongation factor Tu (EF-Tu), belongs to the class of GTP-binding proteins and possesses an intrinsic GTPase activity revealed in the presence of a molar concentration of NaCl ($GTPase^{Na}$) [2]. The crystal structure of SsEF-1α/EF-Tu showed the presence of three structural distinct domains: a N-terminal domain, containing the nucleotide binding site (G-domain), a middle (M) and a C-terminal (C) domain [3,4]. In its active form complexed with GTP, this EF carries the aminoacyl-tRNA on the ribosome [5]; following codon–anticodon recognition, GTP is hydrolysed, and the resulting inactive form bound to GDP dissociates from the ribosome. The switch from the active to the inactive form is associated to a conformational change of the enzymes. The intervention of the elongation factor Ts/1β, that catalyses the GDP/GTP exchange on the factor, promotes the regeneration of the active form [6,7]. The details of the mechanism of action of *Escherichia coli* EF-Tu (EcEF-Tu) have also been elucidated taking advantage of specific antibiotics acting on the elongation factor. In particular, it has been reported that kirromycin freezes EF-Tu·GDP complex on the mRNA-programmed ribosome by preventing the structural rearrangement of the factor [8]; tetracycline was able to inhibit the binding of aminoacyl-tRNA to the A site of mRNA-programmed ribosome [9]. In addition, pulvomycin and GE2270A interfere with ternary complex formation preventing the interaction between EF-Tu·GTP and aminoacyl-tRNA [8,10]. These antibiotics do not seem to be specific for EcEF-Tu only; in fact, kirromycin was

Abbreviations: Ss, *Sulfolobus solfataricus*; Ec, *Escherichia coli*; EF, elongation factor; $GTPase^{Na}$, GTPase activity of SsEF-1α measured in the presence of 3.6 M NaCl.

* Corresponding author. Dipartimento di Studi delle Istituzioni e dei Sistemi Territoriali, Università degli Studi di Napoli "Parthenope", Via Medina 40, I-80133 Napoli, Italy. Tel.: +39 081 7463127; fax: +39 081 7463653.
** Corresponding author. Dipartimento di Biochimica e Biotecnologie Mediche, Università degli Studi di Napoli Federico II, Via S. Pansini 5, I-80131 Napoli, Italy. Tel.: +39 081 7463120; fax: +39 081 7463653.
E-mail addresses: arcari@dbbm.unina.it (P. Arcari), mario.masullo@uniparthenope.it (M. Masullo).
[1] These authors equally contributed to this work.

0300-9084/$ – see front matter © 2011 Elsevier Masson SAS. All rights reserved.
doi:10.1016/j.biochi.2011.08.019

able to enhance the intrinsic GTPase activity of some SsEF-1α mutants, but not that of the wild-type enzyme [11–13]; GE2270A was found to increase the GDP/GTP exchange rate and to reduce the intrinsic GTPase of the archaeal elongation factor [14]. Furthermore, fusidic acid, another eubacterial antibiotic acting on the elongation factor G, was found to interact with its archaeal functional analogue SsEF-2 [15]. It has to be noted that, in an *in vitro* reconstituted system, none of these antibiotics, except tetracycline, were able to inhibit protein synthesis in *S. solfataricus* [16].

All these findings induced us to investigate the effect of eubacterial antibiotic pulvomycin on the molecular and functional properties of SsEF-1α. The results obtained either by fluorescence spectroscopic analysis or through the effect produced by the antibiotic on the elongation factor showed that pulvomycin was able to interact with the SsEF-1α.

2. Materials and methods

2.1. Chemicals, buffers and enzymes

Labelled compounds and chemicals were as already reported [17]. Pulvomycin powder was a gift from Prof. Andrea Parmeggiani and it was used as 28 mM stock solution in absolute ethanol and stored at −80 °C. The spectral quality of the antibiotic was checked as reported [18] and its concentration was determined using a molar absorbance coefficient of 74 582 M^{-1} cm^{-1} at 320 nm in methanol. The following buffers were used: Buffer A: 20 mM Tris·HCl, pH 7.8, 50 mM KCl, 10 mM $MgCl_2$; buffer B: 20 mM Tris·HCl, pH 7.8, 10 mM $MgCl_2$, 1 mM DTT, 3.6 M NaCl.

SsEF-1α and its engineered or chimaeric forms were produced and purified as already reported [17,19,20]. SsRibosome, SstRNA, SsEF-2 and SsFRS were purified as reported [21,22].

2.2. SsEF-1α assays

The preparation of [^{3}H]Val-EctRNAVal, the formation of the ternary complex SsEF-1α·GTP·[^{3}H]Val-EctRNAVal, the protection against spontaneous deacylation of [^{3}H]Val-EctRNAVal and poly(U)-directed poly([^{3}H]Phe) synthesis were carried out as already described [5,14,21].

The ability of SsEF-1α to bind [^{3}H]GDP or to exchange the radiolabelled nucleotide for GDP or GTP was assayed by nitrocellulose filtration as described [17]. Following the titration of 1.0 μM SsEF-1α with 0.4–4 μM [^{3}H]GDP (specific radioactivity 3398 cpm/pmol), the apparent equilibrium dissociation constant (K_d') of the binary complex formed between SsEF-1α and [^{3}H]GDP was determined using Scatchard plots. K_d' for GTP was derived through competitive binding experiments [17] in which 0.5 μM SsEF-1α was incubated in the presence of 10 μM [^{3}H]GDP (specific radioactivity 800 cpm/pmol) and different concentrations (40–300 μM) of GTP.

The intrinsic NaCl-dependent GTPase activity ($GTPase^{Na}$) was measured in the presence of 3.6 M NaCl as reported [2]. The reaction mixture contained 0.5 μM purified elongation factor and 25 μM [γ-^{32}P]GTP (specific activity 400–900 cpm/pmol) in 200 μL of buffer B. The reaction was followed kinetically at 50 °C, and the amount of $^{32}P_i$ released was determined on 40 μl aliquots. The k_{cat} of $GTPase^{Na}$, the K_m for [γ-^{32}P]GTP, and the inhibition constants were determined by Lineweaver–Burk plots as reported [2].

The effect of pulvomycin on the thermophilicity of the $GTPase^{Na}$ was evaluated by determining the initial velocity of [γ-^{32}P]GTP breakdown in the 45–75 °C interval [7]; the data were then treated with the Arrhenius equation

$$\ln v = \ln A + E_a/R \cdot 1/T$$

in which v is the rate of GTP hydrolysis (s^{-1}) at a given temperature T (K), A is the Arrhenius constant (s^{-1}), E_a is the energy of activation (J mol^{-1}), and R is the gas constant (8.314 J mol^{-1} K^{-1}). By plotting ln v against $1/T$, the E_a can be derived from the slope of the straight-line obtained. The energetic parameters of activation ΔH^*, ΔS^* and ΔG^* were calculated at a given temperature by the equations

$$\Delta H^* = E_a - (R \cdot T) \quad \Delta S^* = R \cdot \ln(h \cdot N_A \cdot A/R \cdot T \cdot e) \quad \Delta G^* = \Delta H^* - T\Delta S^*$$

where h is the Plank constant (6.624×10^{-34} J s), N_A is the Avogadro's number (6.023×10^{23} molecules/mol), and e is the base of the natural logarithm (2.718).

The effect of pulvomycin on the chemical denaturation of SsEF-1α was evaluated by exposing the protein to guanidine hydrochloride (GuHCl, Sigma–Aldrich) as already reported [23], determining the residual $GTPase^{Na}$. To this aim, a stock solution of GuHCl (6.6 M) was prepared and mixed in different amounts with protein solutions to give a constant final value of the protein concentration (10 μM) and a variable concentration of GuHCl (0–6 M). Each sample was incubated overnight at room temperature and GuHCl-induced denaturation was evaluated by assaying the residual GTPase activity bringing each sample to a 0.6 M constant value of GuHCl concentration. Under these conditions, the $GTPase^{Na}$ of SsEF-1α was not affected at all.

2.3. Fluorescence measurements

Fluorescence spectra were recorded at 25 °C on a computer assisted Cary Eclipse spectrofluorimeter (Varian) at a scan rate of 60 nm/min using an excitation wavelength of 280 nm; excitation and emission slits were set to 10 nm. Spectra recorded in the presence of pulvomycin were obtained after further additions of a concentrated solution of the antibiotic and a correction for the dilution was applied. Blanks run in the absence of the protein were subtracted. The analysis of the binding affinity was carried out as already reported [24,25] considering that the quenched fluorescence (Q) at respective maximum is a function of the maximum possible quenching (Q_{max}) at an infinite ligand concentration. In particular, the binding affinity of the protein·pulvomycin complex (K_d) was calculated from the equation

$$Q = (Q_{max} \cdot [\text{Pulvomycin}])/(K_d + [\text{Pulvomycin}])$$

through a double reciprocal plot.

3. Results

3.1. Effect of pulvomycin on the functional properties of SsEF-1α

The interaction between SsEF-1α and pulvomycin was studied analysing the effect produced by the antibiotic on the functional properties of the elongation factor.

In a first approach, the ability of pulvomycin to inhibit protein synthesis in a reconstituted system containing purified macromolecular components from *S. solfataricus* was investigated; the antibiotic, at 200 μM concentration, reduced the poly(U)-directed poly(Phe) synthesis rate of about 4-fold (Fig. 1A). The inhibition data obtained at different pulvomycin concentrations (Fig. 1B), treated through a first-order analysis (Fig. 1C), allowed the extrapolation of the concentration of antibiotic leading to 50% inhibition (173 μM).

The effect of the antibiotic was also studied on the partial reactions catalysed by SsEF-1α. Concerning ternary complex formation between Val-$EctRNA^{Val}$, SsEF-1α and guanosine nucleotides, evaluated through the ability of the elongation factor to

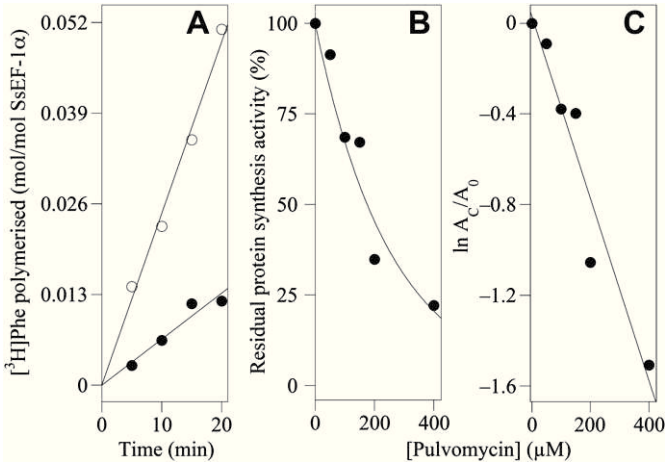

Fig. 1. Effect of pulvomycin on the poly(U)-directed poly(Phe) synthesis at 75 °C. *A* Kinetics of the [^{3}H]Phe incorporation in the absence (open symbol) or in the presence (filled symbol) of 200 μM pulvomycin. The reaction mixture (250 μl) contained 0.5 μM SsEF-1α, 0.25 μM Ssribosome, 80 μg/ml SstRNA, 0.1 μM SsEF-2, 2.0 μM [^{3}H]Phe (specific activity 1514 cpm/pmol) in 25 mM Tris·HCl, pH 7.5 buffer supplemented with 19 mM magnesium acetate, 10 mM NH_4Cl, 10 mM dithiothreitol, 2.4 mM ATP, 1.6 mM GTP, 0.16 mg/ml poly(U) and 3 mM spermine. At the times indicated, 50 μl aliquots were withdrawn and analysed for the amount of [^{3}H]Phe incorporated. *B* Effect of different concentrations of pulvomycin. *C* The data reported in *B* were treated as a first-order behaviour. A_0 represent the activity measured in the absence of pulvomycin, whereas A_C is the activity at the concentration *C* of the antibiotic.

protect [^{3}H]Val-EctRNAVal against spontaneous deacylation [5], pulvomycin was able to decrease the affinity of the elongation factor toward aa-tRNA only in the presence of GTP (Fig. 2A), to an extent similar to that measured in the presence of GDP (Fig. 2B).

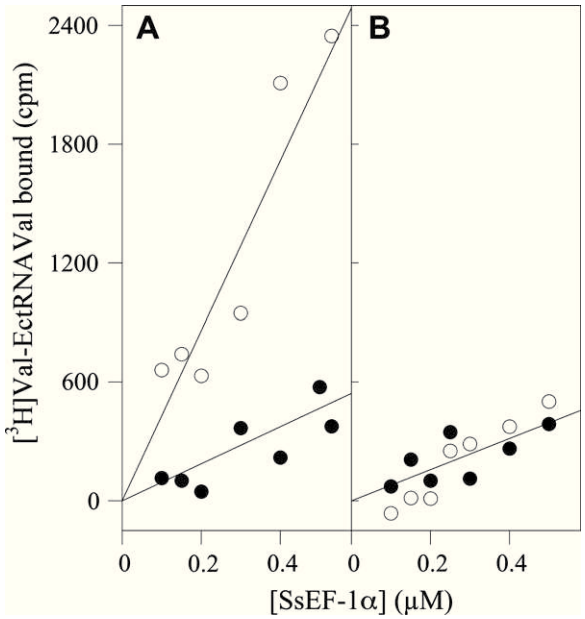

Fig. 2. Effect of pulvomycin on the formation of the ternary complex between SsEF-1α, [^{3}H]ValEc-tRNA^{Val} and GTP or GDP. The reaction mixture (30 μl) prepared in 25 mM Tris·HCl, pH 7.8 buffer, 10 mM NH_4Cl, 10 mM DTT, and 20 mM magnesium acetate, contained 4.6 pmol of [^{3}H]ValEc-tRNA^{Val} (specific activity 1185 cpm/pmol). To allow ternary complex formation the mixture was incubated for 1 h at 0 °C in the presence of the indicated amount of SsEF-1α·GTP (*A*) or SsEF-1α·GDP (*B*), in the absence (open symbols) or in the presence (filled symbols) of 20 μM pulvomycin. The deacylation reaction was then carried out for 1 h at 50 °C and the residual [^{3}H]ValEc-tRNA^{Val} was determined as cold trichloroacetic acid insoluble material.

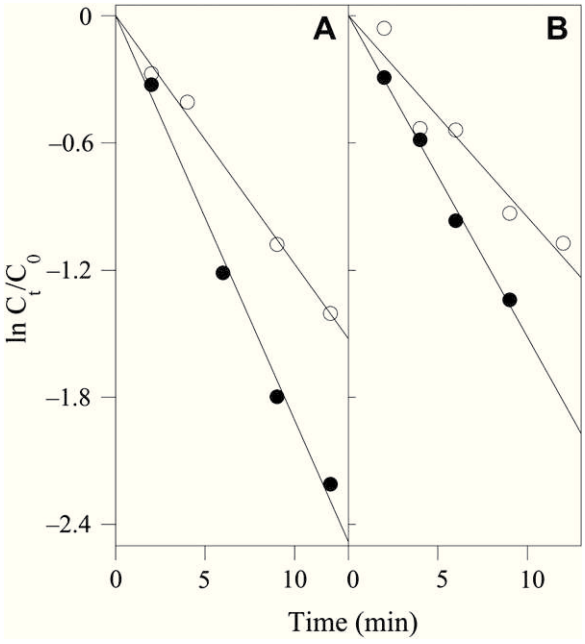

Fig. 3. Effect of pulvomycin on the guanosine nucleotide exchange on the SsEF-1α·[^{3}H]GDP complex. The reaction mixture (250 μl) prepared in buffer A contained 0.5 μM SsEF-1α·[^{3}H]GDP in the absence (empty symbols) or in the presence (filled symbols) of 20 μM pulvomycin. The nucleotide exchange reaction was started at 60 °C by adding 1 mM GDP (A) or GTP (B) final concentration. At the times indicated, the amount of the residual radiolabelled binary complex was determined on 50 μl aliquots by nitrocellulose filtration. The data were treated according to a first-order kinetics.

3.2. Effect of pulvomycin on the interaction between SsEF-1α and guanosine nucleotides

The effect of pulvomycin on the interaction between the elongation factor and guanosine nucleotides was assessed on both the exchange rate and affinity. In presence of pulvomycin, the guanosine nucleotides exchange rate on the archaeal elongation factor was 1.5-fold faster for both GDP (Fig. 3A) and GTP (Fig. 3B). In addition, in the presence of the antibiotic, the guanosine nucleotides apparent equilibrium dissociation constants for GDP and GTP were slightly lower (Table 1) and the effect produced was more evident in the case of GTP. Regarding the slight increased affinity for GDP, the effect of pulvomycin can be ascribed to a higher increase of the association constant with the respect to the dissociation one.

The interaction between pulvomycin and SsEF-1α, was also studied by its effect on the GTPase^{Na}. As reported in Fig. 4A, increasing pulvomycin concentration increased the rate of the intrinsic GTPase catalysed by SsEF-1α, reaching its maximum stimulation effect at 30 μM. This stimulation was not observed for two truncated forms of the archaeal elongation factor lacking the C-terminal (Ss(GM)EF-1α) or the C- and the M-domains (Ss(G)EF-1α) [17], as well as for an engineered elongation factor constituted by

Table 1
Effect of pulvomycin on the affinity of SsEF-1α for guanosine nucleotides at 60 °C.

SsEF-1α	K_d'		k_{-1}	k_{+1}
	GDP (μM)	GTP (μM)	GDP (min^{-1})	GDP (μM^{-1} min^{-1})
− pulvomycin	0.35 ± 0.10	4.7 ± 1.5	0.13 ± 0.02	0.37
+ pulvomycin	0.30 ± 0.11	2.6 ± 2.0	0.19 ± 0.01	0.63

The K_d' and k_{-1} values represent the average of 3–4 different determinations. k_{+1} was calculated as k_{-1}/K_d'.

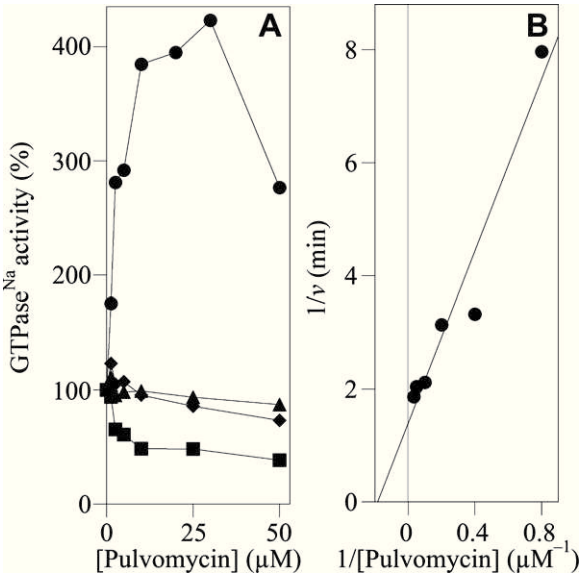

Fig. 4. Effect of pulvomycin on the intrinsic GTPase of SsEF-1α and its engineered forms. *A* The GTPase^{Na} of SsEF-1α (●), Ss(GM)EF-1α (■), Ss(G)EF-1α (▲), and the archaeal/eubacterial chimaeric elongation factor (◆) was determined in the presence of the indicated pulvomycin concentration, as described in Materials and methods. The data were reported as a percentage of the activity measured in the absence of the antibiotic. *B* The data referring to SsEF-1α up to 30 μM pulvomycin were treated by the Lineweaver–Burk equation after the subtraction of the GTPase^{Na} activity of SsEF-1α measured in the absence of pulvomycin (0.166 min^{-1}).

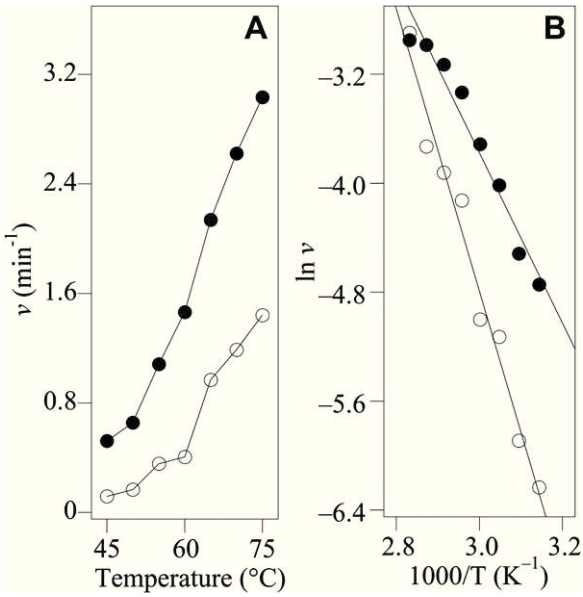

Fig. 5. Effect of pulvomycin on the thermophilicity of the GTPase^{Na} catalysed by SsEF-1α. *A* The rate of GTP breakdown was determined as reported in the Methods section at the indicated temperature, in the absence (empty symbols) or in the presence (filled symbols) of 20 μM pulvomycin. At each temperature, the times used for the determination were selected in order to give a linear relationship between the time and the amount of [γ-^{32}P]GTP hydrolysed. *B* Arrhenius analysis of the data reported in *A*.

the G-domain of SsEF-1 and the M- and C- domains of EcEF-Tu [20]. The data referring to SsEF-1α up to a concentration of pulvomycin of 30 μM followed a saturation behaviour and, through a double reciprocal plot (Fig. 4B), the concentration of pulvomycin required for 50% stimulation (5.4 μM) can be derived from the *X*-axis intercept. The effect of the antibiotic on the kinetic parameters of the GTPase^{Na} was also investigated. The data reported in Table 2 indicated that the increased catalytic efficiency, measured in the presence of 20 μM pulvomycin can be ascribed to an increased affinity for the substrate together with an higher hydrolytic rate. Furthermore, the GTPase^{Na} was competitively inhibited by GDP and the slowly hydrolysable GTP analog GppNHp also in the presence of pulvomycin. In particular, the inhibition power, evaluated through the comparison of the inhibition constants (Table 2), was reduced by 4-fold for both nucleotides, thus confirming the observed increased affinity for the guanosine nucleotides in the presence of the antibiotic.

The effect of pulvomycin on the thermophilicity of GTPase^{Na} was also analysed in the 45–75 °C temperature interval and the antibiotic exerted its stimulatory function at all the tested temperatures (Fig. 5A). The analysis of data through the Arrhenius equation, gave a straight-line also in the presence of the antibiotic, but with a different slope with respect to that obtained in its absence (Fig. 5B). From these data the energetic parameters of activation of GTPase^{Na} in absence or in presence of pulvomycin were calculated and reported in Table 3. The antibiotic reduced the energy of activation of the hydrolytic reaction without changing the free energy of activation. However, a differential effect on the other thermodynamic parameters of activation was observed; in particular, pulvomycin produced a favourable variation of enthalpy of activation that is accompanied by an unfavourable variation of the entropy.

3.3. Effect of pulvomycin on chemical denaturation of SsEF-1α

The effect of antibiotic on the resistance of SsEF-1α against guanidine hydrochloride denaturation was investigated by measuring its residual GTPase activity in the presence of guanidine hydrochloride at increasing concentrations, in the presence or in the absence of 20 μM pulvomycin (Fig. 6). The concentration of denaturant agent to get 50% inactivation of the GTPase^{Na} was 3.0 M in the absence and 3.6 M in the presence of the antibiotic. These results indicated that pulvomycin exerted a protective action against chemical denaturation of SsEF-1α.

3.4. Effects of pulvomycin on fluorescence spectra

The effect of pulvomycin on the molecular properties was also studied by fluorescence spectroscopy in the aromatic region of the fluorescence spectrum (λ_{exc} 280 nm) of SsEF-1α and its truncated forms and compared to that observed for EcEF-Tu. As shown in Fig. 7, pulvomycin exerted for all proteins investigated, a strong

Table 2
Effect of pulvomycin on the kinetic parameters of the GTPase^{Na} catalysed by SsEF-1α at 50 °C.

	K_m (μM)	k_{cat} (min^{-1})	k_{cat}/K_m (min^{-1} μM^{-1})	K_i (GDP) (μM)	K_i (GppNHp) (μM)
− pulvomycin	4.36 ± 1.8	0.18 ± 0.04	0.04	0.12 ± 0.04	0.23 ± 0.08
+ pulvomycin	2.61 ± 1.0	0.47 ± 0.14	0.18	0.47 ± 0.10	0.93 ± 0.15

The K_m and k_{cat} values represent the average of 3–4 different determinations.

Table 3
Effect of pulvomycin on the energetic parameters of activation of GTPase^{Na} of SsEF-1α.

	E_a (kJ mol^{-1})	ΔH^a (kJ mol^{-1})	ΔS^a (J mol K^{-1})	ΔG^a (kJ mol)
− pulvomycin	86	83	−36	95
+ pulvomycin	53	50	−127	92

[a] Calculated at 60 °C.

fluorescence quenching at λ_{max} which was accompanied by the appearance of a new peak at 360 nm; this behaviour can be explained by a combination of both a static and a dynamic quenching [26], as well as by an inner filter effect [27] due to the absorption of pulvomycin at the emission region of spectrum (λ_{max} 320 nm); therefore, these findings impaired the correction for the inner filter effect [26]. Moreover, the presence of a new peak at a higher wavelength could indicate a conformational modification induced by antibiotic involving specific aromatic residues, mainly tryptophans [26]. However, a differential effect on quenching and new peak appearance was exerted by pulvomycin on the different proteins analysed. In particular, a prevalence on the quenching effect was observed in the case of SsEF-1α (Fig. 7A), whereas a higher effect on the new peak appearance was observed in the case of the truncated forms of the elongation factor lacking the C-terminal (Fig. 7B) or both the C- and M- domains (Fig. 7C), but also for EcEF-Tu (Fig. 7D). These results, although to a lesser extent, were also observed using an excitation wavelength of 295 nm (not shown).

The analysis of the quenching effect allowed an evaluation of the binding process [24,25] through the variation of the quenched fluorescence (Q) against pulvomycin concentration (Fig. 8A). In fact, the linearity of the double reciprocal plot (Fig. 8B), allowed the extrapolation of the binding constant from the abscissa axis intercept. The values obtained indicated that intact SsEF-1α and EcEF-Tu showed a similar affinity for the drug being the K_d 11.6 μM and 13.9 μM, respectively. In the case of SsEF-1α the lacking of C-terminal domain lowered the affinity of the elongation factor towards pulvomycin ($K_d = 23.9$ μM), whereas the truncation of both the C- and M-domains induced a less evident effect ($K_d = 16.6$ μM).

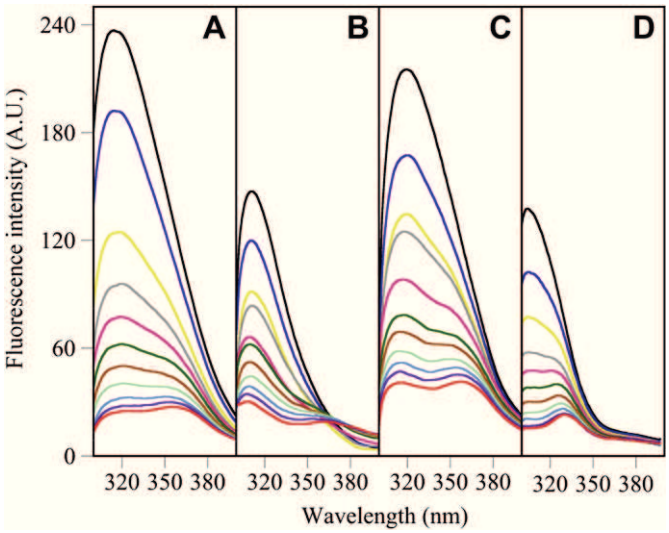

Fig. 7. Effect of pulvomycin on fluorescence spectra of SsEF-1α and its engineered forms. Spectra were recorded in buffer A in the presence of 4 μM SsEF-1α (*A*), Ss(GM)EF-1α (*B*), Ss(G)EF-1α (*C*) or EcEF-Tu (*D*) in the absence (black line) or in the presence of increasing concentration of pulvomycin ranging between 4 (blue) and 38 μM (red) shown by different colors. (For interpretation of the references to colour in this figure legend, the reader is referred to the web version of this article).

4. Discussion

In this work, several aspects of the action of pulvomycin, on the molecular and functional properties of SsEF-1α were investigated. The results obtained indicated that this eubacterial antibiotic, isolated from *Streptoverticillium netropsis* [18], was able to interact with the archaeal elongation factor. It was previously reported that pulvomycin at 1 mM final concentration was not able to inhibit

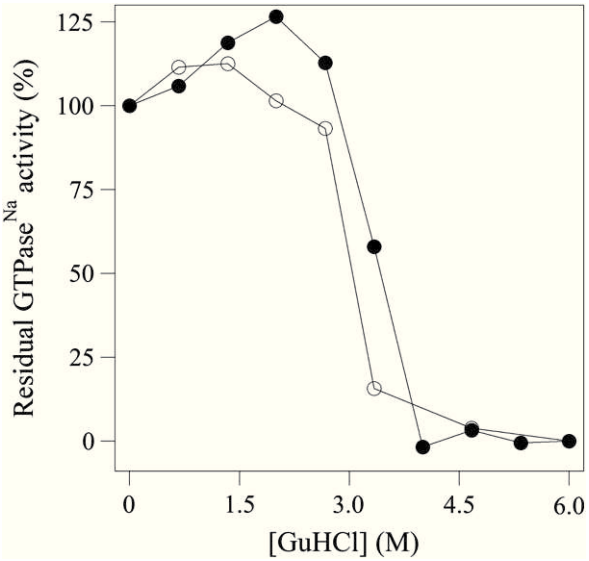

Fig. 6. Effect of pulvomycin on the chemical denaturation of SsEF-1α. The residual GTPase^{Na} was determined, after incubation of the samples at indicated guanidine hydrocloride concentration, as reported in Materials and methods, in the absence (empty symbols) or in the presence (filled symbols) of pulvomycin.

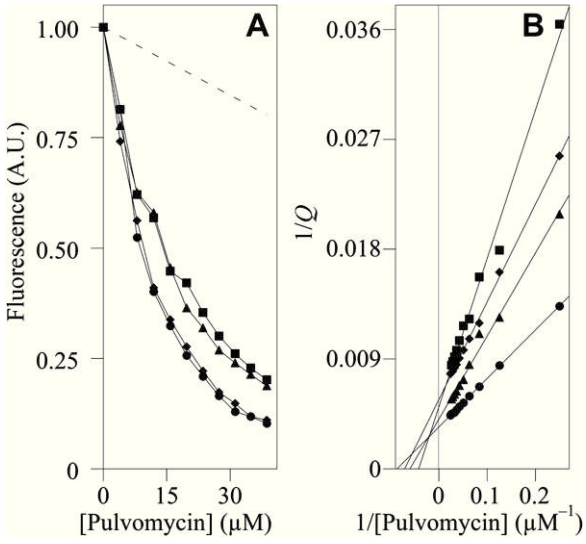

Fig. 8. Quenching analysis of the interaction between pulvomycin and SsEF-1α or its engineered forms. *A* The fluorescence at the respective maximum was plotted against increasing concentration of pulvomycin for SsEF-1α (●, 314 nm), Ss(GM)EF-1α (■, 311 nm), Ss(G)EF-1α (▲, 319 nm), and EcEF-Tu (◆, 310 nm). The dashed line reports the effect on the fluorescence of bovine serum albumin (346 nm), used as a negative control for the interaction. *B* Double reciprocal plot of the data reported in *A*.

protein synthesis in a reconstituted cell-free system from *S. solfataricus* [16]. The availability of purified macromolecular components of *S. solfataricus* required for an *in vitro* protein synthesis assay showed that pulvomycin was able to inhibit poly(U)-directed poly(Phe) synthesis; however, the concentration of antibiotic required to get 50% inhibition (173 μM) was at least two order of magnitude higher than that measurable for both gram-negative and gram-positive eubacterium [28,29], and some methanogenic archaea [30], but at least one order of magnitude lower than that required for *Saccharomyces cerevisiae* [30] or other eukaryotic cells [31]. These findings prompted us an investigation on the effect exerted by pulvomycin on the partial reactions catalysed by SsEF-1α. The results obtained indicated that the antibiotic affected the different functional properties of the elongation factor but at concentrations significantly lower than that required for the inhibition of protein synthesis. This difference can be explained by the finding that the protein synthesis assay was carried out in the presence of several components, mainly ribosomes, EF-2 and synthetic mRNA, rendering the effect of the antibiotic less powerful. However, no effect was exerted by pulvomycin on the intrinsic (Supplementary material Fig. S1) and ribosome-dependent (Supplementary material Fig. S2) GTPase catalysed by SsEF-2. Therefore, a specific effect of pulvomycin on both ribosome and EF-2 can be excluded. On the other hand, this behaviour was also reported for the effects exerted by two other eubacterial antibiotics acting on the partial reactions catalysed by SsEF-1α [14,32]. Regarding the effects on the partial reactions, the presence of the antibiotic reduced the ability of SsEF-1α to form a ternary complex only in the presence of GTP, and the affinity for the aa-tRNA became very similar to that measured using GDP. These findings indicated that, as found for EcEF-Tu, even for an archaeal elongation factor the impairment of the ternary complex formation was the target of this antibiotic action [28].

Regarding the effect of the antibiotic on the interaction with guanosine nucleotides, the results obtained indicated that pulvomycin increased the rate of nucleotide exchange for both GDP and GTP. More pronounced effects were instead observed when the $GTPase^{Na}$ was used as a probe to study the antibiotic interaction. In particular, pulvomycin was able to stimulate the intrinsic NaCl-dependent GTPase catalysed by SsEF-1α, a finding that was already reported for the intrinsic GTPase of EcEF-Tu [33], even though in that case the stimulatory effect was more pronounced. However, the stimulatory effect exerted by pulvomycin cannot be detected for the catalytic activity elicited by the truncated forms of SsEF-1α lacking the C- or the C- and M-domains. These results indicated that the integrity of the elongation factor was required to observe the effect, and that the C-terminal domain was essential for the interaction. The analysis of the energetic parameters of activation could give an explanation of the increased hydrolytic rate of the reaction, measured in the presence of pulvomycin. Indeed, the reduced energy of activation, induced by the antibiotic, was essentially due to a reduced enthalpy of activation, even though an unfavourable entropy factor leads to an unvaried free energy of activation.

The interaction between the archaeal elongation factor and pulvomycin was also demonstrated by the finding that the antibiotic rendered SsEF-1α slightly more resistant to guanidine hydrochloride denaturation. This finding is indicative of a more compact molecular organisation of the elongation factor observed in the presence of pulvomycin. However, a direct stabilising effect of the antibiotic on the protein in the complex cannot be excluded.

Finally, the data obtained from fluorescence spectroscopy, suggested a conformational change induced by the antibiotic upon its interaction with SsEF-1α and confirmed those already reported for EcEF-Tu [8,33]. However, the integrity of the archaeal elongation factor is required to bind the antibiotic with higher affinity. Furthermore, the appearance of a fluorescence band at 360 nm in the presence of pulvomycin for all proteins investigated, is indicative of the exposition to the aqueous solvent of tryptophan residues, even though a resonance energy transfer between close tyrosines and tryptophan(s) residues [26] cannot be excluded. In the primary structure of SsEF-1α two tryptophans and ten tyrosines were present, most of them in the nucleotide binding domain (W209, Y84, Y122, Y161, Y166, Y180, Y210, Y218). Therefore, the finding that the appearance of the 360 nm band was also evident on the truncated forms of the elongation factor, indicated that the main target of the solvent exposition upon antibiotic binding, was the region comprising Trp209 (Fig. 9) to which the resonance energy transfer could occur from tyrosines 161, 166 and 210, surrounding this residue.

Fig. 9. Close-up of the three dimensional structure of the nucleotide binding domain of SsEF-1α (PDB code 1JNY) surrounding W209. Tyrosines 161, 166 and 210 are indicated in red; tryptophan 209 in yellow. The picture was generated using the software iMol (http://www.pirx.com/iMol). (For interpretation of the references to colour in this figure legend, the reader is referred to the web version of this article).

5. Conclusions

In conclusion, the data presented strongly indicated a molecular interaction between an archaeal elongation factor 1α and the eubacterial antibiotic pulvomycin. These findings, besides being useful for studying the interaction between pulvomycin and eukaryotic elongation factor 1α, could be used as probe to investigate phylogenetic relationships among living domains.

Acknowledgements

This work was supported by MiUR, PRIN 2007 and 2009 to MM and PRIN 2008 to PA. We are grateful to Prof. Andrea Parmeggiani for critical reading of the manuscript and for providing samples of pulvomycin.

Appendix. Supplementary data

Supplementary data associated with this article can be found in the online version, at doi:10.1016/j.biochi.2011.08.019.

References

[1] F. Klink, Elongation factors. in: C.R. Woese, R. Wolfe (Eds.), The Bacteria, Archaebacteria, vol. VIII. Academic Press, London, 1985, pp. 379–410.

[2] M. Masullo, E. De Vendittis, V. Bocchini, Archaebacterial elongation factor 1 alpha carries the catalytic site for GTP hydrolysis, J. Biol. Chem. 269 (1994) 20376–20379.
[3] H. Song, M.R. Parsons, S. Rowsell, G. Leonard, S.E. Phillips, Crystal structure of intact elongation factor EF-Tu from *Escherichia coli* in GDP conformation at 2.05 Å resolution, J. Mol. Biol. 285 (1999) 1245–1256.
[4] L. Vitagliano, M. Masullo, F. Sica, A. Zagari, V. Bocchini, The crystal structure of *Sulfolobus solfataricus* elongation factor 1alpha in complex with GDP reveals novel features in nucleotide binding and exchange, EMBO J. 20 (2001) 5305–5311.
[5] G. Raimo, M. Masullo, B. Lombardo, V. Bocchini, The archaeal elongation factor 1alpha bound to GTP forms a ternary complex with eubacterial and eukaryal aminoacyl-tRNA, Eur. J. Biochem. 267 (2000) 6012–6018.
[6] J. Hachmann, D.L. Miller, H. Weissbach, Purification of factor Ts: studies on the formation and stability of nucleotide complexes containing transfer factor Tu, Arch. Biochem. Biophys. 147 (1971) 457–466.
[7] G. Raimo, M. Masullo, G. Savino, G. Scarano, G. Ianniciello, A. Parente, V. Bocchini, Archaeal elongation factor 1β is a dimer. Primary structure, molecular and biochemical properties, Biochim. Biophys. Acta 1293 (1996) 106–112.
[8] A. Parmeggiani, P. Nissen, Elongation factor Tu-targeted antibiotics: four different structures, two mechanisms of action, FEBS Lett. 580 (2006) 4576–4581.
[9] S.E. Heffron, S. Mui, A. Aorora, K. Abel, E. Bergmann, F. Jurnak, Molecular complementarity between tetracycline and the GTPase active site of elongation factor Tu, Acta Crystallogr. D62 (2006) 1392–1400.
[10] S.E. Heffron, F. Jurnak, Structure of an EF-Tu complex with a thiazolyl peptide antibiotic determined at 2.35 Å resolution: atomic basis for GE2270A inhibition of EF-Tu, Biochemistry 39 (2000) 37–45.
[11] M. Masullo, P. Cantiello, B. de Paola, F. Catanzano, P. Arcari, V. Bocchini, G13A substitution affects the biochemical and physical properties of the elongation factor 1 alpha. A reduced intrinsic GTPase activity is partially restored by kirromycin, Biochemistry 41 (2002) 628–633.
[12] M. Masullo, P. Cantiello, B. de Paola, A. Fiengo, L. Vitagliano, A. Zagari, P. Arcari, Valine 114 replacements in archaeal elongation factor 1 alpha enhanced its ability to interact with aminoacyl-tRNA and kirromycin, Biochemistry 41 (2002) 14482–14488.
[13] P. Cantiello, I. Castellano, E. De Vendittis, A. Lamberti, O. Longo, M. Masullo, G. Raimo, M.R. Ruocco, P. Arcari, Interaction of archaeal translation elongation factors with eubacterial protein synthesis inhibitors, Curr. Top. Biochem. Res. 6 (2004) 145–154.
[14] M. Masullo, P. Cantiello, P. Arcari, Archaeal elongation factor 1alpha from *Sulfolobus solfataricus* interacts with the eubacterial antibiotic GE2270A, Extremophiles 8 (2004) 499–505.
[15] E. De Vendittis, B. de Paola, M. Gogliettino, B.S. Adinolfi, T. Duvold, V. Bocchini, Fusidic and helvolic acid inhibition of elongation factor 2 from the archaeon *Sulfolobus solfataricus*, Biochemistry 41 (2002) 14879–14884.
[16] P. Cammarano, A. Teichner, P. Londei, M. Acca, B. Nicolaus, J.L. Sanz, R. Amils, Insensitivity of archaebacterial ribosomes to protein synthesis inhibitors. Evolutionary implications, EMBO J. 4 (1985) 811–816.
[17] M. Masullo, G. Ianniciello, P. Arcari, V. Bocchini, Properties of truncated forms of the elongation factor 1alpha from the archaeon *Sulfolobus solfataricus*, Eur. J. Biochem. 243 (1997) 468–473.
[18] R.J. Smith, D.H. Williams, J.C.J. Barna, I.R. McDermott, K.D. Haegele, F. Piriou, J. Wagner, W. Higgins, Structure revision of the antibiotic pulvomycin, J. Am. Chem. Soc. 107 (1985) 2849–2857.
[19] G. Ianniciello, M. Masullo, M. Gallo, P. Arcari, V. Bocchini, Expression in *Escherichia coli* of thermostable elongation factor 1 alpha from the archaeon *Sulfolobus solfataricus*, Biotechnol. Appl. Biochem. 23 (1996) 41–45.
[20] P. Arcari, M. Masullo, A. Arcucci, G. Ianniciello, B. de Paola, V. Bocchini, A chimeric elongation factor containing the putative guanine nucleotide binding domain of archaeal EF-1 alpha and the M and C domains of eubacterial EF-Tu, Biochemistry 38 (1999) 12288–12295.
[21] G. Raimo, M. Masullo, A. Parente, A. Dello Russo, V. Bocchini, Molecular, functional and structural properties of an archaebacterial elongation factor 2, Biochim. Biophys. Acta 1132 (1992) 127–132.
[22] B. Lombardo, G. Raimo, V. Bocchini, Molecular and functional properties of an archaeal phenylalanyl-tRNA synthetase from the hyperthermophile *Sulfolobus solfataricus*, Biochim. Biophys. Acta 1596 (2002) 246–252.
[23] V. Granata, G. Graziano, A. Ruggiero, G. Raimo, M. Masullo, P. Arcari, L. Vitagliano, A. Zagari, Chemical denaturation of the elongation factor 1α isolated form the hyperthermophilic archaeon *Sulfolobus solfataricus*, Biochemistry 45 (2006) 719–726.
[24] J.S. Johansson, B.R. Gibney, F. Rabanal, K.S. Reddy, P.L. Dutton, A designed cavity in the hydrophobic core of a four-α-helix bundle improves volatile anesthetic binding affinity, Biochemistry 37 (1998) 1421–1429.
[25] J.S. Johansson, D. Scharf, L.A. Davies, K.S. Reddy, R.G. Eckenhoff, A designed four-α-helix bundle that binds the volatile general anesthetic halothane with high affinity, Biophys J. 78 (2000) 982–993.
[26] J.R. Lakowicz, Principles of Fluorescence Spectroscopy, third ed. Springer, New York, 2006.
[27] C.A. Parker, W.T. Rees, Fluorescence spectrometry. A review, Analyst 87 (1962) 83–111.
[28] H. Wolf, D. Assmann, E. Fischer, Pulvomycin, an inhibitor of protein biosynthesis preventing ternary complex formation between elongation factor Tu, GTP, and aminoacyl-tRNA, Proc. Natl. Acad. Sci. USA 75 (1978) 5324–5328.
[29] P. Landini, M. Bandera, A. Soffientini, B.P. Goldstein, Sensitivity of elongation factor Tu (EF-Tu) from different bacterial species to the antibiotics efrotomycin, pulvomycin and MDL 62879, J. Gen. Microbiol. 139 (1993) 769–774.
[30] P. Londei, J.L. Sanz, S. Altamura, H. Hummel, P. Cammarano, R. Amils, A. Böck, H. Wolf, Unique antibiotic sensitivity of archaebacterial polypeptide elongation factors, J. Bacteriol. 167 (1986) 265–271.
[31] B. Schmid, T. Anke, H. Wolf, Action of pulvomycin and kirromycin on eukaryotic cells, FEBS Lett. 96 (1978) 189–191.
[32] A. Lamberti, N.M. Martucci, I. Ruggiero, P. Arcari, M. Masullo, Interaction between the antibiotic tetracycline and the elongation factor 1α from the archaeon *Sulfolobus solfataricus*, Chem. Biol. Drug Des. 78 (2011) 260–268.
[33] A. Parmeggiani, I.M. Krab, S. Okamura, R.C. Nielsen, J. Nyborg, P. Nissen, Structural basis of the action of pulvomycin and GE2270A on elongation factor Tu, Biochemistry 45 (2006) 6846–6857.

Journal of Structural Biology 177 (2012) 506–512

Contents lists available at SciVerse ScienceDirect

Journal of Structural Biology

journal homepage: www.elsevier.com/locate/yjsbi

Crystallographic and spectroscopic characterizations of *Sulfolobus solfataricus* TrxA1 provide insights into the determinants of thioredoxin fold stability

Luciana Esposito [a,1], Alessia Ruggiero [a,b,1], Mariorosario Masullo [c,d], Maria Rosaria Ruocco [d], Anna Lamberti [d], Paolo Arcari [d,e], Adriana Zagari [a,b,e], Luigi Vitagliano [a,*]

[a] *Istituto di Biostrutture e Bioimmagini, CNR, Via Mezzocannone 16, I-80134 Napoli, Italy*
[b] *Dipartimento delle Scienze Biologiche, Sezione di Biostrutture, Università degli Studi di Napoli Federico II, Via Mezzocannone 16, I-80134 Napoli, Italy*
[c] *Dipartimento di Studi delle Istituzioni e dei Sistemi Territoriali, Università degli Studi di Napoli "Parthenope", Via Medina 40, 80133 Napoli, Italy*
[d] *Dipartimento di Biochimica e Biotecnologie Mediche, Università degli Studi di Napoli Federico II, Via S. Pansini 5, I-80131 Napoli, Italy*
[e] *CEINGE Biotecnologie Avanzate s.c.a r.l. – Via Gaetano Salvatore 486, I-80145 Napoli, Italy*

ARTICLE INFO

Article history:
Received 11 August 2011
Received in revised form 20 October 2011
Accepted 30 October 2011
Available online 7 November 2011

Keywords:
Protein structure-stability
Chemical denaturation
Disulfide bonds
Protein structure-function
X-ray crystallography
Circular dichroism

ABSTRACT

Structural characterizations of thioredoxins (Trxs) are important for their involvement in severe pathologies and for their stable scaffold. Here we report a combined structural and spectroscopic characterization of a Trx isolated from the hyperthermophilic archaeon *Sulfolobus solfataricus* (*Ss*TrxA1). Thermal denaturation unveils that *Ss*TrxA1 is endowed with a remarkable stability in the explored temperature range 50–105 °C. The structure of the oxidized form of *Ss*TrxA1 determined at 1.9 Å resolution presents a number of peculiar features. Although the protein was crystallized in a slightly acid medium (pH 6.5) as many as ten intramolecular/intermolecular carboxyl–carboxylate interactions involving glutamic and aspartic acid side chains are found in three independent *Ss*TrxA1 molecules present in the asymmetric unit. Surprisingly for a hyperthermostable protein, the structure of *Ss*TrxA1 is characterized by the presence (a) of a very limited number of intramolecular salt bridges and (b) of a cavity nearby Cys52, a residue that is frequently a phenylananine in other members of the family. Chemical denaturation investigations carried out on *Ss*TrxA1 and *Ss*TrxA2 show that both proteins present a significant stability against guanidine hydrochloride, thus indicating that ionic interactions play a minor role in their stabilization. Compared to Trxs from mesophilic sources, *Ss*TrxA1 displays a longer α-helix 1 and a shorter loop connecting this α-helix with β-strand 2. As these features are shared with Trxs isolated from thermophilic sources, the shortening of this loop may be a general strategy adopted to stabilize this fold. This feature may be exploited for the design of hyperthermostable Trx scaffolds.

1. Introduction

The ubiquitous thioredoxin (Trx) protein family is a member of the thioredoxin fold class of oxidoreductases (Arner and Holmgren, 2000; Carvalho et al., 2006a; Tang and Altman, 2011). The interest for Trxs is twofold. Not only are Trxs involved in fundamental biological processes, but their fold has also been used in interesting applications in protein engineering. In the protein engineering field, the stable fold of these proteins has been exploited in several biotechnological applications (Colas et al., 1996; LaVallie et al., 1993; Moretto et al., 2007).

From the biological point of view, these proteins play a key role in redox regulation of protein activity and redox signaling (Arner and Holmgren, 2000). In particular, the thioredoxin system, composed by Trx, thioredoxin reductase (TrxR), and NADPH, is essential for regulating the redox state of the cell and in protecting against oxidative stress. In this scenario, it is not surprising that Trxs are linked to a variety of disorders (Lillig and Holmgren, 2007; Maulik and Das, 2008).

Investigations carried out on Trxs isolated form thermophilic organisms simultaneously provide information on their biological role and on a possible strategy to generate scaffolds endowed with enhanced stability. It is important to note that, although the Trx system has been discovered decades ago, most of the functional and structural investigations have been performed on eukaryal and eubacteryal Trx systems. Indeed, only limited data are

Abbreviations: RMSD, root mean square deviation; PDB, Protein Data Bank; Trx, thioredoxin; TrxR, thioredoxin reductase; *Ss*TrxA2, *Sulfolobus solfataricus* Trx A2; *Ss*TrxA1, *Sulfolobus solfataricus* Trx A1; *Ec*Trx, *Escherichia coli* Trx; *Tt*Trx, *Thermus thermophilus* Trx; *Sp*Trx, spinach chloroplast M Trx; *St*Trx, *Sulfolobus tokodaii* Trx; GuHCl, guanidine hydrochloride.

* Corresponding author. Fax: +39 0812534560.
E-mail address: luigi.vitagliano@unina.it (L. Vitagliano).

[1] These authors equally contributed.

1047-8477/$ - see front matter © 2011 Elsevier Inc. All rights reserved.
doi:10.1016/j.jsb.2011.10.014

available for proteins involved in the Trx system of archaea, despite more recent work suggests that disulfide bond formation may contribute to the stabilization of proteins even in intracellular environments (Ladenstein and Ren, 2006). We have recently undertaken the functional and structural characterization of the intricate Trx system of the hyperthermophilic archaeon *Sulfolobus solfataricus*. This system includes two distinct Trxs (*Ss*TrxA2 and *Ss*TrxA1) and three potential TrxRs (*Ss*TrxRB1, *Ss*TrxRB2, and *Ss*TrxRB3) (Grimaldi et al., 2008; Ruocco et al., 2004). In our previous studies we have shown that *Ss*TrxA2 and *Ss*TrxA1 are both substrates for *Ss*TrxRB3 (Grimaldi et al., 2008). On the other hand, the other two potential TrxRs (*Ss*TrxRB1 and *Ss*TrxRB2), which share a significant sequence identity with members of the TrxR superfamily, are unable to reduce either *Ss*TrxA2 or *Ss*TrxA1 (Grimaldi et al., 2008). Notably, independent studies have also shown that *Ss*TrxRB3 is able to reduce a PDO-like protein (Pedone et al., 2006). In order to relate the functional properties of these enzymes to their three-dimensional structures and to elucidate the structural basis of their thermostability, we have also undertaken crystallographic investigations on the protein components of the *S. solfataricus* thioredoxin system (Ruggiero et al., 2005; Ruggiero et al., 2009a,b,c). We have previously described the crystal structure of *Ss*TrxRB3, which has provided insights into the determinants of its dual function (thioredoxin reductase and NADH oxidase) and thermostability (Ruggiero et al., 2009b). Moreover, we have also characterized the peculiar dimeric structure of *Ss*TrxA2 (Ruggiero et al., 2009a). We here report a combined structural and spectroscopic characterization of *Ss*TrxA1. This analysis suggests that the extraordinary thermal stability of *Ss*TrxA1 relies on the extension of a specific helix (helix 1) and on the shortening of a loop. As these features are shared with Trxs isolated from thermophilic sources, we suggest that these features represent a common strategy adopted by the evolution to stabilize the Trx structure that can be exploited for the design of hyperthermostable Trx scaffolds.

2. Materials and methods

2.1. Protein expression, purification, and crystallization

*Ss*TrxA1 expression, purification, and crystallization experiments have been conducted as previously reported (Grimaldi et al., 2008). *Ss*TrxA1 structure was solved by molecular replacement as previously described (Ruggiero et al., 2009c).

2.2. Structure refinement

The refinement of the structure was carried by using the program CNS (Brunger, 2007). Refinement runs were followed by manual intervention using the molecular graphic program O (Jones et al., 1991) to correct minor errors in the position of the side chains. Water molecules were identified by evaluating the shape of the electron density and the distance of potential hydrogen bond donors and/or acceptors. The inspection of the maps clearly indicated that, with the exception of few terminal residues or few exposed side chains, the electron density is well-defined for the entire protein. Crystallographic and stereo-chemical statistics of the final models are reported in Table 1. The coordinates of the model and the experimental structure factors of *Ss*TrxA1 have been deposited in the Protein Data Bank with the code 3TCO.

2.3. Circular dichroism spectra and denaturation

*Ss*TrxA1 CD spectra were recorded with a Jasco J-810 spectropolarimeter equipped with a Peltier temperature control system (Model PTC-423-S). Molar ellipticity per mean residue, $[\theta]$ in deg cm^2 dmol^{-1}, was calculated from the equation: $[\theta] = [\theta]_{obs}\cdot mrw\cdot(10\cdot l\cdot C)^{-1}$, where $[\theta]_{obs}$ is the ellipticity measured in degrees, mrw is the mean residue molecular mass (108.5 Da), C is the protein concentration in g l^{-1} and l is the optical path length of the cell in cm. Far-UV measurements (198–250 nm) were carried out using a 0.1 cm optical path length cell and a protein concentration of 0.30 mg ml^{-1}. Other parameters of the CD spectra registration are identical to those adopted in our previous studies (Granata et al., 2006, 2008) . Thermal denaturation curves were recorded over the 50–105 °C temperature range following the CD signal at 222 nm. The curves were registered using a 0.1 cm path length cell and a scan rate of 1.0 °C min^{-1}.

Chemical denaturation was carried out by treating the *Ss*TrxA1/*Ss*TrxA2 with guanidine hydrochloride (GuHCl). A commercial 8 M GuHCl solution (from Sigma) was utilized. Stock solutions of GuHCl, in different amounts, were mixed with protein solutions to give a constant final value of the protein concentration (0.15 mg ml^{-1}). The final concentration of GuHCl was in the range 0.0–7.0 M. All the chemical denaturation experiments were carried out in 20 mM sodium phosphate (pH 7.0) buffer after overnight incubation. The GuHCl-induced denaturations was investigated by CD spectroscopy by following the signal at 220 nm.

Table 1
Data collection and refinement statistics.

Data collection statistics	
Space group	$P2_1$
Cell parameters	
a(Å), b(Å), c(Å), β(°)	51.77, 75.09, 55.35, 112.64
Resolution range (Å)	25.0–1.90
Number of molecules in the asymmetric unit	3
Number of unique observations	28,606
R_{merge}[a]	9.7
Refinement statistics	
Resolution range (Å)	25.0–1.90
R_{factor}[b]/R_{free}[c]	0.189/0.222
Number of protein atoms	2543
Number of water molecules	233
Number of ethylene glycol molecules	8
Root mean square deviations from ideality	
Bonds (Å)	0.0079
Angles (°)	1.30

[a] $R_{merge} = \Sigma_{hkl}\Sigma_i|I_i(hkl) - \langle I(hkl)\rangle|/\Sigma_{hkl}\Sigma_i I_i(hkl)$, where $I_i(hkl)$ is the intensity of an observation and $\langle I(hkl)\rangle$ is the mean value for its unique reflection; summations are over all reflections.

[b] $R_{factor} = \Sigma_h||Fo(h)| - |Fc(h)||/\Sigma_h|Fo(h)|$, where Fo and Fc are the observed and calculated structure-factor amplitudes, respectively.

[c] R_{free} was calculated with 5% of the data excluded from the refinement.

3. Results and discussion

3.1. Overall structure

As previously reported (Ruggiero et al., 2009c), the N-terminal fragment of *Ss*TrxA1 (residues 1–24) is frequently cleaved from the thioredoxin domain upon protein expression and purification. As for *Ss*TrxA2 (Ruggiero et al., 2009c), well diffracting crystals of *Ss*TrxA1 were obtained only for the truncated form of the protein.

On the basis of electron density maps, an accurate tracing could be obtained for the region Lys27–Leu132 for the three copies of the protein, present in the asymmetric unit (hereafter denoted as molecule A, B, and C) (Fig. 1A). Although some extra electron density is evident at the C-terminus of Leu132 for all three chains, residue Lys133 has been built only for molecule A. With the exception of few solvent-exposed side chains, the electron density is well defined for all protein residues (Fig. 1B). *Ss*TrxA1 stereochemical parameters are in line with those reported for well refined protein

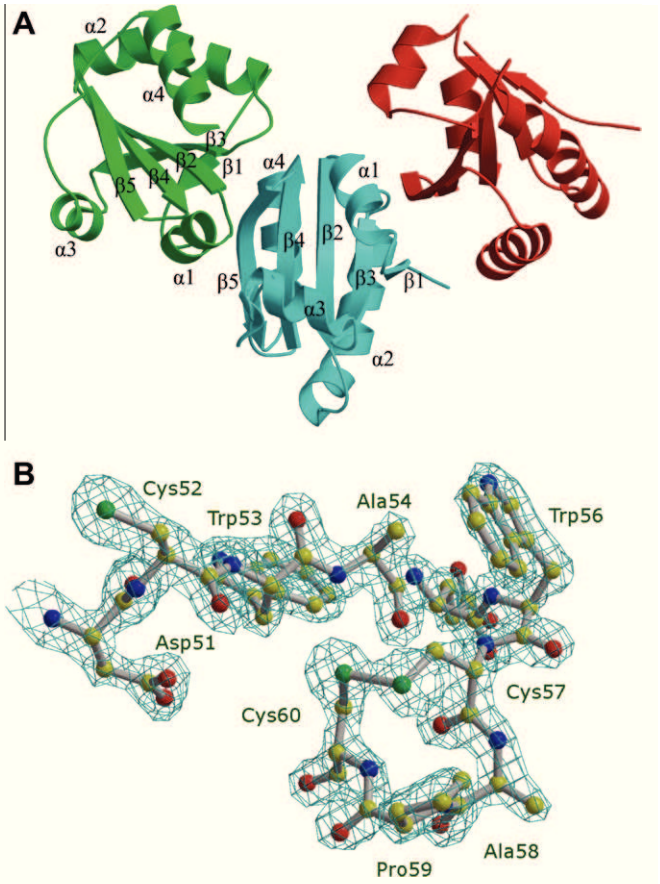

Fig. 1. Overall structure of the three molecules within the asymmetric unit (A) and the 2Fo–Fc omit electron density map of disulfide bond of molecule A countered at 1.7σ (B).

structures. The three independent molecules of the asymmetric unit display very similar structures. Indeed, pairwise RMSD values, calculated on the C^{α} atoms, between these molecules are in the range 0.36–0.56 Å. Unless otherwise specified, the features of molecule A will be described throughout the text.

As expected from the significant sequence identity with other members of the family, *Ss*TrxA1 adopts a typical thioredoxin fold characterized by a central five-stranded β-sheet with a ↑↑↑↓↑ topology surrounded by four α-helices (Fig. 1A). The analysis of *Ss*TrxA1 redox center clearly indicates that the reactive disulfide bridge Cys57–Cys60 of the three molecules is in its oxidized state (Fig. 1B). This finding is not surprising as crystallization experiments were conducted in air. In addition to the two cysteine residues that are involved in the redox center, in TrxA1 sequence there is an extra cysteine residue (Cys52) which is only five residues far from Cys57 of the redox center. The analysis of *Ss*TrxA1 structure indicates that Cys52 is oriented in such a way that it does not interfere with the Cys57–Cys60 disulfide bridge (Fig. 1B). Indeed, the distance between Cys52 side chain and the disulfide bridge of the redox center is ~10 Å. It is important to note that Cys52 is replaced by a bulky Phe residue (i.e. Phe27 in *E. coli* Trx) in Trxs with known three-dimensional structures (Fig. 2). This unusual mutation, which is found in only 11 over 1046 annotated bacterial/archaeal Trx sequences, is likely to generate a cavity in the protein core. Indeed, a comparison of *Ss*TrxA1 and *E. coli* Trx structures shows that the replacement of a bulky Phe side chain with a Cys creates a pocket of about 24 $Å^3$ in the TrxA1 structure (Fig. 3). The analysis of *Ss*TrxA1 structure indicates that there is no local rearrangement to fill the cavity. A careful inspection of the electron density map of the cavity indicates that no ordered water molecule is located inside. This is not surprising considering the hydrophobic nature of the side chains of the residues (Leu83, Val85, Ile91, Ala92, Tyr 95, Val 97 and Leu104) that delimitate this pocket. It is important to note that amino acid replacement that produce similar cavities in the structure of T4 lysozyme significantly destabilize the enzyme ($\Delta T_m \sim 10$ °C) (Eriksson et al., 1992). Therefore, it is somewhat surprising that even proteins endowed with extraordinary thermal stability may tolerate cavities in their 3D structures.

3.2. Comparison with other Trx structures

The comparison of *Ss*TrxA1 with *Ss*TrxA2 (Ruggiero et al., 2009a) and Trxs isolated from *Sulfolobus tokodaii* (*St*Trx) (Ming et al., 2007), *Escherichia coli* (*Ec*Trx) (Katti et al., 1990), *Thermus thermophilus* (*Tt*Trx) (Yanai, H., Yokoyama, S., Kuramitsu, S. PDB code 2CVK), and spinach chloroplast M (*Sp*Trx) (Capitani et al., 2000) yields root mean square deviation (RMSD) values in the range of 0.74–1.08 Å. This is in line with the sequence identity detected between *Ss*TrxA1 and these Trxs (38–45%) (Fig. 2). A detailed comparison of secondary structure elements of these proteins clearly indicates that they are well conserved in the family (Fig. 2). The only significant difference is detected for the α-helix 1, that is significantly shorter in Trxs isolated from mesophilic sources (*Ec*Trx and *Sp*Trx), (Fig. 2). Consequently the loop that connects this helix with strand 2 in mesophilic Trxs is virtually absent in Trxs (*Tt*Trx, *St*Trx, *Ss*TrxA2, *Ss*TrxA1) isolated from thermophilic organisms (Figs. 2 and 4). In line with our previous proposal (Ruggiero et al., 2009c), these findings suggest that the extension of the α-helix 1 and the consequent elimination of the loop may be related to the stability of these proteins. It is important to note that the local sequences of the proteins that exhibit a longer helix also present a deletion of a single residue in this region. The observation that the local sequences of both thermophilic and mesophilic Trxs present a significant level of variability may indicate that the deletion of a residue in this region may be sufficient for the elongation of the helix and, possibly, for increasing the fold stability.

3.3. SsTrxA1 crystal packing and oligomeric state

Previous characterizations of *Ss*TrxA1 and *Ss*TrxA2 by gel filtration showed that the elution behavior of both proteins was indicative of a dimeric state (Grimaldi et al., 2008). Accordingly, the crystallographic analysis of *Ss*TrxA2 led to the identification of a symmetric dimeric assembly in the crystalline state (Ruggiero et al., 2009a) whose stability was validated by analyses of the interface carried out using the program PISA (Krissinel and Henrick, 2007). The inspection of *Ss*TrxA1 crystal packing of the three independent molecules present in the asymmetric unit did not lead to the identification of symmetric dimers. Nevertheless, significant intermolecular interactions are detected in the crystal state (Table 2). Interestingly, these interactions are not random between crystal mates, but they are recurrent. Indeed, as reported in Table 2, the interface detected between molecule A and B closely resembles the one formed by molecules B and C and by molecule C and copy of molecule A (A#) generated by the translation along the ***a*** axis. This packing leads to the generation of a polymer-like assembly of *Ss*TrxA1 that extends for the entire crystal (Fig. S1). The interface area calculated by using the program PISA is ~450 $Å^2$. In addition to the hydrogen bonding interactions, each recurrent interface is characterized by the presence of two molecules of ethylene glycol, that was used as cryoprotectant in freezing the crystals. The position of these ethylene glycol molecules is stabilized by H-bonding interactions with protein atoms and, occasionally, with water molecules. In addition, they make extensive contacts with hydrophobic atoms that are exposed in the protein monomers. The similar

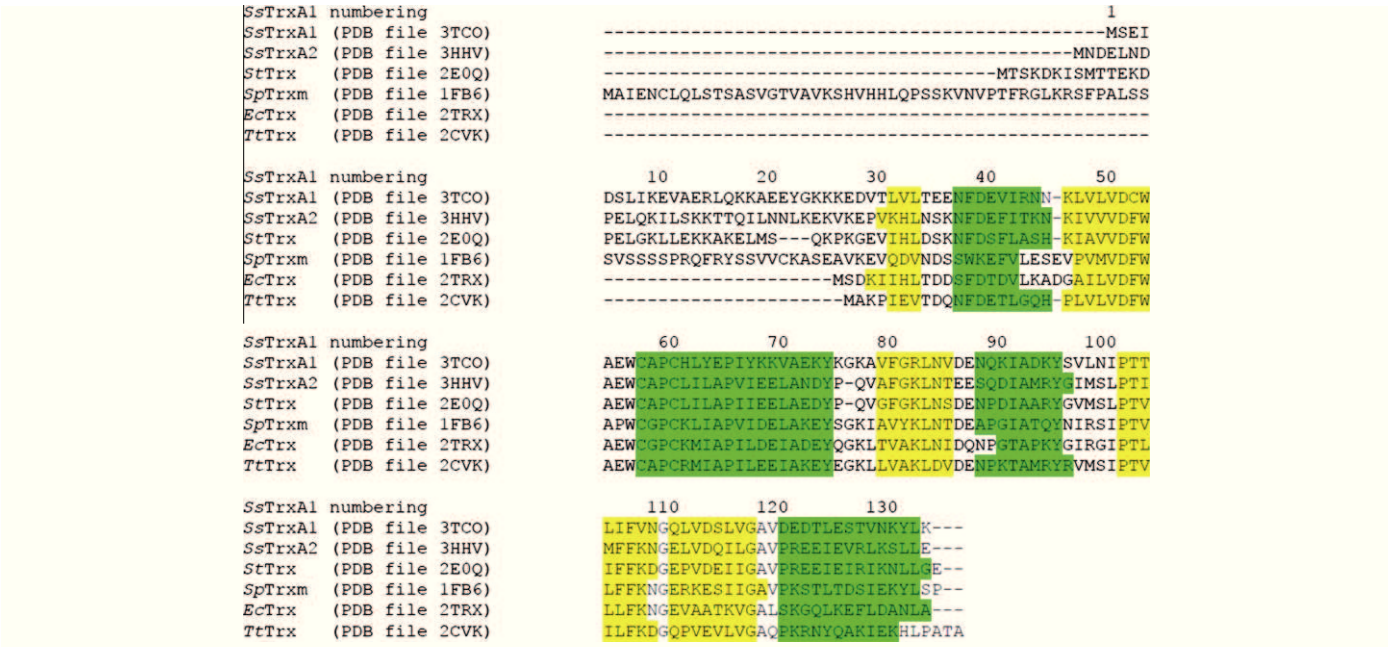

Fig. 2. Sequence alignment of *Ss*TrxA1, *Ss*TrxA2, *Ec*Trx, *Sp*Trxm, *Tt*Trx, and *St*Trx. α-helices and β-sheets are denoted in green and yellow, respectively. The residue numbering refers to *Ss*TrxA1 sequence. (For interpretation of the references to color in this figure legend, the reader is referred to the web version of this article.)

location of these two ethylene glycol molecules in the three recurrent interfaces A–B, B–C, and C–A# confirms their high similarity. In addition to these six ethylene glycol molecules located at the recurrent interface two additional molecules have been found in other packing regions of the asymmetric unit.

3.4. A peculiar feature of SsTrxA1 structure: carboxyl–carboxylate interactions

An interesting feature of SsTrxA1 structure is the presence of an unusual high number of carboxyl–carboxylate interactions (Table 3), despite the rather standard conditions used for protein crystallization (30% (w/v) PEG4000 and 0.2 M $(NH_4)_2SO_4$ – pH of the solution 6.5). Although there are several examples of carboxyl–carboxylate interactions in protein structures (Flocco and Mowbray, 1995), occasionally with important physiological roles (Ito et al., 1995; Mazzarella et al., 2006b; Vergara et al., 2010) and even at rather high pH values (Mazzarella et al., 2006a), the structure of SsTrxA1 is characterized by a peculiar abundance of these pairs. As reported in Table 3, there are seven intra-molecular and four intermolecular carboxyl–carboxylate interactions. In the three recurrent interfaces of the polymer-like association the side chain of Asp113 is bonded to the side chain of Glu36. At the B–C interface, the side chain of Asp113 also binds the side chain of Glu40. Two intramolecular interactions, those linking Glu27 to Glu72 and Glu121 to Glu125, are conserved in the three molecules of the asymmetric unit. On the other hand, the interaction between Asp51 and Glu64 side chain is observed only in molecule A. Asp51 has the same conformation in the three molecules of the asymmetric unit. This conformation is also similar to that observed for the corresponding residue (Asp26) in EcTrx. On the other hand, Glu64 protrudes toward the solvent in molecules B and C. The close similarity of the local structure of the three SsTrxA1 molecules suggests that the energy of the two rotameric states of Glu64 is regulated by minor local effects. It is important to note that in EcTrx the ionization of Asp26 affects the stability of the thiolate anion of Cys32 in EcTrx (Cys57 in SsTrxA1) (Carvalho et al., 2006b; Holmgren, 1995) (Chivers and Raines, 1997; Chivers et al., 1997). Indeed, the deprotonation of Cys32 may be hampered by a deprotonated

Fig. 3. Superimposition of *Ss*TrxA1 (cyan) with *Ec*Trx (red). The residues that delimitate the cavity created by the replacement of Phe27 *Ec*Trx with Cys52 *Ss*TrxA1 are drawn in ball-and-stick in *Ss*TrxA1 structure. (For interpretation of the references to color in this figure legend, the reader is referred to the web version of this article.)

Asp. Current resolution does not provide insights into the protonation of these two carboxylic groups (Asp51 or Glu64) that interact in molecule A. Nevertheless, the formation of the bond attenuates

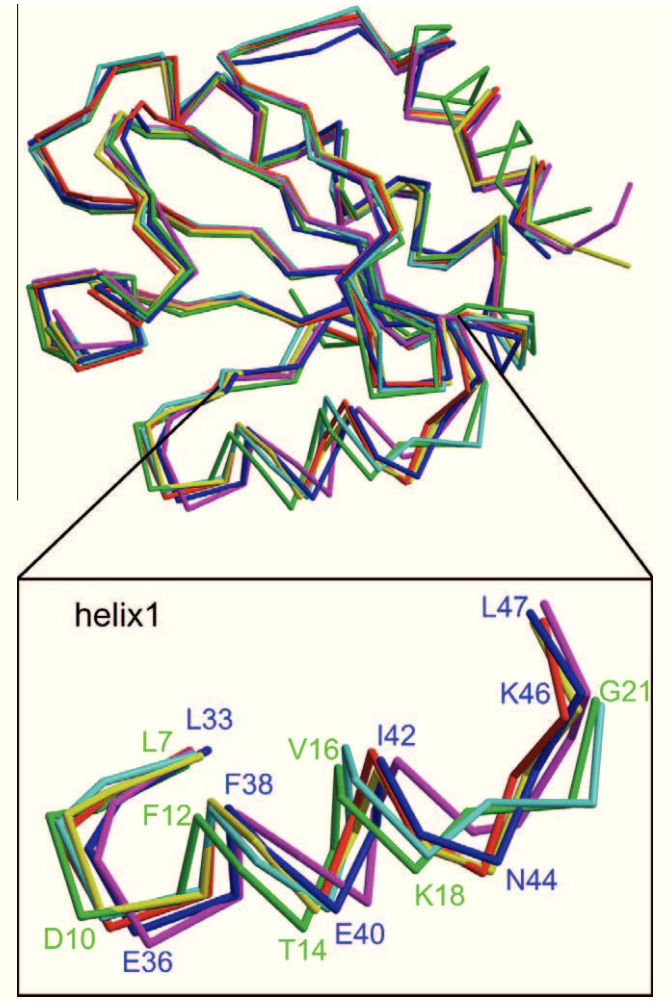

Fig. 4. Superimposition of *Ss*TrxA1 structure (blue) with the 3D models of *Ss*TrxA2 (red), *Ec*Trx (green), *Sp*Trxm (cyan), *Tt*Trx (yellow), and *St*Trx (magenta). It is evident that helix 1, highlighted in the snapshot, is longer in Trxs isolated from thermophilic organisms. Residues of helix 1 of *Ss*TrxA1 and *Ec*Trx are drawn in blue and green, respectively.

Table 2
Recurrent intermolecular H-bond interactions between different molecules in TrxA1 crystals.

	Residues and atoms	Distance (Å)
Molecules A–B	Gln110 NE2–Ala78 O	3.05
	Leu111 O–Asn45 ND2	2.85
	Val112 O–Asn37 ND2	2.99
	Asp113 OD1–Glu36 OE1	2.81[b]
Molecules B–C	Gln110 NE2–Ala78 O	2.90
	Leu111 O–Asn45 ND2	2.86
	Val112 O–Asn37 ND2	2.88
	Ser114 OG–Glu40 OE1	2.26
	Asp113 OD1–Glu36 OE1	2.65[b]
	Asp113 OD1–Glu40 OE1	3.04[b]
Molecules C–A#[a]	Gln110 NE2–Ala78 O	3.15
	Leu111 O–Asn45 ND2	2.83
	Val112 O–Asn37 ND2	2.90
	Ser114 OG–Glu40 OE1	2.53
	Asp113 OD1–Glu36 OE1	2.56[b]

[a] A# denotes a symmetry copy of A. The symmetry operation is a translation along the ***a*** axis.
[b] These H-bonds are generated by carboxyl–carboxylate interactions (see the text for details).

Table 3
Carboxyl–carboxylate interactions.

	Residues	Distance (Å)
Intra-molecular		
Molecule A	Glu27–Glu72	2.76
	Asp51–Glu64	2.81
	Glu121–Glu125	2.85
Molecule B	Glu27–Glu72	2.93
	Glu121–Glu125	2.84
Molecule C	Glu27–Glu72	2.69
	Glu121–Glu125	2.48
Inter-molecular		
Interface A–B	Asp113–Glu36	2.81
Interface B–C	Asp113–Glu36	2.65
	Asp113–Glu40	3.04
Interface C–A# [a]	Asp113–Glu36	2.56

[a] A# denotes a symmetry copy of A. The symmetry operation is a translation along the **a** axis.

the charge on Asp, thus facilitating the deprotonation of nucleophilic Cys57 which is responsible for the attack of the disulfide bond of the substrate.

3.5. Salt bridges in SsTrxA1 structure

Over the years, several structural determinants of protein stabilization have been proposed and evaluated (Petsko, 2001; Kumar and Nussinov, 2001). Although these analyses have unveiled that no mechanism has a general validity, it seems that an important role in protein stabilization is played by the occurrence of salt bridges (Kumar et al., 2000; Kumar and Nussinov, 2004). Moreover, previous studies have suggested that electrostatic interactions may be responsible for the remarkable stability of *St*Trx (Ming et al., 2007). As *Ss*TrxA1 is endowed with a remarkable thermal stability (see also below) we carried out a detailed analysis of the ion pairs in *Ss*TrxA1. As shown in Table 4, the three independent molecules in the asymmetric unit present on average only three intramolecular salt bridges. Moreover, there is a single ion pair (Glu27–Lys75) that is observed in all three independent copies of *Ss*TrxA1. Collectively, the finding that these ion pairs are weakly conserved among different independent molecules of *Ss*TrxA1 in the crystal state and that their total number is in line with that observed in mesophilic Trx does not provide support to a possible role of these interactions in the thermostabilization of *Ss*TrxA1.

3.6. Spectroscopic characterization of SsTrxA1 by using circular dichroism

In order to gain further insights into the determinants of *Ss*TrxA1 stability, we also carried out a spectroscopic characterization of the protein by using circular dichroism. In line with previous biochemical observations, this analysis confirms that *Ss*TrxA1 is endowed with a remarkable thermostability (Fig. 5). Indeed, the direct com-

Table 4
Salt bridges.

	Residues	Distance
Intra-molecular		
Molecule A	Glu27–Lys75	2.81
	Lys73–Glu125	2.46
	Lys73–Glu121	3.33
Molecule B	Glu27–Lys75	2.68
	Lys69–Glu121	3.20
Molecule C	Glu64–Lys68	3.43
	Lys69–Glu121	2.53
	Lys73–Glu121	2.82
	Lys73–Glu125	2.86

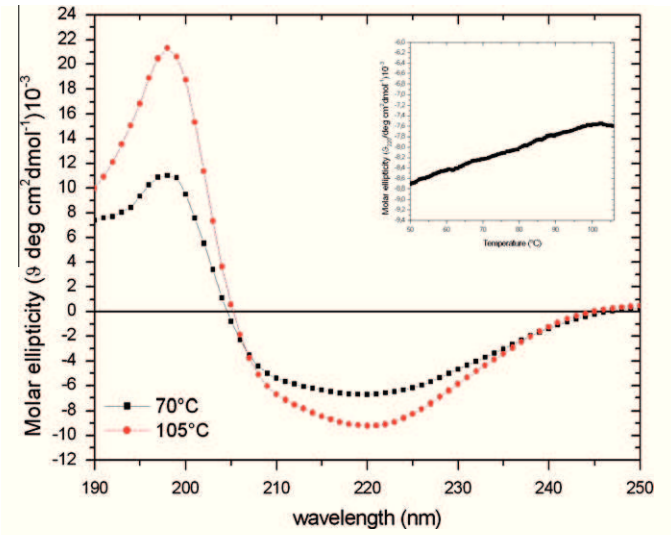

Fig. 5. Far-UV circular dichroism spectrum of *Ss*TrxA1 at 70 (red) and 105 (black) °C. The evolution of the CD signal at 220 nm in the temperature range 50–105 °C is reported in the inset. (For interpretation of the references to color in this figure legend, the reader is referred to the web version of this article.)

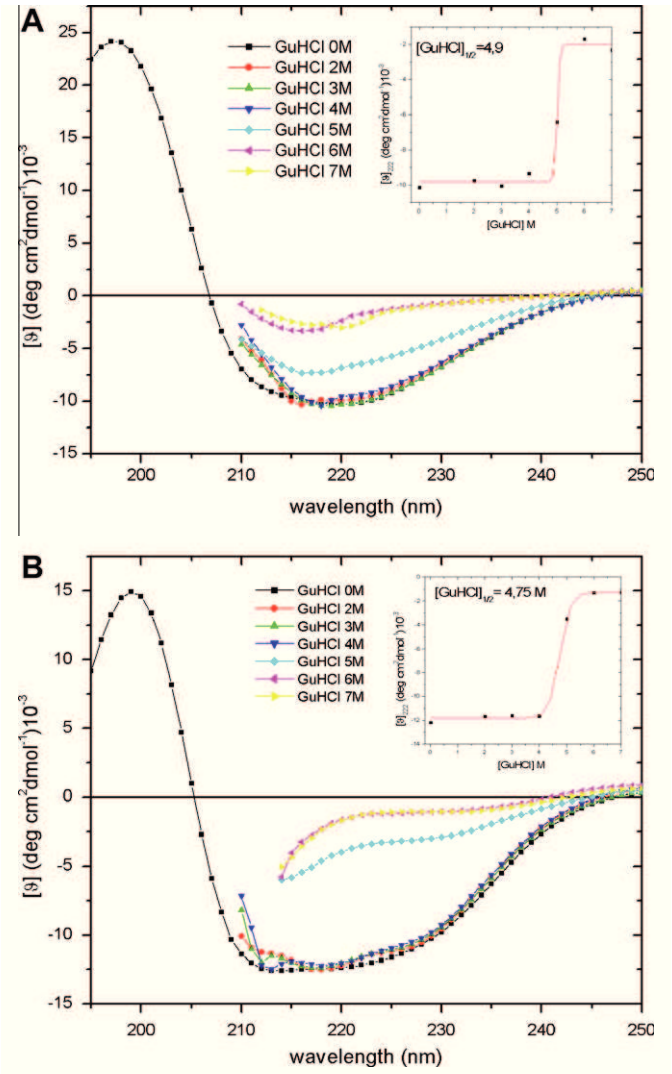

Fig. 6. Thermal denaturation curves of *Ss*TrxA1 (A) and *Ss*TrxA2 (B) obtained by treating the proteins with GuHCl. The CD signal at 222 nm is reported in the insets.

parison of the far-UV CD spectrum of the protein kept for one hour at 105 °C is very similar to that collected at 70 °C. Accordingly, a thermal denaturation experiment carried out in the temperature range 50–105 °C only reveals a negligible variation of the CD signal at 220.

We then evaluated the effect of a charged chemical denaturant (GuHCl), which is commonly supposed to weaken protein salt bridges (Ibarra-Molero et al., 1999; Makhatadze et al., 1998), on the stability of *Ss*TrxA1. The analysis of the CD spectra unveils that the secondary structure elements of *Ss*TrxA1 are virtually unchanged by the addition of GuHCl up to 4 M (Fig. 6A). Denaturating effects are detected for higher concentrations. Similar experiments conducted on *Ss*TrxA2, which also presents a limited number of salt bridges, led to similar results (Fig. 6B). The significant stability of both *Ss*TrxA1 and *Ss*TrxA2 against GuHCl suggests that the contribution of salt bridges to the stability of both proteins may be limited.

4. Conclusions

The spectroscopic and crystallographic characterization of *Ss*TrxA1 suggests that ion pairs do not contribute to the remarkable thermal stability of the enzyme. On the basis of the present structure and of comparisons of Trx structures isolated from either thermophilic or mesophilic organisms, we suggest that other effects, such as the shortening or removal of the loop connecting secondary structure elements, play a role in *Ss*TrxA1 stability. The close similarity of secondary structure content in other thermophilic Trxs such as SsTrxA2, StTrx, and TtTrx suggests that this mechanism may be of general validity within this widespread protein family. Along this line, it has been shown that secondary structure content has also an important role in the stabilization of *Alicyclobacillus acidocaldarius* Trx (Leone et al., 2004). This observation may have an important impact in the design of Trx variants endowed with an increased stability. Indeed, on analogy with the result of the evolution, the shortening of the loop connecting the α-helix 1 and the β-strand 2 may increase the stability of Trx scaffolds used for biotechnological applications. Under this regard, it is relevant that the addition of *Ss*TrxA2 to cultured neuroblastoma cells protected them from the oxidative stress induced by diclofenac, an anti-inflamatory drug (Cecere et al., 2010).

Finally, it is important to note that it has been previously shown that the thermostability of *Ss*TrxRB3 (Ruggiero et al., 2009b), the enzyme that reduces both *Ss*TrxA1 and *Ss*TrxA2, likely relies on clusters of interacting ion pairs. Collectively, these observations suggest that the thermostability of functionally related proteins isolated from the same organism can be based on different structural determinants.

Acknowledgments

The authors thank Dr. Maria Angela Lanzotti for the help in the early stage of this project and Mr. Maurizio Amendola, Dr. Giuseppe Perretta and Mr. Giosuè Sorrentino for technical assistance. The financial support of PRIN 2007 and 2009-MIUR, Rome (Italy) is also acknowledged.

Appendix A. Supplementary data

Supplementary data associated with this article can be found, in the online version, at doi:10.1016/j.jsb.2011.10.014.

References

Arner, E.S., Holmgren, A., 2000. Physiological functions of thioredoxin and thioredoxin reductase. Eur. J. Biochem. 267, 6102–6109.

Brunger, A.T., 2007. Version of the crystallography and NMR system. Nat. Protoc. 2, 2728–2733.
Capitani, G., Markovic-Housley, Z., DelVal, G., Morris, M., Jansonius, J.N., et al., 2000. Crystal structures of two functionally different thioredoxins in spinach chloroplasts. J. Mol. Biol. 302, 135–154.
Carvalho, A.P., Fernandes, P.A., Ramos, M.J., 2006a. Similarities and differences in the thioredoxin superfamily. Prog. Biophys. Mol. Biol. 91, 229–248.
Carvalho, A.T., Fernandes, P.A., Ramos, M.J., 2006b. Determination of the DeltapKa between the active site cysteines of thioredoxin and DsbA. J. Comput. Chem. 27, 966–975.
Cecere, F., Iuliano, A., Albano, F., Zappelli, C., Castellano, I., et al., 2010. Diclofenac-induced apoptosis in the neuroblastoma cell line SH-SY5Y: possible involvement of the mitochondrial superoxide dismutase. J. Biomed. Biotechnol. 2010, 801726.
Chivers, P.T., Raines, R.T., 1997. General acid/base catalysis in the active site of *Escherichia coli* thioredoxin. Biochemistry 36, 15810–15816.
Chivers, P.T., Prehoda, K.E., Volkman, B.F., Kim, B.M., Markley, J.L., et al., 1997. Microscopic p*Ka* values of *Escherichia coli* thioredoxin. Biochemistry 36, 14985–14991.
Colas, P., Cohen, B., Jessen, T., Grishina, I., McCoy, J., Brent, R., 1996. Genetic selection of peptide aptamers that recognize and inhibit cyclin-dependent kinase 2. Nature 380, 548–550.
Eriksson, A.E., Baase, W.A., Zhang, X.J., Heinz, D.W., Blaber, M., et al., 1992. Response of a protein structure to cavity-creating mutations and its relation to the hydrophobic effect. Science 255, 178–183.
Flocco, M.M., Mowbray, S.L., 1995. Strange bedfellows: interactions between acidic side-chains in proteins. J. Mol. Biol. 254, 96–105.
Granata, V., Graziano, G., Ruggiero, A., Raimo, G., Masullo, M., et al., 2006. Chemical denaturation of the elongation factor 1alpha isolated from the hyperthermophilic archaeon Sulfolobus solfataricus. Biochemistry 45, 719–726.
Granata, V., Graziano, G., Ruggiero, A., Raimo, G., Masullo, M., et al., 2008. Stability against temperature of Sulfolobus solfataricus elongation factor 1 alpha, a multi-domain protein. Biochim. Biophys. Acta 1784, 573–581.
Grimaldi, P., Ruocco, M.R., Lanzotti, M.A., Ruggiero, A., Ruggiero, I., et al., 2008. Characterisation of the components of the thioredoxin system in the archaeon Sulfolobus solfataricus. Extremophiles 12, 553–562.
Holmgren, A., 1995. Thioredoxin structure and mechanism: conformational changes on oxidation of the active-site sulfhydryls to a disulfide. Structure 3, 239–243.
Ibarra-Molero, B., Loladze, V.V., Makhatadze, G.I., Sanchez-Ruiz, J.M., 1999. Thermal versus guanidine-induced unfolding of ubiquitin. An analysis in terms of the contributions from charge–charge interactions to protein stability. Biochemistry 38, 8138–8149.
Ito, N., Komiyama, N.H., Fermi, G., 1995. Structure of deoxyhaemoglobin of the antarctic fish Pagothenia bernacchii with an analysis of the structural basis of the root effect by comparison of the liganded and unliganded haemoglobin structures. J. Mol. Biol. 250, 648–658.
Jones, T.A., Zou, J.Y., Cowan, S.W., Kjeldgaard, M., 1991. Improved methods for building protein models in electron density maps and the location of errors in these models. Acta Crystallogr. A A47, 110–119.
Katti, S.K., LeMaster, D.M., Eklund, H., 1990. Crystal structure of thioredoxin from *Escherichia coli* at 1.68 A resolution. J. Mol. Biol. 212, 167–184.
Krissinel, E., Henrick, K., 2007. Inference of macromolecular assemblies from crystalline state. J. Mol. Biol. 372, 774–797.
Kumar, S., Nussinov, R., 2001. How do thermophilic proteins deal with heat? Cell. Mol. Life Sci. 58, 1216–1233.
Kumar, S., Nussinov, R., 2004. Different roles of electrostatics in heat and in cold: adaptation by citrate synthase. ChemBioChem 5, 280–290.
Kumar, S., Tsai, C.J., Nussinov, R., 2000. Factors enhancing protein thermostability. Protein Eng. 13, 179–191.
Ladenstein, R., Ren, B., 2006. Protein disulfides and protein disulfide oxidoreductases in hyperthermophiles. FEBS J. 273, 4170–4185.
LaVallie, E.R., DiBlasio, E.A., Kovacic, S., Grant, K.L., Schendel, P.F., et al., 1993. A thioredoxin gene fusion expression system that circumvents inclusion body formation in the *E. Coli* cytoplasm. Biotechnology (NY) 11, 187–193.
Leone, M., Di Lello, P., Ohlenschlager, O., Pedone, E.M., Bartolucci, S., et al., 2004. Solution structure and backbone dynamics of the K18G/R82E Alicyclobacillus acidocaldarius thioredoxin mutant: a molecular analysis of its reduced thermal stability. Biochemistry 43, 6043–6058.
Lillig, C.H., Holmgren, A., 2007. Thioredoxin and related molecules–from biology to health and disease. Antioxid. Redox Signal. 9, 25–47.
Makhatadze, G.I., Lopez, M.M., Richardson 3rd, J.M., Thomas, S.T., 1998. Anion binding to the ubiquitin molecule. Protein Sci. 7, 689–697.
Maulik, N., Das, D.K., 2008. Emerging potential of thioredoxin and thioredoxin interacting proteins in various disease conditions. Biochim. Biophys. Acta 1780, 1368–1382.
Mazzarella, L., Vergara, A., Vitagliano, L., Merlino, A., Bonomi, G., et al., 2006a. High resolution crystal structure of deoxy hemoglobin from Trematomus bernacchii at different pH values: the role of histidine residues in modulating the strength of the root effect. Proteins 65, 490–498.
Mazzarella, L., Bonomi, G., Lubrano, M.C., Merlino, A., Riccio, A., et al., 2006b. Minimal structural requirements for root effect: crystal structure of the cathodic hemoglobin isolated from the antarctic fish Trematomus newnesi. Proteins 62, 316–321.
Ming, H., Kato, Y., Miyazono, K., Ito, K., Kamo, M., et al., 2007. Crystal structure of thioredoxin domain of ST2123 from thermophilic archaea Sulfolobus tokodaii strain7. Proteins 69, 204–208.
Moretto, N., Bolchi, A., Rivetti, C., Imbimbo, B.P., Villetti, G., et al., 2007. Conformation-sensitive antibodies against alzheimer amyloid-beta by immunization with a thioredoxin-constrained B-cell epitope peptide. J. Biol. Chem. 282, 11436–11445.
Pedone, E., Limauro, D., D'Alterio, R., Rossi, M., Bartolucci, S., 2006. Characterization of a multifunctional protein disulfide oxidoreductase from Sulfolobus solfataricus. FEBS J. 273, 5407–5420.
Petsko, G.A., 2001. Structural basis of thermostability in hyperthermophilic proteins, or ''there's more than one way to skin a cat''. Methods Enzymol. 334, 469–478.
Ruggiero, A., Ruocco, M.R., Grimaldi, P., Arcari, P., Masullo, M., et al., 2005. Crystallization and preliminary X-ray crystallographic analysis of Sulfolobus solfataricus thioredoxin reductase. Acta Crystallogr., Sect. F: Struct. Biol. Cryst. Commun. 61, 906–909.
Ruggiero, A., Masullo, M., Marasco, D., Ruocco, M.R., Grimaldi, P., et al., 2009a. The dimeric structure of Sulfolobus solfataricus thioredoxin A2 and the basis of its thermostability. Proteins 77, 1004–1008.
Ruggiero, A., Masullo, M., Ruocco, M.R., Grimaldi, P., Lanzotti, M.A., et al., 2009b. Structure and stability of a thioredoxin reductase from Sulfolobus solfataricus: a thermostable protein with two functions. Biochim. Biophys. Acta 1794, 554–562.
Ruggiero, A., Lanzotti, M.A., Ruocco, M.R., Grimaldi, P., Marasco, D., et al., 2009c. Crystallization and preliminary X-ray crystallographic analysis of two dimeric hyperthermostable thioredoxins isolated from Sulfolobus solfataricus. Acta Crystallogr., Sect. F: Struct. Biol. Cryst. Commun. 65, 604–607.
Ruocco, M.R., Ruggiero, A., Masullo, L., Arcari, P., Masullo, M., 2004. A 35 kDa NAD(P)H oxidase previously isolated from the archaeon Sulfolobus solfataricus is instead a thioredoxin reductase. Biochimie 86, 883–892.
Tang, G.W., Altman, R.B., 2011. Remote thioredoxin recognition using evolutionary conservation and structural dynamics. Structure 19, 461–470.
Vergara, A., Vitagliano, L., Merlino, A., Sica, F., Marino, K., et al., 2010. An order–disorder transition plays a role in switching off the root effect in fish hemoglobins. J. Biol. Chem. 285, 32568–32575.

Chem Biol Drug Des 2011; **78:** 260–268

Research Article

doi: 10.1111/j.1747-0285.2011.01142.x

Interaction Between the Antibiotic Tetracycline and the Elongation Factor 1α from the Archaeon *Sulfolobus solfataricus*

Anna Lamberti[1], Nicola M. Martucci[1,2], Immacolata Ruggiero[1], Paolo Arcari[1,3,*] and Mariorosario Masullo[1,3,4,*]

[1]*Dipartimento di Biochimica e Biotecnologie Mediche, Università di Napoli Federico II, Via S. Pansini 5, I-80131 Napoli, Italy*
[2]*Dipartimento di Scienze Farmacobiologiche, Università degli Studi 'Magna Graecia' di Catanzaro, Complesso 'Ninì Barbieri', I-88021 Roccelletta di Borgia, Catanzaro, Italy*
[3]*CEINGE Biotecnologie Avanzate scarl, Via Gaetano Salvatore 486, I-80145 Napoli, Italy*
[4]*Dipartimento di Studi delle Istituzioni e dei Sistemi Territoriali, Università di Napoli 'Parthenope', Via Medina 40, I-80133 Napoli, Italy*
**Corresponding authors: Mariorosario Masullo, mario.masullo@uniparthenope.it, Paolo Arcari, arcari@unina.it*
Anna Lamberti and Nicola M. Martucci equally contributed to this work.

The interaction between tetracycline and the archaeal elongation factor 1α from *Sulfolobus solfataricus* was investigated. The effects produced by this eubacterial antibiotic indicated that this interaction involved the G-domain of the elongation factor 1α from *S. solfataricus*, although also the M-domain was required. In fact, in the presence of the antibiotic, an increase in the fluorescence quantum yield of the aromatic region was observed for elongation factor 1α from *S. solfataricus* and its truncated form lacking the C-terminal domain, but not for that lacking also the M-domain. The increase in quantum yield was restored when the G-domain of elongation factor 1α from *S. solfataricus* was fused to the M and the C-domains of the eubacterial analogue elongation factor Tu. Tetracycline inhibits protein synthesis catalysed by elongation factor 1α from *S. solfataricus*; this is accompanied by an increase in the GDP/GTP exchange rate and a slight inhibition of the intrinsic GTPase, suggesting that a main effect of the antibiotic was exerted on the GTP-bound form of the enzyme. Furthermore, the mixed inhibition observed for GTPase confirmed that the interaction, besides the G-domain, involved also other region(s) of elongation factor 1α from *S. solfataricus*. These results can be useful for studying potential side effects arising from the interaction between tetracycline and eukaryotic elongation factors.

Key words: antibiotic, elongation factor 1α, protein synthesis, *Sulfolobus solfataricus*, tetracycline

Abbreviations: Ec, *Escherichia coli*; EcEF-Tu, *Escherichia coli* EF-Tu; EF, elongation factor; $GTPase^{Na}$, NaCl-dependent GTPase of SsEF-1α; SsEF-1α, elongation factor 1α from *Sulfolobus solfataricus*.

Received 23 July 2010, revised 1 February 2011 and accepted for publication 23 April 2011

Translation elongation factor 1α from *Sulfolobus solfataricus* (SsEF-1α) is the functional homologue of the eubacterial elongation factor Tu (EF-Tu) that belongs to the family of GTP-binding proteins (1). The primary role of SsEF-1α/EF-Tu is the delivery of the aminoacyl-tRNA to the A site of mRNA-programmed ribosome during the elongation cycle (2,3), even though for both enzymes, other biological functions have been reported (4–6). The crystal structure of SsEF-1α/EF-Tu showed the presence of three structural domains (7–10): a GDP/GTP-binding domain (G-domain), a middle (M) and a C-terminal (C) domain; in the fulfilment of its main role, SsEF-1α/EF-Tu, in its active form bound to GTP, elicits a GTPase activity that produces the corresponding GDP-bound form that dissociates from the ribosome. The switch from the active to the inactive form is associated with a conformational change of the enzymes (11). The regeneration of the active form is ensured by the intervention of the elongation factor Ts/1β which catalyses the GDP/GTP exchange on the factor. The details of the mechanism of action of *Escherichia coli* EF-Tu (EcEF-Tu) have also been investigated taking advantage of specific antibiotics acting on the elongation factor; in particular, kirromycin hinders the dissociation of EF-Tu•GDP from the mRNA-programmed ribosome inducing a GTP-bound conformation on EF-Tu (12). Pulvomicyn and GE2270A interfere with ternary complex formation both preventing the interaction between EF-Tu•GTP and aa-tRNA (12,13). More recently, the resolution of the three-dimensional structure of a complex formed between tetracycline and the EF-Tu•GDP complex (14) reopens the question of the molecular target(s) of this antibiotic that probably reflects different modes of action and/or resistant mechanisms in different pathogens (14). In fact, over the years several studies have been reported in which ribosomal proteins (15–17) or specific sites of 16S rRNA molecules (18–23) are claimed to be involved in the weak interaction between tetracycline and ribosome (24). Therefore, the resolution of the structure of a complex between tetracycline and EF-Tu in its GDP-bound form (14) revalued early reports focusing on the involvement of this elongation factor in the mechanism of action of tetracycline (25–31). The details of the molecular contacts between the antibiotic and the

elongation factor pointed to a binding site entirely located on the G-domain of EF-Tu; however, the crystallographic unit contains an (EF-Tu•GDP•tetracycline)$_2$ dimer in which intramolecular contacts are formed by the two G and the two M-domains of the EF-Tu molecules in the dimer. Therefore, the packaging of the complex might involve different portions of the proteins and it is not restricted to the nucleotide-binding domain of the elongation factor.

Regarding the interaction between archaeal protein synthesis elongation factors and eubacterial antibiotics, we have reported that kirromycin was able to enhance the intrinsic GTPase activity of some SsEF-1α mutants, but not that of the wild-type enzyme (32–34); vice versa, GE2270A was found to increase the GDP/GTP exchange rate and to reduce the intrinsic GTPase of the archaeal elongation factor (35). In addition, fusidic acid, another eubacterial antibiotic acting on the elongation factor G, was found to interact with its archaeal functional analogue SsEF-2 (36). It has to be noted that in an *in vitro* reconstituted system, none of these three antibiotics were able to inhibit protein synthesis in *S. solfataricus* (37); vice versa, it has been reported that tetracycline was able to inhibit protein synthesis in an *in vitro* cell-free reconstituted system in *S. solfataricus* (37) and *Sulfolobus acidocaldarius* (38), even though the concentration of antibiotic leading to half inhibition was at least one order of magnitude higher than that reported for eubacterial protein synthesis. All these considerations prompted us an investigation into the interaction between tetracycline and SsEF-1α. The results obtained indicated that the antibiotic interacts with the archaeal elongation factor, as revealed by fluorescence analysis but also based on the influence that tetracycline exerted on specific partial reactions catalysed by the elongation factor. Finally, the availability of engineered forms of SsEF-1α confirmed that the middle domain of the elongation factor is important for the interaction with the antibiotic.

Materials and Methods

Chemicals, buffers and enzymes

Labelled compounds and chemicals were as already reported (39). Tetracycline (Sigma–Aldrich, Milan, Italy) was prepared as 50 mM stock solution in water and stored at −80 °C. The antibiotic concentration was assessed by absorbance reading at 360 nm, using a molar extinction coefficient of 15.80 1/mM•cm (40). The following buffers were used: Buffer A: 20 mM Tris•HCl, pH 7.8, 50 mM KCl, 10 mM $MgCl_2$; buffer B: 20 mM Tris•HCl, pH 7.8, 10 mM $MgCl_2$, 1 mM DTT, 3.6 M NaCl.

Elongation factor 1α from *S. solfataricus* and its engineered or chimaeric forms were produced and purified as already reported (39,41,42). SsRibosome, SstRNA, SsEF-2 and SsFRS were purified as reported (43,44).

SsEF-1α assays

The preparation of [^{3}H]Val–EctRNA^{Val}, the formation of the ternary complex SsEF-1α•Gpp(NH)p•[^{3}H]Val–EctRNA^{Val} and the protection against spontaneous deacylation of [^{3}H]Val–EctRNA^{Val} were carried out as already described (45). Poly(U)-directed poly([^{3}H]Phe) synthesis was assayed as reported (35,43).

The ability of SsEF-1α to bind [^{3}H]GDP or to exchange the radiolabelled nucleotide for GDP or GTP was assayed by nitrocellulose filtration as described (39). The apparent equilibrium dissociation constant (K'_d) of the binary complex formed between SsEF-1α and [^{3}H]GDP was determined by Scatchard plots titrating 1.0 μM SsEF-1α with 0.4–4 μM [^{3}H]GDP (specific radioactivity 7443 cpm/pmol). K'_d for GTP was derived from competitive binding experiments in which 0.5 μM SsEF-1α was incubated in the presence of 14 μM [^{3}H]GDP (specific radioactivity 1183 cpm/pmol) and different concentrations (40–300 μM) of GTP.

The intrinsic GTPase of SsEF-1α was measured in the presence of 3.6 M NaCl (GTPase^{Na}) as reported (46). The kinetic parameters were determined in buffer B using 0.5 μM SsEF-1α and 1.5–30 μM [γ–^{32}P]GTP (specific radioactivity 8582–551 cpm/pmol). The reaction was followed kinetically at 60 °C and the amount of $^{32}P_i$ released determined on 50–μL aliquots.

The effect of tetracycline on the heat inactivation of SsEF-1α was evaluated by incubating 4 μM protein in buffer A at selected temperatures in the 87–96 °C interval. After the heat treatment, 40-μL aliquots were cooled on ice for 30 min and then analysed for their residual [^{3}H]GDP-binding ability or GTPase^{Na} as reported earlier. The data were analysed through a first-order kinetic equation, and the rate constants of the heat inactivation process obtained (k_{in}) were used to draw an Arrhenius plot, from which the energetic parameters of activation can be derived as reported (39).

Fluorescence spectra were recorded on a Cary Eclipse spectrofluorimeter (Varian Inc., Mulgrave, Australia) at a scan rate of 60 nm/min using an excitation wavelength of 280 nm; excitation and emission slits were set to 10 nm. Blanks run in the absence of the protein were subtracted. Spectra recorded in the presence of tetracycline were corrected for the inner filter effect because of the absorbance of the antibiotic, using a molar absorption coefficient at 280 nm of 17.49 1/mM•cm determined from a linear Beer–Lambert plot of absorbance versus tetracycline concentration.

Results

Effects of tetracycline on the molecular properties of SsEF-1α

The effect of tetracycline on the molecular properties of SsEF-1α was studied by fluorescence spectroscopy. As shown in Figure 1A, a 4–molar excess of antibiotic over protein concentration induced a less than 1 nm red shift with a 10% increase in the quantum yield, in the aromatic region of the fluorescence spectrum (λ_{max} 314 nm). This behaviour was also observed for the eubacterial counterpart EcEF-Tu (Figure 1D, λ_{max} 310 nm) for which the interaction with the antibiotic was also observed crystallographically (14). The availability of (i) two truncated forms of SsEF-1α lacking either the C-terminal (Ss(GM)EF-1α) or both the middle and C-terminal domains [Ss(G)EF-1α, (39)] or (ii) a chimaeric form constituted by the G-domain of SsEF-1α and the M and C-domains of EcEF-Tu (41)

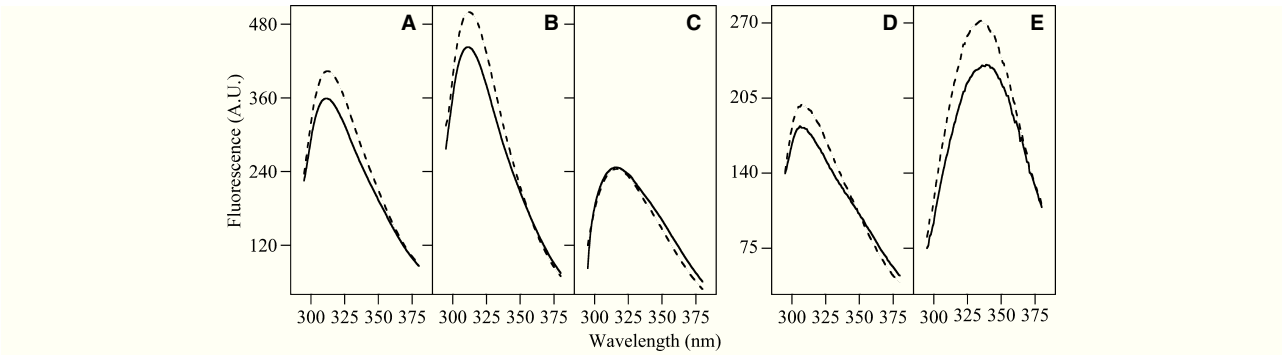

Figure 1: Effect of tetracycline on the fluorescence spectra of elongation factor 1α from *Sulfolobus solfataricus* (SsEF-1α), *Escherichia coli* EF-Tu (EcEF-Tu) and the engineered forms of the archaeal elongation factor. Spectra were recorded as described in Materials and Methods, at 25 °C in the absence (continuous line) or in the presence (dashed line) of 16 μM tetracycline using 4.5 μM of each protein. (A) SsEF-1α, (B) Ss(GM)EF-1α, (C) Ss(G)EF-1α, (D) EcEF-Tu, (E) archaeal/eubacterial chimaeric elongation factor.

allowed the identification of the protein's portion involved in the interaction between the elongation factor and tetracycline. In fact, in the case of Ss(GM)EF-1α (Figure 1B, λ_{max} 310 nm), the antibiotic induced a similar quantum yield increase with respect to the intact factor; on the other hand, this increase was not observed with the truncated form lacking both M and C-terminal domains (Figure 1C, λ_{max} 314 nm). These results indicated that the domain M of the elongation factor is essential to observe the interaction between SsEF-1α and the antibiotic. Concerning the chimaera, a result similar to the intact factors was observed (Figure 1E, λ_{max} 330 nm), although the antibiotic produced a slight higher blue shift (∼7 nm); this finding indicated that tetracycline induced a more compact conformation on the chimaeric elongation factor.

For all proteins investigated, except the domain G of SsEF-1α, an increase in the quantum yield at increasing tetracycline concentration with a saturation behaviour was observed (Figure 2A). In fact, using a double reciprocal plot, straight lines were obtained (Figure 2B). From the intercept on the abscissa axis, a value of the tetracycline concentration to reach half the maximum fluorescence can be derived; in particular, the value derived for SsEF-1α (229 μM, F_{max} 490) was significantly higher than that found for the chimaera (104 μM, F_{max} 378), EcEF-Tu (57 μM, F_{max} 87) and Ss(GM)EF-1α (50 μM, F_{max} 222). These findings, besides indicating that eubacterial EcEF-Tu has an affinity for tetracycline higher than archaeal SsEF-1α, confirm that the M-domain of the elongation factor plays a role in the antibiotic binding. Finally, eubacterial domains were able to increase the affinity for the antibiotic with respect to the archaeal domain.

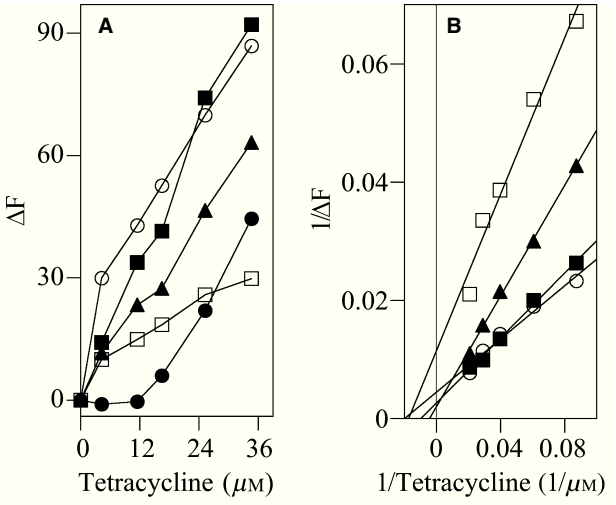

Figure 2: Effect of tetracycline on the fluorescence intensity of elongation factor 1α from *Sulfolobus solfataricus* (SsEF-1α), *Escherichia coli* EF-Tu (EcEF-Tu) and the engineered forms of the archaeal elongation factor. (A) The increase in the fluorescence intensity upon excitation at 280 nm caused by tetracycline was measured at 314 nm for SsEF-1α (▲), 310 nm for Ss(GM)EF-1α (○), 314 nm for Ss(G)EF-1α (●), 310 nm for EcEF-Tu (□) or 330 nm for the archaeal/eubacterial chimaeric elongation factor (■). The concentration of each protein was 4.5 μM. (B) The data reported in (A) were treated as a double reciprocal plot, except that referred to Ss(G)EF-1α.

Effect of tetracycline on the functional properties of SsEF-1α

The interaction between SsEF-1α and tetracycline was also studied in terms of the effect produced by the antibiotic on the functional properties of the elongation factor.

We first analysed the ability of tetracycline to inhibit protein synthesis using a reconstituted system containing purified macromolecular components from *S. solfataricus*. The effect of tetracycline on the kinetics of [^{3}H]Phe polymerisation at 75 °C, reported in Figure 3A, indicated that at 2 mM antibiotic, a reduction of threefold of the rate was observed. The effect of different concentration of tetracycline on poly(Phe) incorporation is reported in Figure 3B. The concentration of antibiotic leading to 50% inhibition was derived from a first-order analysis of the data (Figure 3C). The value obtained (1.1 mM) was identical to that measured using a cell-free reconstituted system (37), even though it was at least one order of magnitude higher than that required for the eubacterial process.

To identify the partial reaction catalysed by SsEF-1α possibly affected by this antibiotic, we tested the ability of SsEF-1α to

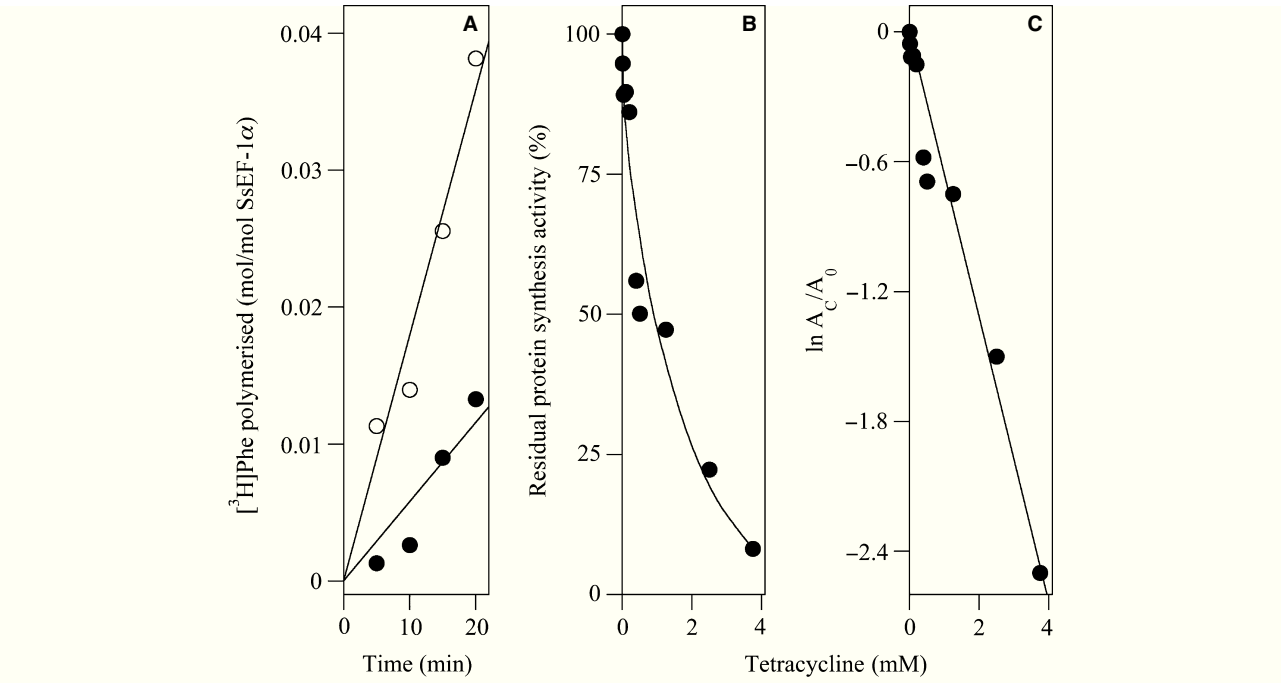

Figure 3: Effect of tetracycline on the poly(U)-directed poly(Phe) synthesis catalysed by elongation factor 1α from *Sulfolobus solfataricus* (SsEF-1α). (A) 250 μL of the reaction mixture contained 25 mM Tris•HCl pH 7.5, 19 mM magnesium acetate, 10 mM NH_4Cl, 10 mM dithiothreitol, 2.4 mM ATP, 1.6 mM GTP, 0.16 mg/mL poly(U), 3 mM spermine, 0.25 μM Ssribosome, 80 μg/mL SstRNA, 0.1 μM SsEF–2, 2.0 μM [^{3}H]Phe (specific activity 1268 cpm/pmol). The reaction was started by addition of 0.5 μM final concentration of SsEF-1α in the absence (○) or presence (●) of 2 mM tetracycline and carried out at 75 °C. At the times indicated, 50-μL aliquots were withdrawn, chilled on ice and then analysed for the amount of [^{3}H]Phe incorporated. (B) Effect of different concentrations of tetracycline. At each antibiotic concentration, the assay was carried out as reported in (A). (C) The data reported in (B) were treated as a first-order behaviour. A_0 represents the activity measured in the absence of tetracycline, whereas A_C is the activity at the concentration C of tetracycline.

interact with aa-tRNA in the absence or in the presence of tetracycline. As shown in Figure 4, the amount of ternary complex formed between heterologous Val–EctRNA^{Val}, SsEF-1α and nucleotides was almost identical either in the absence or in the presence of tetracycline, as revealed by the ability of the elongation factor to protect [^{3}H]Val–EctRNA^{Val} against spontaneous deacylation. In addition, the antibiotic did not affect the affinity for the nucleotide in ternary complex formation, still remaining lower for GDP (Figure 4B) with respect to that for GppNHp (Figure 4A), a slowly hydrolysable GTP analogue.

Effect of tetracycline on the interaction between SsEF-1α and guanosine nucleotides

The effect of tetracycline on guanosine nucleotide exchange ability of SsEF-1α was also studied. As shown in Figure 4, the presence of tetracycline caused a 2.1-fold faster [^{3}H]GDP/GTP exchange rate on SsEF-1α (Figure 5A), whereas in the case of [^{3}H]GDP/GDP exchange, both rates resulted undistinguishable from each other (Figure 5B). The effect of the antibiotic on the GDP binding was also evaluated in terms of the equilibrium dissociation constant of the binary complex formed with the elongation factor. The data reported in Table 1 indicated that tetracycline slightly reduces the affinity for both GDP and GTP, and in the case of the nucleotide diphosphate, the reduced affinity measured in the presence of the antibiotic can be ascribed to a selective reduction in the association rate constant.

To better evaluate the effect of the antibiotic on the interaction between SsEF-1α and guanosine nucleotides, we have checked whether tetracycline affected the intrinsic GTPase of the elongation factor and its truncated forms triggered by high concentration of NaCl (39,46). The results shown in Figure 5 indicate that tetracycline inhibited the GTPase^{Na} of SsEF-1α but not that elicited by its engineered forms. The inhibition level observed for SsEF-1α depended on the antibiotic concentration (Figure 6A), even though a complete inhibition was not reached even in the presence of 120 μM antibiotic, a concentration corresponding to about 200-fold molar excess over the elongation factor. However, the concentration of tetracycline for half inhibition of SsEF-1α GTPase can be calculated as about 322 μM (Figure 6B). The effect of the antibiotic on the kinetic parameters of the reaction (Table 2) indicated that tetracycline exerted a mixed inhibition; in fact, besides a reduced maximum hydrolytic rate, also a slight reduced affinity for the nucleotide was observed.

Effect of tetracycline on the heat stability of SsEF-1α

The interaction between tetracycline and SsEF-1α was also studied through the effect exerted by the antibiotic on the heat inactivation kinetics of the GTPase^{Na} catalysed by SsEF-1α in the interval 87–96 °C. As shown in Figure 7A, the antibiotic did not affect the first-order behaviour of the heat inactivation kinetic at all the temperature investigated. The analysis according to the Arrhenius

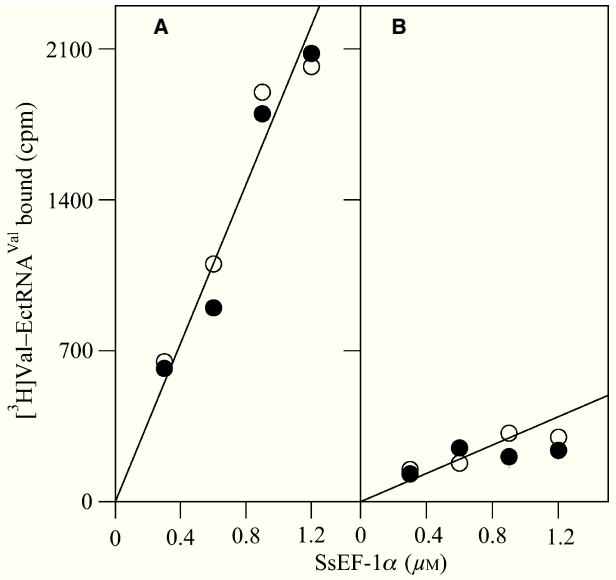

Figure 4: Effect of the tetracycline on the formation of the ternary complex between elongation factor 1α from *Sulfolobus solfataricus* (SsEF-1α), [^{3}H]ValEc–tRNA^{Val} and GDP or GppNHp. The mixture (30 μL) contained 25 mM Tris•HCl, pH 7.8, 10 mM NH_4Cl, 10 mM DTT, 20 mM magnesium acetate and 4.6 pmol of [^{3}H]ValEc–tRNA^{Val} (specific radioactivity 1521 cpm/pmol) and was incubated for 1 h at 0 °C to allow ternary complex formation in the presence of the indicated amount of SsEF-1α·GppNHp (A) or SsEF-1α·GDP (B), in the absence (○) or in the presence (●) of 50 μM tetracycline. The deacylation reaction was carried out for 1 h at 50 °C, and the residual [^{3}H]ValEc–tRNA^{Val} was determined as cold trichloroacetic acid insoluble material.

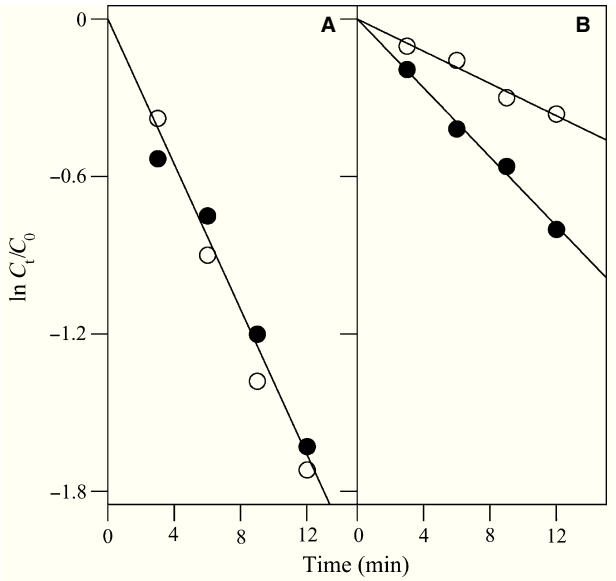

Figure 5: Effect of tetracycline on the nucleotide exchange rate catalysed by elongation factor 1α from *Sulfolobus solfataricus* (SsEF-1α). The reaction mixture (300 μL) prepared in buffer A contained 0.5 μM SsEF-1α·[^{3}H]GDP in the absence (○) or in the presence (●) of 50 μM tetracycline. The nucleotide exchange reaction was started at 60 °C by adding 1 mM GDP (A) or GTP (B) final concentration. At the times indicated, the amount of the residual radiolabelled binary complex was determined on 30-μL aliquots by nitrocellulose filtration. The data were treated according to a first-order kinetic.

equation of the kinetic constants of the heat inactivation process (Figure 7B) allowed the calculation of the energetic parameters of the activation. The data reported in Table 3 indicated that tetracycline increased the rate of the heat inactivation through a reduction in the energy of activation without affecting the free energy associated with the process.

Discussion

Tetracycline, a broad-spectrum antibiotic produced by the *Streptomyces* genus of Actinobacteria, is a protein synthesis inhibitor acting on 30S ribosome subunit of eubacteria (47). More recently, a direct interaction between this antibiotic and the EF-Tu from *E. coli* was reported by crystallographic studies pointing to a different mode of action of tetracycline (14). Because different eubacterial antibiotics, like kirromycin (32,33), GE2270A (35) and fusidic acid, (36) interact with the homologous archaeal elongation factors from *S. solfataricus*, a study on the interaction between tetracycline and SsEF-1α was undertaken. The availability of three engineered forms of the archaeal elongation factor (39,41) allowed a dissection of the molecular requirements involved in the interaction.

The interaction between SsEF-1α and tetracycline was demonstrated either by fluorescence spectroscopy in the aromatic region of the spectrum or by the effects produced by the antibiotic on some functional properties of the elongation factor; in particular, spectroscopic data showed in the presence of the antibiotic an increase in the quantum yield in the fluorescence spectrum of SsEF-1α. A similar behaviour was also observed for EcEF-Tu, Ss(GM)EF-1α and the chimaeric elongation factor containing the nucleotide-binding domain of SsEF-1α and the other two domains of EcEF-Tu, but not for Ss(G)EF-1α. These results indicated that the M-domain of archaeal/eubacterial factor is essential for the interaction with tetracycline. However, the value of the tetracycline concentration to reach half the maximum fluorescence for SsEF-1α was higher than that found for the chimeara, EcEF-Tu and Ss(GM)EF-1α in the order, thus indicating that

Table 1: Effect of tetracycline on the affinity of SsEF-1α for guanosine nucleotides at 60 °C

	K_d'		k_{-1}	k_{+1}
SsEF-1α	GDP (μM)	GTP (μM)	GDP (1/min)	GDP (1/μM•min)
− Tetracycline	0.3 ± 0.08	6.0 ± 1.3	0.13 ± 0.03	0.43
+ Tetracycline	0.5 ± 0.1	9.0 ± 2.0	0.12 ± 0.04	0.24

SsEF-1α, elongation factor 1α from *Sulfolobus solfataricus*.
The K_d' and k_{-1} values represent the average of 3–4 different determinations.
k_{+1} was calculated as k_{-1}/K_d'.

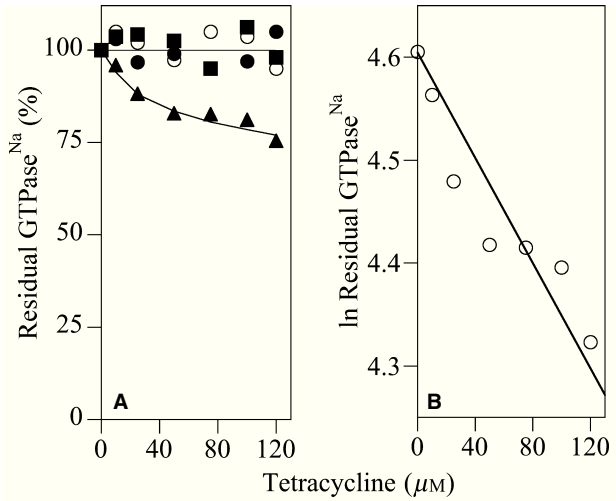

Figure 6: Effect of tetracycline on the intrinsic GTPase of SsEF-1α and its engineered forms. (A) The GTPase^{Na} activity of SsEF-1α (▲), Ss(GM)EF-1α (○), Ss(G)EF-1α (●) and the archaeal/eubacterial chimaeric elongation factor (■) was determined in the presence of the indicated tetracycline concentration, as described in Materials and Methods. The data were referred to the value measured in the absence of the antibiotic. (B) The data referring to SsEF-1α were linearised using a first-order behaviour equation.

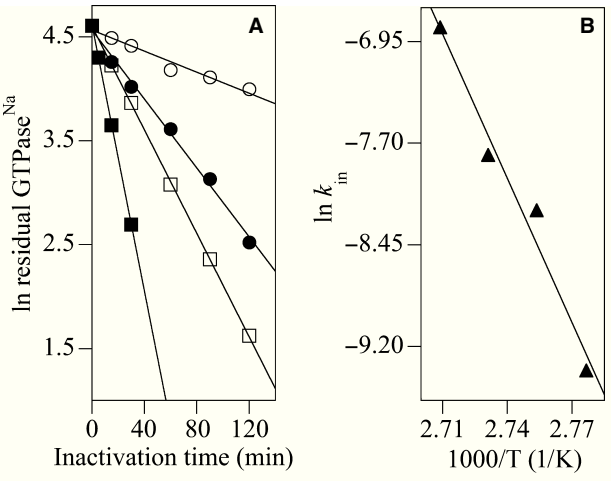

Figure 7: Effect of tetracycline on the heat inactivation of the GTPase^{Na} of elongation factor 1α from *Sulfolobus solfataricus* (SsEF-1α). (A) 4 μM SsEF-1α was incubated at 87 (○), 90 (●), 93 (□) or 96 °C (■) in the presence of 16 μM tetracycline, and at the indicated time intervals, aliquots were withdrawn and placed at 0 °C. The residual GTPase activity was determined as reported in Materials and Methods and referred to an untreated sample kept at 0 °C for all the experiment of the heat treatment. The data were treated as a first-order kinetic and reported as the natural logarithm of the residual activity. (B) Arrhenius analysis of the heat inactivation kinetic rate constants (k_{in}) derived from the slope of the equations reported in (A).

Table 2: Effect of tetracycline on the kinetic parameters of the GTPase^{Na} catalysed by SsEF-1α at 60 °C

	K_m (μM)	k_{cat} (1/s)	k_{cat}/K_m (1/s·μM)
− Tetracycline	2.5 ± 0.8	0.50 ± 0.12	0.20
+ Tetracycline	4.5 ± 1.3	0.36 ± 0.14	0.08

SsEF-1α, elongation factor 1α from *Sulfolobus solfataricus*.
The K_m and k_{cat} values represent the average of 3–4 different determinations.

Table 3: Effect of tetracycline on the energetic parameters of activation of the inactivation process

	E_a (kJ/mol)	ΔH^* (kJ/mol)	ΔS^* (J/mol•K)	ΔG^* (kJ/mol)
− Tetracycline	361	358	665	119
+ Tetracycline	177	174	164	115

ΔH^*, ΔS^* and ΔG^* were calculated at 87 °C.

the eubacterial elongation factor has an higher affinity for the antibiotic with respect to the archaeal one.

Regarding the effects on the functional properties of the enzyme, tetracycline, although at concentration at least one order of magnitude higher than that required for the eubacterial process, was able to inhibit protein synthesis. In addition, the antibiotic slightly reduced the affinity of SsEF-1α for guanosine nucleotides. In the case of GDP, the increased equilibrium dissociation constant of the binary complex SsEF-1α•GDP can be ascribed to a greater decrease in the association rate constant than the dissociation one. In the case of the GDP/GTP exchange reaction on the archaeal elongation factor, tetracycline has a more pronounced effect, making the rate faster and more similar to GDP/GDP.

The effects of the antibiotic on the intrinsic GTPase catalysed by SsEF-1α in the presence of NaCl appeared limited and undetectable on the truncated forms of the factor. This behaviour, in contrast to the data reported on the spectroscopic properties, can be attributed to the high concentration of NaCl (3.6 M) needed to induce the GTPase activity of both intact (46) and engineered forms of the elongation factor (39,41). However, the concentration of antibiotic needed to get a 50% inhibition of the intrinsic GTPase of SsEF-1α (322 μM) is very similar to that derived from fluorescence titration and of the same order of magnitude than that required to inhibit to 50% the protein synthesis *in vitro* in some micropathogens (400–850 μM) but also in a cell-free reconstituted system of *S. solfataricus* and *S. acidocaldarius* (37,48).

The interaction between SsEF-1α and tetracycline caused a reduction of the heat inactivation of the archaeal elongation factor, as demonstrated by a lower value of the energy of activation of the process. The analysis of the thermodynamic parameters of the heat inactivation process at 87 °C (Table 3) indicated that the antibiotic reduced both the enthalpy and the entropy of activation without affecting the

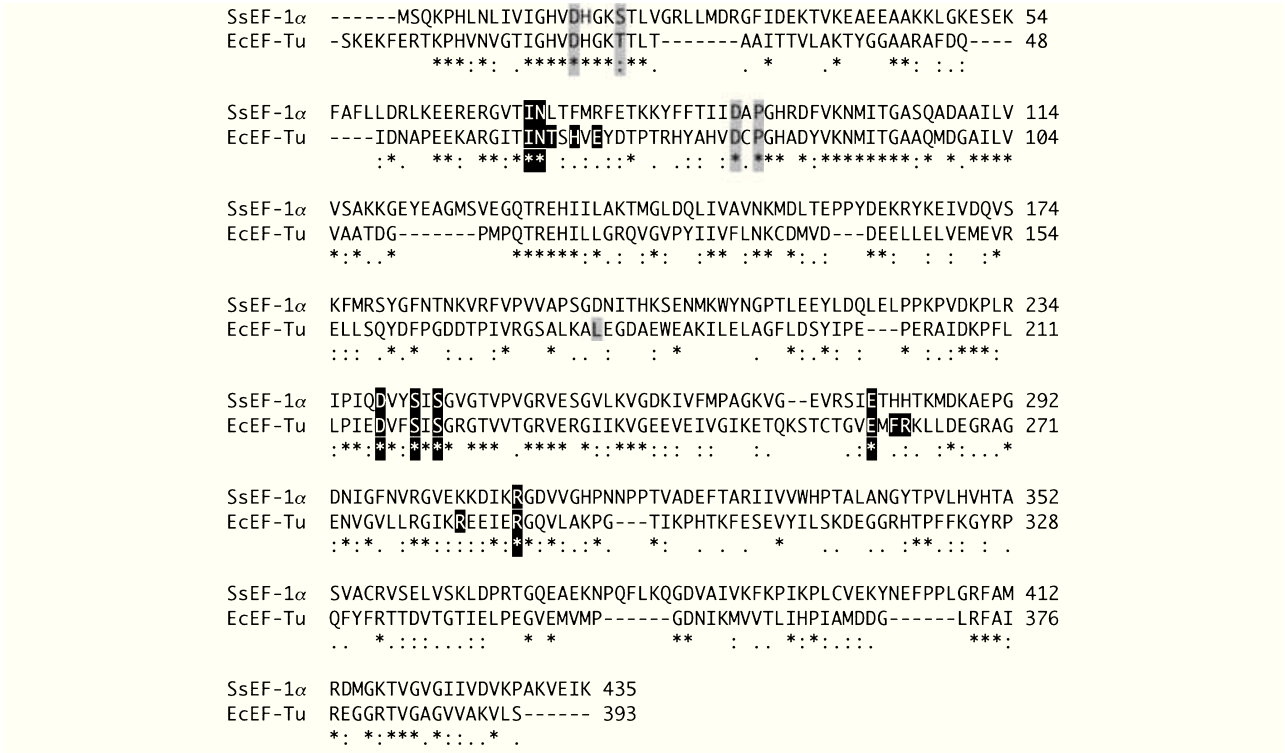

Figure 8: Alignment between the primary structure of elongation factor 1α from *Sulfolobus solfataricus* and *Escherichia coli* EF-Tu (EcEF-Tu). The alignment was carried out using the proteomics tools available at http://www.expasy.ch. Residues involved in tetracycline binding in EcEF-Tu belonging to the nucleotide-binding domain are highlighted in grey. Those participating in the dimerisation induced by tetracycline are in white and shaded in black. Conserved residues are indicated by an asterisk, conservative substitutions by a colon and semi-conservative substitutions by a dot.

free energy associated with the process. This finding can be explained by a less favourable entropic factor induced by tetracycline in the attainment of the activation state of the inactivation process.

The interaction between SsEF-1α and tetracycline was also analysed in terms of amino acid residues of the elongation factor involved, through the alignment between the primary structures of EcEF-Tu and SsEF-1α (Figure 8). Among the residues identified in the catalytic domain of EcEF-Tu involved in the binding of the antibiotic (14), those of the consensus sequences of guanosine nucleotide-binding proteins (Asp21, Thr25, Asp80, and Pro82, EcEF-Tu numbering) as expected are conserved in SsEF-1α. Regarding the other residues involved in the interaction with the antibiotic and belonging to this domain (Thr64, Ser65, Val67 and Leu178, EcEF-Tu numbering), although a Ser65 → Thr and a Val67 → Met were found as conservative substitutions, the other two residues were not conserved in SsEF-1α (Thr65 → Leu and Leu178 → Asp, EcEF-Tu numbering, respectively). Concerning the amino acid residues involved in the dimer formation through protein–protein interaction, those participating in the stabilisation of the conserved flexible region Ile220 → Arg223 were also present in SsEF-1α; vice versa, differences were found in the residues belonging to the Arg262 → Leu264 loop, even though some of the residues involved in its stabilisation were conserved (Asp216 and Glu259).

Conclusions

In conclusion, the data presented demonstrate the interaction between an archaeal elongation factor 1α and the eubacterial antibiotic tetracycline. These results, besides being useful for studying the interaction between tetracycline and eukaryotic elongation factors and hence for the assessment of potential side effects, could provide a basis for the development of new drugs whose mechanism of action is based on the interaction between specific amino acid residues of target proteins and reactive portions in the structure of this family of antibiotics.

Acknowledgments

This work was supported by PRIN 2007 and 2008 (Miur, Rome) to MM and PA, respectively.

References

1. Dever T.E., Glynias M.J., Merrick W. (1987) GTP–binding domain: three consensus sequence elements with distinct spacing. Proc Natl Acad Sci USA;84:1814–1818.

2. Abel K., Journak F. (1996) A complex profile of protein elongation: translating chemical energy into molecular movement. Structure;4:229–238.
3. Krab I., Parmeggiani A. (1998) EF–Tu, a GTPase odyssey. Biochim Biophys Acta;1443:1–22.
4. Blumenthal T., Carmichael G.G. (1979) RNA replication: function and structure of Qbeta-replicase. Annu Rev Biochem;48:525–548.
5. Suzuki H., Ueda T., Taguchi H., Takeuchi N. (2007) Chaperone properties of mammalian mitochondrial translation elongation factor Tu. J Biol Chem;282:4076–4084.
6. Negrutskii B.S., El'skaya A.V. (1998) Eukaryotic translation elongation factor 1 alpha: structure, expression, functions, and possible role in aminoacyl-tRNA channeling. Prog Nucleic Acid Res Mol Biol;60:47–78.
7. Kjeldgaard M., Nyborg J. (1992) Refined structure of elongation factor EF-Tu from *Escherichia coli*. J Mol Biol;223:721–742.
8. Song H., Parsons M.R., Rowsell S., Leonard G., Phillips S.E. (1999) Crystal structure of intact elongation factor EF-Tu from *Escherichia coli* in GDP conformation at 2.05 Å resolution. J Mol Biol;285:1245–1256.
9. Vitagliano L., Masullo M., Sica F., Zagari A., Bocchini V. (2001) The crystal structure of *Sulfolobus solfataricus* elongation factor 1 alpha in complex with GDP reveals novel features in nucleotide binding and exchange. EMBO J;20:5305–5311.
10. Vitagliano L., Ruggiero A., Masullo M., Cantiello P., Arcari P., Zagari A. (2004) The crystal structure of *Sulfolobus solfataricus* elongation factor 1 alpha in complex with magnesium and GDP. Biochemistry;43:6630–6636.
11. Sprinzl M. (1994) Elongation factor Tu: a regulatory GTPase with an integrated effector. Trends Biochem Sci;19:245–250.
12. Krab I., Parmeggiani A. (2002) Mechanisms of EF–Tu, a pioneer GTPase. Prog Nucleic Acid Res;71:513–551.
13. Heffron S.E., Jurnak F. (2000) Structure of an EF–Tu complex with a thiazolyl peptide antibiotic determined at 2.35 Å resolution: atomic basis for GE2270A inhibition of EF–Tu. Biochemistry;39:37–45.
14. Heffron S.E., Mui S., Aorora A., Abel K., Bergmann E., Jurnak F. (2006) Molecular complementarity between tetracycline and the GTPase active site of elongation factor Tu. Acta Crystallogr;62:1392–1400.
15. Connamacher R.H., Mandel H.G. (1968) Studies on the intracellular localization of tetracycline in bacteria. Biochim Biophys Acta;166:475–486.
16. Maxwell I.H. (1968) Studies of the binding of tetracycline to ribosomes *in vitro*. Mol Pharmacol;4:25–37.
17. Williams Smith H. (1979) Antibiotic-resistant *Escherichia coli* in market pigs in 1956–1979: the emergence of organisms with plasmid-borne trimethoprim resistance. J Hyg (Lond);84:467–477.
18. Moazed D., Noller H.F. (1987) Interaction of antibiotics with functional sites in 16S ribosomal RNA. Nature;327:389–394.
19. Brodersen D.E., Clemons W.M. Jr, Carter A.P., Morgan-Warren R.J., Wimberly B.T., Ramakrishnan V. (2000) The structural basis for the action of the antibiotics tetracycline, pactamycin, and hygromycin B on the 30S ribosomal subunit. Cell;103:1143–1154.
20. Pioletti M., Schlünzen F., Harms J., Zarivach R., Glühmann M., Avila H., Bashan A., Bartels H., Auerbach T., Jacobi C., Hartsch T., Yonath A., Franceschi F. (2001) Crystal structures of complexes of the small ribosomal subunit with tetracycline, edeine and IF3. EMBO J;20:1829–1839.
21. Hinrichs W., Kisker C., Düvel M., Müller A., Tovar K., Hillen W., Saenger W. (1994) Structure of the Tet repressor-tetracycline complex and regulation of antibiotic resistance. Science;264:418–420.
22. Orth P., Saenger W., Hinrichs W. (1999) Tetracycline-chelated Mg^{2+} ion initiates helix unwinding in Tet repressor induction. Biochemistry;38:191–198.
23. Nonaka L., Connell S.R., Taylor D.E. (2005) 16S rRNA mutations that confer tetracycline resistance in Helicobacter pylori decrease drug binding in *Escherichia coli* ribosomes. J Bacteriol;187:3708–3712.
24. Epe B., Woolley P. (1984) The binding of 6-demethylchlortetracycline to 70S, 50S and 30S ribosomal particles: a quantitative study by fluorescence anisotropy. EMBO J;3:121–126.
25. Gordon J. (1969) Hydrolysis of guanosine 5′-triphosphate associated with binding of aminoacyl transfer ribonucleic acid to ribosomes. J Biol Chem;244:5680–5686.
26. Lucas-Lenard J., Tao P., Haenni A.L. (1969) Further studies on bacterial polypeptide elongation. Cold Spring Harb Symp Quant Biol;34:455–462.
27. Ravel J.M., Shorey R.L., Garner C.W., Dawkins R.C., Shive W. (1969) The role of an aminoacyl-tRNA-GTP-protein complex in polypeptide synthesis. Cold Spring Harb Symp Quant Biol;34:321–330.
28. Shorey R.L., Ravel J.M., Garner C.W., Shive W. (1969) Formation and properties of the aminoacyl transfer ribonucleic acid-guanosine triphosphate-protein complex. J Biol Chem;244:4555–4564.
29. Skoultchi A., Ono Y., Waterson J., Lengyel P. (1970) Peptide chain elongation; indications for the binding of an amino acid polymerization factor, guanosine 5′-triphosphate–aminoacyl transfer ribonucleic acid complex to the messenger-ribosome complex. Biochemistry;9:508–514.
30. Spirin A.S., Kostiashkina O.E., Jonák J. (1976) Contribution of the elongation factors to resistance of ribosomes against inhibitors: comparison of the inhibitor effects on the factor-free translation systems. J Mol Biol;101:553–562.
31. Semenkov Yu.P., Makarov E.M., Makhno V.I., Kirillov S.V. (1982) Kinetic aspects of tetracycline action on the acceptor (A) site of *Escherichia coli* ribosomes. FEBS Lett;144:125–129.
32. Masullo M., Cantiello P., de Paola B., Catanzano F., Arcari P., Bocchini V. (2002) G13A substitution affects the biochemical and physical properties of the elongation factor 1 alpha. A reduced intrinsic GTPase activity is partially restored by kirromycin. Biochemistry;41:628–633.
33. Masullo M., Cantiello P., de Paola B., Fiengo A., Vitagliano L., Zagari A., Arcari P. (2002) Valine 114 replacements in archaeal elongation factor 1 alpha enhanced its ability to interact with aminoacyl–tRNA and kirromycin. Biochemistry;41:14482–14488.
34. Cantiello P., Castellano I., De Vendittis E., Lamberti A., Longo O., Masullo M., Raimo G., Ruocco M.R., Arcari P. (2004) Interaction of archaeal translation elongation factors with eubacterial protein synthesis inhibitors. Curr Top Biochem Res;6:145–154.
35. Masullo M., Cantiello P., Arcari P. (2004) Archaeal elongation factor 1alpha from *Sulfolobus solfataricus* interacts with the eubacterial antibiotic GE2270A. Extremophiles;8:499–505.

36. De Vendittis E., de Paola B., Gogliettino M., Adinolfi B.S., Duvold T., Bocchini V. (2002) Fusidic and helvolic acid inhibition of elongation factor 2 from the archaeon *Sulfolobus solfataricus*. Biochemistry;41:14879–14884.
37. Cammarano P., Teichner A., Londei P., Acca M., Nicolaus B., Sanz J.L., Amils R. (1985) Insensitivity of archaebacterial ribosomes to protein synthesis inhibitors. Evolutionary implications. EMBO J;4:811–816.
38. Aagaard C., Phan H., Trevisanato S., Garrett R.A. (1994) A spontaneous point mutation in the single 23S rRNA gene of the thermophilic arachaeon *Sulfolobus acidocaldarius* confers multiple drug resistance. J Bacteriol;176:7744–7747.
39. Masullo M., Ianniciello G., Arcari P., Bocchini V. (1997) Properties of truncated forms of the elongation factor 1alpha from the archaeon *Sulfolobus solfataricus*. Eur J Biochem;243:468–473.
40. Kenawy E.R., Bowlin G.L., Mansfield K., Layman J., Simpson D.G., Sanders E.H., Wnek G.E. (2002) Release of tetracycline hydrochloride from electrospun poly(ethylene–co–vinylacetate), poly(lactic acid), and a blend. J Control Release;81:57–64.
41. Arcari P., Masullo M., Arcucci A., Ianniciello G., de Paola B., Bocchini V. (1999) A chimeric elongation factor containing the putative guanine nucleotide binding domain of archaeal EF-1 alpha and the M and C domains of eubacterial EF-Tu. Biochemistry;38:12288–12295.
42. Ianniciello G., Masullo M., Gallo M., Arcari P., Bocchini V. (1996) Expression in *Escherichia coli* of thermostable elongation factor 1 alpha from the archaeon *Sulfolobus solfataricus*. Biotechnol Appl Biochem;23:41–45.
43. Raimo G., Masullo M., Parente A., Dello Russo A., Bocchini V. (1992) Molecular, functional and structural properties of an archaebacterial elongation factor 2. Biochim Biophys Acta;1132:127–132.
44. Lombardo B., Raimo G., Bocchini V. (2002) Molecular and functional properties of an archaeal phenylalanyl-tRNA synthetase from the hyperthermophile *Sulfolobus solfataricus*. Biochim Biophys Acta;1596:246–252.
45. Raimo G., Masullo M., Lombardo B., Bocchini V. (2000) The archaeal elongation factor 1alpha bound to GTP forms a ternary complex with eubacterial and eukaryal aminoacyl–tRNA. Eur J Biochem;267:6012–6018.
46. Masullo M., De Vendittis E., Bocchini V. (1994) Archaebacterial elongation factor 1 alpha carries the catalytic site for GTP hydrolysis. J Biol Chem;269:20376–20379.
47. Chopra I., Roberts M. (2001) Tetracycline antibiotics: mode of action, applications, molecular biology, and epidemiology of bacterial resistance. Microbiol Mol Biol Rev;65:232–260.
48. Katiyar S.K., Edlind T.D. (1991) Enhanced antiparasitic activity of lipophilic tetracyclines: role of uptake. Antimicrob Agents Chemother;35:2198–2202.